

NACA  
RM-E51114 53

CONFIDENTIAL

Copy  
RM E51114

NACA RM E51114

UNCLASSIFIED



GROUP 4  
Downgraded at 3 year  
intervals; declassified  
after 12 years

# RESEARCH MEMORANDUM

Classification Changed to  
**UNCLASSIFIED**  
Authority  
DOD DIR 5200.10

PERFORMANCE AND OPERATIONAL CHARACTERISTICS OF A  
PYTHON TURBINE-PROPELLER ENGINE AT

SIMULATED ALTITUDE CONDITIONS

By Carl L. Meyer and LaVern A. Johnson

Lewis Flight Propulsion Laboratory  
Cleveland, Ohio

JPL LIBRARY  
CALIFORNIA INSTITUTE OF TECHNOLOGY

CLASSIFIED  
SECRET

FEB 18 1952

CLASSIFIED DOCUMENT

This material contains information affecting the National Defense of the United States within the meaning of the espionage laws, Title 18, U.S.C., Secs. 793 and 794, the transmission or revelation of which in any manner to unauthorized person is prohibited by law.

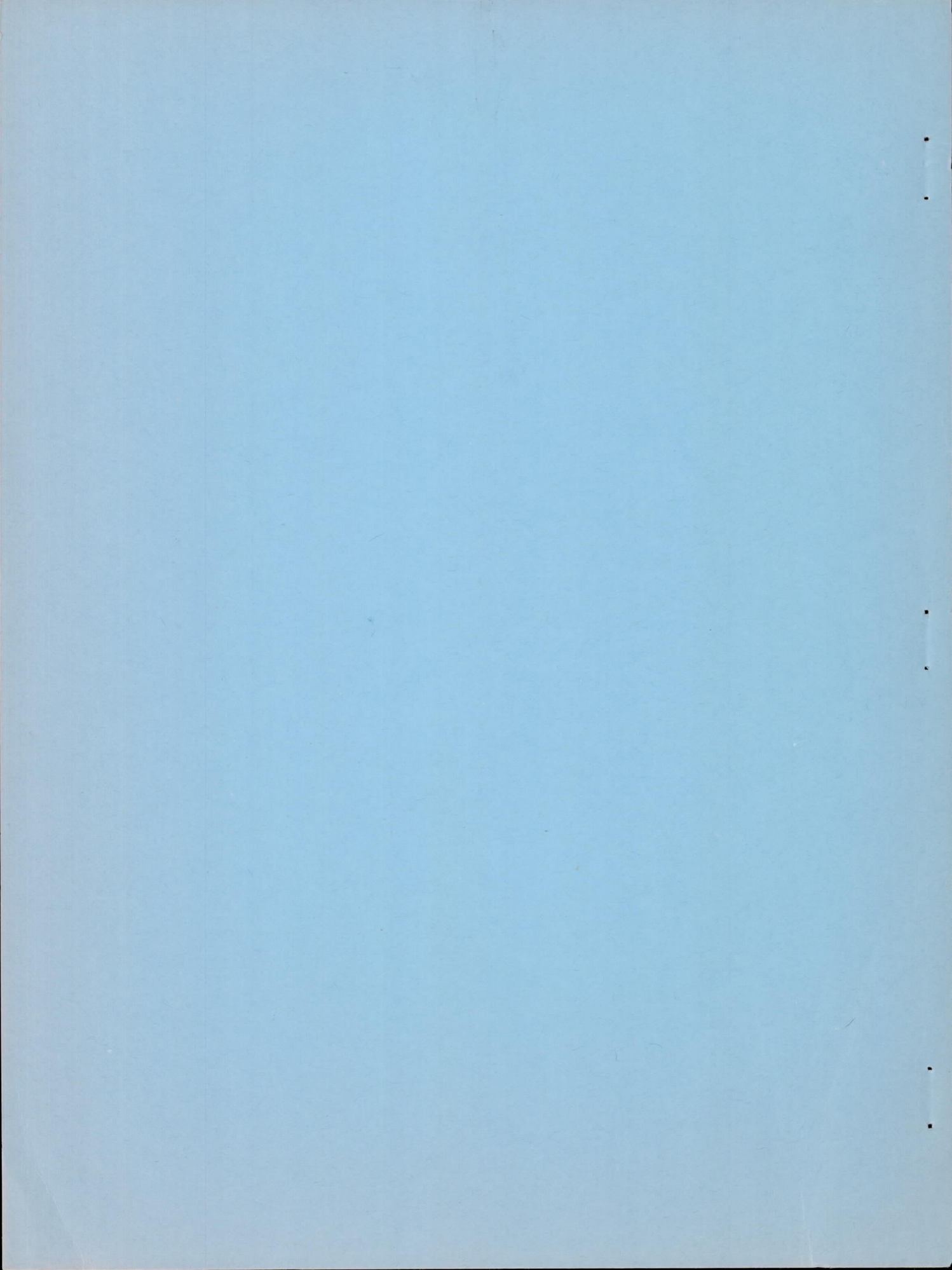
## NATIONAL ADVISORY COMMITTEE FOR AERONAUTICS

WASHINGTON

February 6, 1952

UNCLASSIFIED

CONFIDENTIAL



## NATIONAL ADVISORY COMMITTEE FOR AERONAUTICS

RESEARCH MEMORANDUMPERFORMANCE AND OPERATIONAL CHARACTERISTICS OF A PYTHON  
TURBINE-PROPELLER ENGINE AT SIMULATED  
ALTITUDE CONDITIONS

By Carl L. Meyer and LaVern A. Johnson

## SUMMARY

2308

The performance and operational characteristics of a Python turbine-propeller engine have been investigated over a range of engine operating conditions at simulated altitudes from 5000 to 40,000 feet in the NACA Lewis altitude wind tunnel. For the performance phase of the investigation, a single cowl-inlet ram pressure ratio was maintained and independent control of engine speed and fuel flow was used to obtain a range of power at each engine speed.

Engine performance data obtained at a given altitude could not be used to predict performance accurately at other altitudes by use of the standard air pressure and temperature generalizing factors.

Specific fuel consumption based on shaft horsepower decreased as the shaft horsepower increased at a given engine speed. At a given altitude condition and turbine-inlet total temperature, there was an optimum engine speed at which maximum shaft horsepower was obtained. At a given engine speed and turbine-inlet total temperature, a greater portion of the total available energy was converted to propulsive power as the altitude increased.

Windmilling starts were made at altitudes up to 40,000 feet; the minimum true airspeed required for successful windmilling starts increased as the altitude was raised. In general, the engine control prevented large overshoots or undershoots of engine speed during starts, accelerations, and decelerations.

## INTRODUCTION

An investigation to determine the performance and operational characteristics of a Python turbine-propeller engine over a range of simulated altitude conditions has been conducted in the NACA Lewis altitude wind tunnel. Instrumentation was installed in the engine to permit

evaluation of the performance of the individual components operating as integral parts of the engine as well as over-all engine performance. In the performance phase of the investigation, data were obtained over a range of engine speeds and exhaust-nozzle areas at altitudes from 10,000 to 40,000 feet at a single cowl-inlet ram pressure ratio; independent control of engine speed and fuel flow was used to obtain a range of power at each engine speed. Analyses of turbine, compressor, and combustion-chamber performance are presented in references 1, 2, and 3, respectively; and an investigation of the dynamic characteristics of the engine is reported in reference 4.

Performance and certain operational characteristics of the over-all engine are reported herein. Data are presented to show the performance of the engine over a range of engine speeds at each of four altitudes, the effect of altitude on nongeneralized performance at a given engine speed, the applicability of a generalization method for predicting engine performance at altitudes other than the test altitude, and the effect of exhaust-nozzle area on performance. Performance deterioration, apparently resulting from dust and oil accumulations in the compressor, is discussed. The division of energy between the propeller and jet is shown for a range of engine speeds, altitudes, and exhaust-nozzle areas. All engine performance data are also presented in tabular form. Operational characteristics discussed include windmilling drag and engine speed for a range of propeller blade angles, and starting, acceleration, and deceleration with the normal engine control system.

## DESCRIPTION OF ENGINE

### General

The main components of the Python turbine-propeller engine (fig. 1) are a 14-stage axial-flow compressor, 11 cylindrical combustion chambers, a two-stage turbine, an exhaust cone, a tail pipe with a fixed-area exit, and a reduction-gear assembly. The engine is fitted with two 4-blade, constant-speed, contra-rotating propellers. The maximum diameter of the engine is 54.5 inches, the length from the center line of the forward propeller to the end of the exhaust cone is  $182\frac{2}{3}$  inches, and the net dry weight without propellers is about 3150 pounds. For the engine used in the present investigation, the standard tail pipe has a length of 66 inches and an exit diameter of 23 inches.

The operating limits of the engine as established by the manufacturer are:

258

Operating condition	Engine speed (rpm)	Tail-pipe gas temperature		Time limit (min)
		(°C)	(°F)	
Maximum take-off	8000	590	1094	5
Maximum climb	7800	560	1040	30
Maximum cruise	7600	530	986	continuous
Minimum flight idling	6500 $\pm$ 100	---	---	---
Ground idling	3500 - 4000	580	1076	10

At maximum take-off operating conditions, the engine has a nominal static sea-level rating of 3670 shaft horsepower and 1150 pounds of jet thrust.

The engine is of the reverse-flow type (fig. 1). Air enters the engine through a screened annular cowling after which the air-flow passage is divided circumferentially into 11 convergent throats through which the air is swept inward through 180° to the entry annulus of the compressor. Thus, flow through the compressor is in the forward direction. Air from the compressor passes through an annular angled section where it is turned outward 90°, after which the air-flow passage is divided circumferentially into 11 combustion-chamber-inlet ducts through which the air is turned rearward 90° to the combustion chambers. Air is bled from the fifth compressor stage for cooling the rear bearing and rear face of the turbine disk and from the tenth compressor stage for cooling the front face of the turbine disk. A more complete description of the compressor is given in reference 2.

The 11 direct-flow-type combustion chambers (reference 3) are equally spaced around the outer circumference of the compressor casing. A vaporizing-type fuel system is used during normal engine operation; fuel from the main fuel nozzles and a portion of the air from the compressor enter the primary combustion zone through a mixing chamber or vaporizer. For starting purposes, nine combustion chambers include starting fuel nozzles and two chambers include combination spark plugs and starting fuel nozzles; cross-fire tubes are provided for ignition of the other combustion chambers. The fuel used throughout the investigation conformed to specification MIL-F-5616 (kerosene).

Gases from the combustion chambers flow through the two-stage turbine (reference 1) and exhaust to atmosphere through the exhaust cone and tail pipe. Each turbine stage consists of a stator and rotor; both rotor stages are mounted on a common disk.

The turbine shaft drives the compressor directly and the propeller shaft through a two-stage planetary-reduction gear. A floating-type annulus (or ring) gear in the reduction gear assembly is prevented from rotating by two hydraulic pistons which provide a means of determining shaft torque.

## Control

Fuel flow is controlled by a flow-control unit, which is sensitive to throttle position and cowl-inlet total pressure, in conjunction with a variable displacement pump. During normal engine operation, fuel from the flow-control unit flows through a distributor where it is divided into 11 equal parts and distributed to each of the main fuel nozzles. During starting, the initial fuel flow is directly from the flow-control unit to the starting fuel nozzles; a spring loaded valve prevents fuel from entering the distributor during starting until the fuel pressure increases to a given value. An electro-hydraulic valve in the fuel line to the starting fuel nozzles permits flow only while the ignition is on.

A propeller constant-speed unit controls engine speed over a range from approximately 75 to 100 percent of full engine speed. At engine speeds between approximately 50 and 75 percent of full speed, propeller pitch is held constant by a fine pitch stop which is normally retractable to facilitate ground starting and landing; engine speeds within this range are controlled by fuel flow. Minimum flight idling engine speed is normally the minimum engine speed at which the constant speed unit is effective.

A single lever, or throttle, is normally used to operate the engine. The necessary relation between engine speed and fuel flow is obtained by connecting both the propeller constant-speed unit control and the fuel-flow throttle to a single lever through an oil-servo unit and suitable cam-operated linkages. The engine will operate at approximately 50 percent of full engine speed with the single control lever in the fully closed position. As the single lever is advanced through the first portion of its travel, engine speed will increase to about 75 percent of full speed but the propeller blade angle remains constant. As the lever is further advanced, the propeller blade angle and the engine speed are gradually increased, resulting in a progressive increase in power.

A reverse torque switch in the reduction gear causes the propeller blade angle to increase whenever the propeller windmills the engine. To make flight windmilling starts possible, the reverse torque switch is inoperative when the ignition is on.

The normal single-lever control was not flexible enough to be used throughout the various phases of the present investigation. For the performance investigation, the propeller fine pitch stop was omitted and the propeller constant-speed unit valve and the fuel throttle were separately operated to permit independent control of engine speed and fuel flow. For the windmilling investigation, the constant-speed unit valve was replaced by a manually operated valve with which it was possible to control the flow of hydraulic oil to the propeller and thus control propeller blade angle. For the investigation of starting, acceleration, and deceleration characteristics, the normal single-lever control and a 20° propeller fine pitch stop were used.

2308

## INSTALLATION AND INSTRUMENTATION

2308  
The altitude wind tunnel in which the investigation was conducted is a closed-throat return-flow tunnel with a test section 20 feet in diameter and 40 feet long. The engine was installed in a wing segment (fig. 2) that was supported in the test section by the tunnel balance frame. The normal cowling over the forward section of the engine and NACA designed cowling over the exhaust cone and tail pipe were used throughout the investigation. Air was supplied to the engine from the tunnel air stream.

Instrumentation for measuring steady-state pressures and temperatures was installed at various stations (fig. 1) within the engine. Schematic diagrams of the instrumentation at individual stations are shown in figure 3. Pressures at the cowl inlet and in the tail pipe were measured with water-filled manometers and those at the compressor outlet (or combustion-chamber inlet) and turbine inlet were measured with mercury-filled manometers; all pressures were photographically recorded. Temperatures at the cowl inlet and compressor outlet were measured with iron-constantan thermocouples and those in the tail pipe were measured with chromel-alumel thermocouples; all temperatures were automatically recorded with self-balancing potentiometers.

Engine speed was measured by means of a stroboscopic tachometer in conjunction with a continuously indicating tachometer. Torque was sensed by means of the built-in hydraulic torquemeter which had been calibrated by the manufacturer to give propeller-shaft torque in terms of torquemeter pressure; torquemeter pressure was measured by a Bourdon gage. Fuel flow was measured by calibrated rotameters. The instrument panel included a series of gages for an indication of various operating temperatures and pressures, including turbine-inlet temperature, compressor-discharge pressure, and distributor fuel pressure. For the windmilling investigation, propeller blade angle was sensed by an NACA indicator attached to one of the blades of the rear propeller.

## PROCEDURE

## Performance Investigation

Throughout the performance investigation, independent control of engine speed and fuel flow was used to obtain a range of fuel flows and, consequently, a range of powers at each engine speed. With the standard 23-inch-diameter tail pipe, which had no exhaust nozzle, performance data were obtained at engine speeds from 6800 to 8000 rpm at altitudes from 10,000 to 30,000 feet and at engine speeds from 7400 to 8000 rpm at an altitude of 40,000 feet; data were not obtained at engine speeds below 7400 rpm at an altitude of 40,000 feet because of the limited range of

powers available. With a 24-inch-diameter tail pipe and tail-pipe exit diameters of 20, 22, and 24 inches, performance data were obtained at engine speeds from 7600 to 8000 rpm at altitudes from 10,000 to 40,000 feet.

All performance data were obtained at a cowl-inlet ram pressure ratio of about 1.03. Ram pressure ratio is defined as the ratio of cowl-inlet (station 1) total pressure to free-stream (tunnel test section) static pressure. The cowl-inlet air temperatures were held at approximately NACA standard values corresponding to the simulated conditions at altitudes of 10,000 and 20,000 feet; for altitudes of 30,000 and 40,000 feet, the cowl-inlet air temperature was held at about 440° R. The value of ram pressure ratio is a compromise value selected from two considerations. First, a deteriorated condition of the tunnel drive fan prohibited more realistic values of ram pressure ratio for the present investigation. Second, it was considered desirable to select a ram pressure ratio which could be maintained over the range of altitudes, engine speeds, and engine powers. Tunnel refrigeration equipment had the capacity to reduce the air temperature to about 415° R; however, the time required to reduce the temperature and the desirability of selecting a temperature that could be maintained over the range of engine conditions resulted in a compromise at the higher altitudes.

Symbols and methods of calculation are given in the appendix.

#### Operational Investigation

The standard 23-inch-diameter tail pipe was used throughout the operational investigation.

Windmilling. - For the windmilling investigation, a manually operated valve was used to control propeller blade angle and, consequently, windmilling engine speed. Steady-state windmilling data were obtained over a range of propeller blade angles at altitudes from 10,000 to 40,000 feet at a true airspeed of about 135 miles per hour and at true airspeeds from 100 to 175 miles per hour at an altitude of 20,000 feet.

Starting, acceleration, and deceleration. - The normal single-lever control and a 20° propeller fine pitch stop were used. Windmilling starting characteristics were investigated at altitudes from 5000 to 40,000 feet at true airspeeds ranging from about 120 to 280 miles per hour. Acceleration characteristics were investigated within the aforementioned altitude range at true airspeeds ranging from about 130 to 290 miles per hour. Deceleration characteristics were investigated at altitudes from 5000 to 35,000 feet at true airspeeds from about 160 to 310 miles per hour. In all cases, the true airspeed is that immediately preceding the transient; no attempt was made to hold airspeed constant during the transient.

2308

2808

Before attempting a windmilling start, the altitude and airspeed conditions were established with the propeller at full-feathered blade angle. Then, in quick succession, the ignition was turned on, the fuel valve was opened, and the unfeathering pump was started to reduce propeller blade angle. A successful start was considered to be one from which the engine could be accelerated to an engine speed of approximately 6500 rpm. At established altitude and airspeed conditions, accelerations and decelerations were accomplished by rapid movement of the single-lever control to the proper positions. The data for the starts, accelerations, and decelerations were obtained by photographing a panel of instruments with a motion-picture camera at a rate of about 9 frames per second.

## RESULTS AND DISCUSSION

### Engine Performance

All engine performance data obtained with the various tail-pipe configurations are presented in table I.

The inlet air temperatures deviated from NACA standard values, particularly at altitudes of 30,000 and 40,000 feet for which the inlet-air temperature was held at about 440° R. Therefore, all performance data presented graphically in nongeneralized form have been adjusted to NACA standard conditions at the respective altitudes by the use of the factors  $\theta_a$  and  $\delta_a$  (see appendix). Performance data adjusted by this method may be somewhat different from data obtained under actual standard conditions because the effect of Reynolds number is not considered; however, the method permits a reasonable evaluation of the data at standard altitude conditions.

Engine deterioration. - During the early phase of the present investigation, loss of power at a given tail-pipe temperature was noted with increased engine operating time. This loss in power is associated with the accumulation of dust and oil on the compressor blading, resulting in reduced mass flow and pressure ratio. The amount of dust that passed through the engine may have been greater during the wind-tunnel investigation than would have been encountered under normal operating conditions. The variation of engine performance with operating time is shown in figure 4 as plots of air flow, fuel flow, turbine-inlet total temperature, ratio of shaft enthalpy drop to total enthalpy drop (see appendix), and jet thrust against shaft horsepower for various engine operating times; data are presented for altitudes of 10,000, 20,000, 30,000, and 40,000 feet.

The trend of engine performance with operating time was similar, in general, at altitudes from 10,000 to 30,000 feet (figs. 4(a) to 4(c)); however, the effect of operating time on performance decreased with

increasing altitude until at an altitude of 40,000 feet there was essentially no change in performance with increased operating time within the range noted (fig. 4(d)). In general and for a given shaft horsepower, as engine operating time increased, air flow decreased, fuel flow (and, consequently, specific fuel consumption based on shaft horsepower) was essentially unchanged, turbine-inlet temperature increased, the ratio of shaft enthalpy drop to total enthalpy drop increased slightly, and jet thrust decreased at altitudes of 10,000 to 30,000 feet. At a given turbine-inlet total temperature, both shaft horsepower and jet thrust decreased with increased operating time because of the loss in air flow.

Data are not available to indicate the effect of engine operating time on performance at all engine speeds for the various altitudes. It was not possible, therefore, to adjust the data so as to eliminate the effects of engine deterioration. In table I and where possible in the various figures, the approximate engine time is noted.

Engine performance maps. - Performance data for a range of engine speeds at an altitude of 10,000 feet are presented in figure 5 as plots of air flow, turbine-inlet total temperature, fuel flow, specific fuel consumption based on shaft horsepower, and jet thrust against shaft horsepower. A portion of these data and similar data for altitudes of 20,000, 30,000, and 40,000 feet have been crossplotted in figure 6 in the form of engine performance maps for each of the four altitudes. The performance maps selected show shaft horsepower against engine speed at various constant values of turbine-inlet total temperature, fuel flow, and jet thrust; these maps summarize engine performance at each of the four altitudes within the range of shaft horsepowers and engine speeds investigated.

Within operating temperature and engine speed limits and by use of independent control of engine speed and fuel flow, a given shaft horsepower is available over a range of engine speeds and a range of shaft horsepowers is available at a given engine speed. Turbine-inlet total temperature, fuel flow, and jet thrust increase nearly linearly with shaft horsepower at a given engine speed. Use of a normal single-lever control would restrict engine operation within the performance map to an operating line defined by a single available shaft horsepower at a given engine speed, altitude, and airspeed.

In general, shaft horsepower at a given fuel flow decreased with increasing engine speed. At a given altitude condition and turbine-inlet temperature, in general, there was an optimum engine speed at which maximum shaft horsepower was obtained; the maximum value of shaft horsepower occurred at higher engine speeds as the turbine-inlet total temperature increased. Jet thrust increased with increasing engine speed primarily because of the increased air flow. Specific fuel consumption

8032

2508  
based on shaft horsepower at an altitude of 10,000 feet (fig. 5(d)) decreased with increasing shaft horsepower at a given speed and with decreasing engine speed at a given shaft horsepower. If jet thrust were accounted for in the specific fuel consumption, the effect of engine speed on specific fuel consumption would be smaller since jet thrust increases with engine speed at a given shaft horsepower. The minimum specific fuel consumption based on shaft horsepower was approximately 0.9 pound per hour per shaft horsepower at engine speeds of about 7600 to 8000 rpm. Air flow (fig. 5(a)) at a given engine speed decreases somewhat with increasing shaft horsepower because of the increased compressor-pressure ratio.

Altitude. - Performance data for an engine speed of about 7600 rpm at altitudes of 10,000, 20,000, 30,000, and 40,000 feet are presented in figure 7 as plots of air flow, turbine-inlet total temperature, fuel flow, specific fuel consumption based on shaft horsepower, and jet thrust against shaft horsepower. The relation between turbine-inlet total temperature and shaft horsepower was used to superimpose temperature contours on figures 7(c) to 7(e).

Air flow decreased slightly with increasing shaft horsepower, as previously discussed, and decreased with increasing altitude primarily because of the reduction in air density (fig. 7(a)). As altitude increased, the shaft horsepower at a given turbine-inlet total temperature and the fuel flow required to produce a given turbine-inlet total temperature decreased, primarily because of the reduced air flow (figs. 7(b) and 7(c)). At each altitude, the lowest values of specific fuel consumption based on shaft horsepower was obtained at or near maximum temperature and power. For a given turbine-inlet total temperature, the minimum specific fuel consumption based on shaft horsepower was obtained at an altitude near 30,000 feet (fig. 7(d)). Jet thrust increased nearly linearly with shaft horsepower at each altitude and decreased with increasing altitude at a given turbine-inlet total temperature or shaft horsepower (fig. 7(e)).

The factors  $\delta_0$  and  $\theta_0$  were applied to the performance data of figure 5 and to similar data for the other altitudes at which data were obtained. The resultant data were cross-plotted to obtain generalized performance parameters for each altitude at a corrected engine speed of 8300 rpm, which is approximately the maximum corrected engine speed at which data were obtained at an altitude of 10,000 feet. The variation of corrected turbine-inlet total temperature, corrected fuel flow, and corrected jet thrust with corrected shaft horsepower at a corrected engine speed of 8300 rpm is shown in figure 8 for altitudes of 10,000, 20,000, 30,000, and 40,000 feet and a cowl-inlet ram pressure ratio of about 1.03. For a given corrected shaft horsepower, the corrected turbine-inlet total temperature and corrected fuel flow increased and the corrected jet thrust decreased as the altitude was increased from

10,000 to 40,000 feet. The pressure and temperature generalizing factors  $\delta_0$  and  $\theta_0$  could not, therefore, be applied to data obtained at a given altitude to predict performance accurately at some other altitude.

Engine deterioration cannot be eliminated from figure 8. However, considering the results of figure 4, the corrected performance for an altitude of 40,000 feet should be relatively unaffected by deterioration; also, data for an altitude of 10,000 feet were obtained earliest in the investigation and therefore should not be seriously affected by deterioration. A relatively true indication of the effect of altitude on generalized performance, therefore, should be noted by comparison of the curves for altitudes of 10,000 and 40,000 feet in figure 8.

It is shown in reference 2 that an increase in altitude from 10,000 to 40,000 feet at a given corrected engine speed decreased compressor efficiency and corrected air flow over the range of corrected turbine-inlet total temperature. Reference 3 indicates a slight tendency for combustion efficiency to decrease with increasing altitude. The loss in compressor efficiency and corrected air flow with increasing altitude made it necessary that the corrected turbine-inlet total temperature increase to maintain a given corrected shaft horsepower. To permit the higher corrected turbine-inlet temperature at a given shaft horsepower and to account for any loss in combustion efficiency, the corrected fuel flow increased with increasing altitude. The loss in corrected jet thrust at a given corrected shaft horsepower was primarily due to the loss in corrected air flow.

Exhaust-nozzle area. - Engine performance data for exhaust-nozzle diameters of 20, 22, and 24 inches, obtained at an engine speed of about 7600 rpm and an altitude of 10,000 feet, are presented in figure 9 as plots of turbine-inlet total temperature, specific fuel consumption based on shaft horsepower, and jet thrust against shaft horsepower; turbine-inlet temperature contours are superimposed on the curves of specific fuel consumption and jet thrust.

At a given turbine-inlet total temperature, jet thrust and specific fuel consumption based on shaft horsepower decreased and shaft horsepower increased as the exhaust-nozzle area increased. If jet thrust were accounted for in the specific fuel consumption, the effect of exhaust-nozzle area on specific fuel consumption would be smaller. The greater available turbine-pressure ratio with large exhaust-nozzle area resulted in a greater percentage of the available power being delivered to the shaft and consequently less being available in the jet.

2308

## Engine-Power Division

The division of power is expressed as the ratio of equivalent propeller-shaft enthalpy drop to total available enthalpy drop and the ratio of jet enthalpy drop to total available enthalpy drop. The method of calculating these ratios is given in the appendix.

The jet and shaft enthalpy-drop ratios are shown in figure 10 as functions of shaft horsepower for a range of corrected engine speeds at an altitude of 10,000 feet. In general, both jet and shaft enthalpy-drop ratios at a given engine speed increased with increasing shaft horsepower. At a given shaft horsepower, an increase in engine speed had essentially no effect on jet enthalpy-drop ratio, but reduced the shaft enthalpy-drop ratio because of the increasing power requirements of the compressor. The maximum total available enthalpy drop at any engine speed is limited by the operating temperature limits of the engine.

The jet and shaft enthalpy-drop ratios are shown in figure 11 as functions of shaft horsepower for a range of altitudes at an engine speed of about 7600 rpm; turbine-inlet total-temperature contours are superimposed on these curves. Though shaft horsepower at a given turbine-inlet total temperature decreased with increasing altitude, jet and shaft enthalpy-drop ratios at a given temperature, in general, increased with increasing altitude. Thus, a greater percentage of the total available enthalpy drop was converted to propulsive power as the altitude was increased at a given turbine-inlet temperature and engine speed.

The jet and shaft enthalpy-drop ratios are shown in figure 12 as functions of shaft horsepower for a range of exhaust-nozzle areas at an engine speed of about 7600 rpm and an altitude of 10,000 feet; turbine-inlet total-temperature contours are superimposed. At a given shaft horsepower or at a given turbine-inlet total temperature, the jet enthalpy-drop ratio decreased and the shaft enthalpy-drop ratio increased as the exhaust-nozzle area increased. As the exhaust-nozzle area was increased, the sum of jet and shaft enthalpy-drop ratios increased at a given shaft horsepower and remained essentially constant at a given turbine-inlet total temperature.

## Engine Operational Characteristics

Windmilling. - Drag and engine speed against propeller blade angle are presented in figure 13 for windmilling conditions over a range of altitudes at a true airspeed of 135 miles per hour and over a range of true airspeeds at an altitude of 20,000 feet. The drag presented is

defined as the installation drag at a given propeller blade angle minus the installation drag at full-feathered propeller blade angle; installation drag was determined from tunnel balance-scale measurements.

In general, both drag and windmilling engine speed at a given propeller blade angle increased as the altitude decreased and as the true airspeed increased. Peak values of drag occurred at a propeller blade angle of about  $15^{\circ}$ ; peak values of windmilling engine speed occurred at a propeller blade angle of about  $22^{\circ}$ . Though windmilling runs were not made at true airspeeds above 175 miles per hour, the need for feathering the propeller to prevent excessive drag at any airspeed and possible overspeeding of the engine at higher true airspeeds is evident.

Starting. - The effect of altitude on the minimum true airspeed required for successful windmilling starts is shown in figure 14; the normal single-lever control and a  $20^{\circ}$  propeller fine pitch stop were used. Successful windmilling starts were obtainable at a true airspeed of about 120 miles per hour up to an altitude between 15,000 and 20,000 feet; windmilling starts were not attempted at lower airspeeds. As the altitude was increased from 20,000 to 40,000 feet, progressively higher true airspeeds were required for successful starts. For the marginal starts noted in figure 14, the engine was started and accelerated to an operable engine speed but excessive turbine-inlet temperatures were encountered. The investigation did not include the determination of possible maximum true airspeed for windmilling starts; successful windmilling starts were made at true airspeeds up to 280 miles per hour.

Flight conditions and various engine variables during windmilling starts are shown against time in figure 15 for two altitudes at an initial true airspeed of about 280 miles per hour and for two initial airspeeds at an altitude of 25,000 feet. The flight conditions noted are tunnel true airspeed and cowl-inlet ram pressure ratio. The engine variables noted include turbine-inlet temperature, compressor-outlet total pressure, distributor fuel pressure (an indication of fuel flow), and engine speed. It is to be noted that at low distributor fuel pressures, a small change in pressure causes a relatively large change in fuel flow. As previously discussed, the altitude and airspeed conditions were established at full-feathered propeller blade angle. Then, in quick succession, the ignition was turned on, the fuel valve was opened (single control lever fully closed), and the unfeathering pump was started. With the single control lever fully closed, the engine will normally accelerate to about 50 percent of maximum engine speed; therefore, the accelerations noted consist of essentially two phases. As the engine speed approached 50 percent, the single control lever was advanced to permit continued acceleration to an engine speed of about 6500 rpm. The camera was started manually at the same time as the

unfeathering pump. Since a measure of propeller blade angle was not available for these data, the actual beginning of the transient is not accurately defined; the zero time noted in the figures is the first frame of the film.

No attempt was made to maintain tunnel true airspeed constant during the transient; as the propeller blade angle decreased during the unfeathering process and as the engine speed increased during the acceleration, the blockage caused by the engine propeller caused the true airspeed to decrease. The airspeed reached a minimum before maximum engine speed was reached. Cowl-inlet ram pressure ratio remained nearly constant during the transient, varying a maximum of about 0.01.

The accuracy of the measurement of turbine-inlet temperature is questionable. It appears from the turbine-inlet temperature curve, however, that in some cases partial burning occurred for the first few seconds; full combustion, as indicated by a rapid rise in temperature, occurred after about 4 seconds at which time the engine was windmilling at an appreciable engine speed. Since the normal control was used, there was no large overshoot of turbine-inlet temperature or engine speed. The apparent "flat spot" in the fuel-distributor pressure curve for the low true airspeed at an altitude of 25,000 feet (fig. 15(b)) is apparently due to a leveling off of fuel flow before the single-lever control was advanced. In most cases, the camera was stopped before steady-state operation was obtained after the transient.

The time required for the start and acceleration, until an engine speed of 6500 rpm was initially obtained, increased from about 11 seconds at an altitude of 25,000 feet to about 15.5 seconds at an altitude of 35,000 feet for the same initial true airspeed of 280 miles per hour (fig. 15(a)); for an altitude of 25,000 feet, this time increased from about 11 seconds at an airspeed of 280 miles per hour to 34 seconds at an airspeed of 144 miles per hour (fig. 15(b)). The maximum turbine-inlet temperature encountered during the transients was about the same for the two altitudes and an airspeed of 280 miles per hour (fig. 15(a)), but was higher for the lower of the two airspeeds at an altitude of 25,000 feet (fig. 15(b)).

It was necessary that the reverse torque switch be inoperative during a windmilling start until the engine was driving the propeller; it was occasionally necessary, therefore, to hold the ignition on longer than normally or to use an additional switch to keep the reverse torque switch inoperative after the ignition was off.

Acceleration. - Flight conditions and various engine variables during accelerations, from an engine speed of 6600 to 6800 rpm to an engine speed of 8000 rpm, are shown in figure 16 for two altitudes at an initial true airspeed of about 290 miles per hour and for two initial

true airspeeds at an altitude of 25,000 feet. The tunnel true airspeed and the cowl-inlet ram pressure ratio tended to increase very slightly during the transient.

It was desired to make the accelerations by quick movement of the single control lever from its initial position to the position for rated engine speed and power. Trends of the fuel distributor pressure indicate that the fuel flow did not increase uniformly. Some overshoot of engine speed is apparent for each acceleration. Adequate data are available to note apparent steady-state operation after the transient only for the low airspeed at an altitude of 25,000 feet (fig. 16(b)).

The time required for the acceleration until an engine speed of 8000 rpm was initially obtained increased, for an airspeed of 290 miles per hour, from about 4.3 seconds at an altitude of 25,000 feet to about 7.8 seconds at an altitude of 35,000 feet (fig. 16(a)); for an altitude of 25,000 feet, this time increased from about 4.3 seconds at a true airspeed of 292 miles per hour to about 5.2 seconds at an airspeed of 158 miles per hour (fig. 16(b)).

Deceleration. - Flight conditions and various engine variables during decelerations, from an engine speed of 8000 rpm to an engine speed of 6600 to 6800 rpm, are shown in figure 17 for two true airspeeds at an altitude of 25,000 feet. The tunnel true airspeed and the cowl-inlet ram pressure ratio tended to decrease very slightly during the transients.

It was desired to make these decelerations by quick movement of the single control lever from its initial setting to the final setting. Trends of the fuel distributor pressure for the deceleration at the higher airspeed indicate that the control was not moved uniformly to its final setting; this trend is reflected by the remaining engine variables and thus the deceleration was not accomplished in the shortest possible time. The time required for a given deceleration apparently increased with increasing airspeed. For the decelerations shown, the control prevented any notable undershoot of engine speed.

#### SUMMARY OF RESULTS

The performance and operational characteristics of a Python turbine-propeller engine were investigated over a range of engine operating conditions at simulated altitudes from 5000 to 40,000 feet. The results of this investigation may be summarized as follows:

1. Engine performance data obtained at a given altitude could not be used to accurately predict performance at other altitudes by the application of the standard air pressure and temperature generalizing factors.

2308

2. Turbine-inlet total temperature, fuel flow, and jet thrust increased and specific fuel consumption based on shaft horsepower decreased with increasing shaft horsepower at constant engine speed; air flow at a given engine speed decreased slightly with increasing shaft horsepower. Air flow and, consequently, jet thrust increased with increasing engine speed. For a given altitude condition and turbine-inlet total temperature, there was an optimum engine speed at which maximum shaft horsepower was obtained. For a given turbine-inlet total temperature and engine speed, there was an optimum altitude at which minimum specific fuel consumption based on shaft horsepower was obtained.

3. At a given altitude and shaft horsepower, increasing the engine speed lowered the portion of the total available energy absorbed by the propeller and had essentially no effect on the portion absorbed by the jet. As the altitude was increased at a given engine speed and turbine-inlet total temperature, a greater portion of the total available energy was converted to propulsive power.

4. For windmilling conditions, maximum values of drag and windmilling engine speed occurred at propeller blade angles of about  $15^{\circ}$  and  $22^{\circ}$ , respectively.

5. Windmilling starts and accelerations were made at altitudes as high as 40,000 feet; decelerations were made at altitudes up to 35,000 feet. The minimum true airspeed required for successful windmilling starts increased with increasing altitude. The time required for windmilling starts and accelerations increased with increasing altitude and decreasing airspeed; for decelerations, the time required increased with increasing airspeed. In general, the engine control prevented large overshoots or undershoots of engine speed during starts, accelerations, and decelerations.

Lewis Flight Propulsion Laboratory  
National Advisory Committee for Aeronautics  
Cleveland, Ohio

## APPENDIX - CALCULATIONS

## Symbols

The following symbols are used in this report:

A	cross-sectional area, sq ft
$C_T$	thermal expansion ratio, ratio of hot exhaust-nozzle area to cold exhaust-nozzle area
$c_p$	specific heat at constant pressure, Btu/(lb)(°R)
$D - D_f$	installation drag at a given propeller blade angle minus installation drag at full-feathered propeller blade angle
$F_j$	jet thrust, lb
$f_{TM}$	torquemeter calibration factor, (min/rev)(sq in./lb)(shp)
$f/a$	fuel-air ratio
$g$	acceleration due to gravity, 32.2 ft/sec <sup>2</sup>
ghp	gear horsepower
H	enthalpy, Btu/lb
J	mechanical equivalent of heat, 778 ft-lb/Btu
N	engine speed, rpm
P	total pressure, lb/sq ft absolute
p	static pressure, lb/sq ft absolute
$p_{TM}$	torquemeter pressure, lb/sq in. gage
R	gas constant, 53.4 ft-lb/(lb)(°R)
shp	shaft horsepower
T	total temperature, °R
$T_i$	indicated temperature, °R
t	static temperature, °R

$V$	velocity, ft/sec
$W_a$	air flow, lb/sec
$W_c$	compressor leakage air flow, lb/sec
$W_f$	fuel flow, lb/hr
$W_g$	gas flow, lb/sec
$W_{rb}$	rear-bearing cooling-air flow, lb/sec
$W_t$	turbine cooling-air flow, lb/sec
$\beta$	propeller blade angle, deg
$\gamma$	ratio of specific heats
$\delta_a$	ratio of absolute ambient static pressure to absolute static pressure of NACA standard atmosphere at the respective altitude
$\delta_0$	ratio of absolute ambient static pressure to absolute static pressure of NACA standard atmosphere at sea level
$\theta_a$	ratio of absolute ambient static temperature to absolute static temperature of NACA standard atmosphere at the respective altitude
$\theta_0$	ratio of absolute ambient static temperature to absolute static temperature of NACA standard atmosphere at sea level

## Subscripts:

$j$	jet
$n$	turbine nozzle
$0$	tunnel-test-section air stream
$1$	cowl or compressor inlet
$2$	compressor outlet or combustion-chamber inlet
$3$	turbine inlet or combustion-chamber outlet
$5$	tail pipe

The following performance parameters generalized to NACA standard sea-level conditions are used:

$F_j/\delta_0$	corrected jet thrust, lb
$N/\sqrt{\theta_0}$	corrected engine speed, rpm
$\text{shp}/\delta_0\sqrt{\theta_0}$	corrected shaft horsepower
$T_3/\theta_0$	corrected turbine-inlet total temperature, °R
$W_{a,1}\sqrt{\theta_0}/\delta_0$	corrected air flow, lb/sec
$W_f/\delta_0\sqrt{\theta_0}$	corrected fuel flow, lb/hr

#### Methods of Calculation

Shaft horsepower. - A hydraulic piston-type torquemeter located in the reduction gearing was used to sense shaft torque which, together with measured values of engine speed, permitted determination of shaft horsepower. The torquemeter had been calibrated by the engine manufacturer so that shaft torque could be determined from the torquemeter pressure. The relation between the torquemeter calibration factor and torquemeter pressure is shown in figure 18. The calibration factor includes the ratio of shaft torque to torque at the torquemeter station; torque at the torquemeter station varies directly with torquemeter pressure. Shaft horsepower was determined from the following relation:

$$\text{shp} = f_{\text{TM}} p_{\text{TM}}^N \quad (1)$$

where  $p_{\text{TM}}$  and  $N$  were measured and  $f_{\text{TM}}$  was determined from figure 18.

The total horsepower delivered to the reduction gear by the turbine is greater than the shaft horsepower because of power losses in the reduction gearing, bearings, and so forth. The power loss was obtained from a calibration curve (fig. 19), furnished by the manufacturer, showing the ratio of power loss to shaft horsepower as a function of shaft horsepower. This curve had been calculated from a measurement of the oil temperature rise in, and the oil flow through, the gear box.

Temperatures. - Total temperatures were obtained from indicated temperatures by use of a thermocouple recovery factor of 0.85 and the relation:

2308

$$T = \frac{T_1 \left(\frac{P}{p}\right)^\gamma}{1 + 0.85 \left[ \left(\frac{P}{p}\right)^\gamma - 1 \right]} \quad (2)$$

Turbine-inlet total temperature was determined by assuming the turbine power equal to the sum of the power absorbed by the compressor, the propeller, and the losses in the reduction gearing:

$$W_{g,3}H_3 - W_{g,5}H_5 = (W_{a,2}H_2 - W_{a,1}H_1) + \frac{550(\text{shp} + \text{ghp})}{J} \quad (3)$$

Then

$$T_3 = H_3/c_p$$

Gas flow. - Gas flow through the tail pipe may be determined from pressure and temperature measurements at station 5 by use of the relation:

$$W_{g,5} = p_5 C_T A_5 \sqrt{\frac{2\gamma_5 g}{(\gamma_5 - 1) R t_5} \left[ \left(\frac{P_5}{p_5}\right)^{\frac{\gamma_5 - 1}{\gamma_5}} - 1 \right]} \quad (4)$$

Gas flow or air flow at any station in the engine may be determined from  $W_{g,5}$  by proper consideration of various leakage and cooling air flows and engine fuel flow; turbine gas flow is

$$W_{g,3} = W_{g,5} - (W_c + W_t) \quad (5)$$

Gas flows determined by this method were of the proper order of magnitude but data scatter was considered excessive; the data scatter was attributed to difficulty in accurately measuring small impact pressures.

It was observed in reference 1 that the turbine nozzles were choked and that the effective turbine-nozzle flow area was constant for the range of engine and altitude conditions of the present investigation. The following equation was used in the final calculation of gas flow:

$$W_{g,3} = \frac{P_3 \sqrt{\gamma_3}}{\sqrt{T_3}} \sqrt{\frac{g}{R}} \frac{A_n}{\left(\frac{\gamma_3+1}{2}\right)^{\frac{\gamma_3+1}{2(\gamma_3-1)}}} \quad (6)$$

The average effective turbine-nozzle flow area  $A_n$  was calculated from this equation, using gas flows determined from equations (4) and (5), turbine-inlet temperatures based on gas flows from equation (4), and measured values of  $P_3$ . Using the average effective turbine-nozzle flow area thus determined, measured values of  $P_3$ , and turbine-inlet temperatures based on gas flows from equation (4), a new value of  $W_{g,3}$  was obtained from equation (6). Turbine-inlet temperatures based on the new values of  $W_{g,3}$  showed a negligible change when compared with the original values.

Air flow. - Air flow at station 1 may be determined from

$$W_{a,1} = W_{g,3} + W_{rb} + W_c + W_t - \frac{W_f}{3600} \quad (7)$$

This is the air flow used in the present report.

Jet thrust. - Jet thrust was determined from:

$$F_j = \frac{W_{g,5}}{g} \quad V_j = \frac{W_{g,5}}{g} \sqrt{\frac{2\gamma_5 g R}{(\gamma_5 - 1)} \frac{T_5}{\left(\frac{P_5}{P_0}\right)^{\frac{\gamma_5 - 1}{\gamma_5}}} \left[ \left(\frac{P_5}{P_0}\right)^{\frac{\gamma_5 - 1}{\gamma_5}} - 1 \right]} \quad (8)$$

where  $W_{g,5} = W_{g,3} + (W_c + W_t)$ .

Enthalpy ratios. - The enthalpy ratios were calculated in the following manner:

$$\frac{\text{Jet enthalpy drop}}{\text{Total enthalpy drop}} = \frac{H_5 - H_j}{H_3 - H_j}$$

$$\frac{\text{Shaft enthalpy drop}}{\text{Total enthalpy drop}} = \frac{\frac{550}{J} (\text{shp} + \text{ghp})}{H_3 - H_j}$$

2208

where  $H_j$  represents the enthalpy of the jet based on the static temperature of the exhaust gas when  $p_j = p_0$ . All other enthalpies are based on total temperatures.

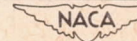
## REFERENCES

- 2308
1. Farley, John M., and Prince, William R.: Turbine Performance Characteristics of a Python Turbine-Propeller Engine Investigated in Altitude Wind Tunnel. NACA RM E50J12, 1951.
  2. Jansen, Emmert T., and McAulay, John E.: Compressor Performance Characteristics of a Python Turbine-Propeller Engine Investigated in Altitude Wind Tunnel. NACA RM E50K24, 1951.
  3. Campbell, Carl E.: Combustion-Chamber Performance Characteristics of a Python Turbine-Propeller Engine Investigated in Altitude Wind Tunnel. NACA RM E51G25, 1951.
  4. Krebs, Richard P., Himmel, Seymour C., Blivas, Darnold, and Shames, Harold: Dynamic Investigation of Turbine-Propeller Engine under Altitude Conditions. NACA RM E50J24, 1950.

TABLE I - PERFORMANCE DATA FOR

(a) Standard

Run	Altitude (ft)	Ram pressure ratio $P_1/P_0$	Cowl-inlet total pressure $P_1$ (lb/sq ft abs.)	Tunnel static pressure $P_0$ (lb/sq ft abs.)	Cowl-inlet total temperature $T_1$ (°R)	Tunnel static temperature $t_0$ (°R)	Engine speed N (rpm)	Torque-meter pressure $P_{TM}$ (lb/sq in. gage)	Shaft horsepower (shp)	Engine fuel flow $W_f$ (lb/hr)	Specific fuel consumption $W_f/shp$ (lb)/(hr) (shp)	Engine air flow (recalculated) $W_{a,1}$ (lb/sec)
1	10,000	1.028	1492	1451	485	481	8006	229	2578	2330	0.904	39.68
2		1.028	1494	1454	485	481		213	2398	2170	.905	39.71
3		1.027	1495	1455	483	479		190	2159	2055	.961	39.99
4		1.028	1488	1448	484	480		127	1419	1645	1.159	40.19
5		1.028	1497	1456	479	475		38	410	1125	2.744	41.34
6		1.026	1491	1453	489	485	7806	227	2491	2240	.899	37.30
7		1.026	1475	1437	486	482		211	2316	2080	.898	37.47
8		1.026	1489	1451	488	484		190	2085	1920	.921	37.81
9		1.026	1487	1449	484	480		121	1317	1510	1.147	38.74
10		1.027	1485	1446	490	486		51	316	1010	3.196	38.74
11		1.026	1488	1450	485	481	7606	214	2289	2060	.900	36.18
12		1.026	1486	1448	484	480		200	2139	1975	.923	36.50
13		1.026	1489	1451	488	484		180	1924	1820	.946	36.65
14		1.026	1485	1448	486	482		110	1165	1420	1.219	37.42
15		1.027	1479	1440	482	478		25	241	900	3.734	38.42
16		1.026	1489	1451	488	484	7406	190	1978	1880	.950	34.52
17		1.026	1481	1444	487	483		178	1852	1810	.977	34.62
18		1.025	1494	1457	490	487		158	1641	1660	1.012	34.97
19		1.026	1486	1449	493	489		101.5	1045	1310	1.254	35.41
20		1.025	1487	1451	487	484		30	289	910	3.149	36.71
21		1.025	1489	1453	490	487	7205	164	1658	1675	1.010	33.22
22		1.025	1489	1452	490	487		151	1524	1600	1.050	33.73
23		1.026	1485	1448	486	482		130.5	1314	1470	1.119	34.14
24		1.025	1489	1452	487	484		89	889	1220	1.372	34.53
25		1.025	1475	1439	491	488		32	302	875	2.897	34.76
26		1.027	1486	1447	490	486	6805	130	1235	1400	1.134	30.41
27		1.026	1493	1455	491	487		121	1148	1360	1.185	31.05
28		1.026	1490	1452	490	486		102	965	1220	1.264	31.10
29		1.027	1493	1454	489	485		73	686	1050	1.531	31.91
30		1.026	1487	1449	487	483		34	307	810	2.638	32.22
31	20,000	1.029	993	965	456	452	8006	179	2013	1810	0.899	27.10
32		1.028	1000	973	456	452		167.5	1883	1680	.892	27.50
33		1.028	1002	975	455	451		151.5	1699	1550	.912	27.74
34		1.027	994	968	455	452		108	1204	1265	1.051	27.67
35		1.027	998	972	454	451		34	361	840	2.327	27.97
36		1.028	996	969	456	452	7806	172.5	1891	1675	.886	26.59
37		1.028	1003	976	457	453		159	1740	1555	.894	26.90
38		1.027	1002	976	457	454		141.5	1445	1420	.919	27.04
39		1.028	998	971	453	449		139.5	1522	1385	.910	27.36
40		1.027	995	969	454	451		94.5	1024	1125	1.039	27.46
41		1.026	1000	975	452	449		29	292	750	2.568	27.78
42		1.027	996	970	456	453	7606	159.5	1701	1515	.891	25.82
43		1.027	1005	979	461	458		147	1565	1430	.914	25.85
44		1.027	995	969	456	453		147	1565	1420	.907	26.02
45		1.027	1003	977	457	454		131	1392	1315	.945	26.35
46		1.027	992	966	455	452		90	949	1065	1.122	26.45
47		1.027	994	968	455	452		30	296	717	2.422	27.10
48		1.027	997	971	454	451	7406	150	1556	1415	.909	24.64
49		1.026	990	965	452	449		139.5	1444	1345	.931	24.73
50		1.027	997	971	450	447		126	1303	1250	.959	25.32
51		1.027	992	966	454	451		86	883	1010	1.144	25.28
52		1.025	997	973	452	449		28.5	272	680	2.500	26.27
53		1.027	994	968	454	451	7205	133.5	1345	1285	.955	23.54
54		1.027	990	964	458	455		125.5	1262	1250	.990	23.19
55		1.026	988	963	458	455		124	1246	1225	.983	23.22
56		1.027	997	971	455	452		113	1134	1150	1.014	23.93
57		1.026	997	972	456	453		77.5	773	925	1.197	24.33
58		1.025	989	965	454	451		27	249	645	2.590	24.79
59		1.028	1000	973	455	451	6805	86.5	816	940	1.152	22.11
60		1.028	994	964	454	450		76.5	720	875	1.215	22.23
61	1.027	990	964	455	452		62	582	800	1.375	22.33	
62	1.026	995	970	454	451		29	255	595	2.333	23.15	
63	30,000	1.027	643	626	437	434	8006	121.5	1376	1265	0.919	18.02
64		1.027	643	626	438	435		115	1303	1170	.898	18.01
65		1.027	645	628	437	434		103.5	1173	1085	.925	18.08
66		1.027	644	627	436	433		77	869	885	1.018	18.33
67		1.026	637	621	436	433		26	266	575	2.162	18.22
68		1.026	643	627	438	435	7806	116.5	1287	1160	.901	17.46
69		1.027	643	626	438	435		110	1215	1095	.901	17.83
70		1.027	642	625	437	434		97.5	1077	983	.913	17.99
71		1.027	640	623	437	434		70.5	773	815	1.054	18.12
72		1.027	636	619	436	433		32.5	336	570	1.696	17.97



2308

PYTHON TURBINE-PROPELLER ENGINE

tail pipe

Engine air flow (initial) $W_{a,1}$ (lb/sec)	Engine fuel-air ratio $f/a$	Turbine-inlet total temperature $T_3$ (°R)	Exhaust-nozzle-inlet total temperature $T_5$ (°R)	Jet thrust $F_j$ (lb)	Corrected engine speed $N/\sqrt{\theta_0}$ (rpm)	Corrected shaft horsepower $shp/\theta_0\sqrt{\theta_0}$	Corrected fuel flow $W_f/\theta_0\sqrt{\theta_0}$ (lb/hr)	Corrected air flow $W_{a,1}\sqrt{\theta_0}/\theta_0$ (lb/sec)	Corrected turbine-inlet temperature $T_3/\theta_0$ (°R)	Corrected Jet thrust $F_j/\theta_0$ (lb)	Approximate engine time (hr)	Run
40.04	0.0163	1957	1452	955	8318	3906	3530	55.68	2112	1392	3.2	1
40.20	.0152	1884	1389	914	8318	3626	3281	55.61	2033	1330		2
40.07	.0145	1830	1352	892	8334	3238	3111	55.86	1983	1298		3
40.84	.0114	1641	1206	806	8326	2155	2499	56.46	1774	1178		4
41.25	.0076	1372	1012	693	8366	622	1708	57.48	1499	1007		5
37.75	.0167	1986	1486	867	8071	3751	3373	52.52	2125	1263	13.1	6
37.72	.0154	1894	1410	833	8103	3541	3180	53.17	2039	1227		7
37.94	.0141	1820	1352	801	8079	3146	2897	53.26	1952	1167		8
38.74	.0108	1598	1186	720	8118	1999	2292	54.39	1728	1052		9
37.89	.0072	1362	1014	603	8064	477	1526	54.87	1455	881		10
36.63	.0158	1907	1435	790	7903	3470	3123	50.81	2058	1153	13.9	11
36.85	.0150	1853	1391	781	7910	3249	3000	51.28	2003	1141		12
36.21	.0138	1790	1341	741	7872	2903	2746	51.63	1919	1081		13
37.27	.0105	1555	1160	658	7895	1767	2154	52.67	1674	961		14
37.42	.0065	1291	960	569	7925	369	1378	54.16	1402	836		15
34.33	.0151	1864	1416	704	7665	2985	2837	48.63	1999	1026	15.0	16
34.32	.0145	1813	1374	691	7680	2813	2749	48.91	1948	1012		17
35.32	.0132	1737	1313	664	7643	2458	2487	49.20	1851	963	14.5	18
36.40	.0103	1543	1166	606	7628	1572	1970	50.19	1638	885		19
36.04	.0069	1298	978	522	7665	436	1373	51.71	1392	762		20
32.71	.0140	1775	1358	612	7436	2492	2518	46.87	1892	891	14.8	21
33.19	.0132	1727	1322	613	7436	2292	2406	47.62	1840	893		22
33.80	.0120	1641	1249	595	7479	1993	2230	48.05	1767	869		23
35.50	.0098	1492	1134	557	7457	1341	1840	48.61	1600	811		24
33.83	.0070	1303	989	478	7436	458	1327	49.51	1386	703		25
30.88	.0128	1658	1292	501	7030	1865	2114	43.04	1771	732	16.7	26
31.55	.0122	1622	1264	506	7023	1723	2041	43.75	1729	736	18.5	27
32.96	.0109	1535	1192	491	7030	1452	1836	43.87	1639	716	16.8	28
31.44	.0091	1427	1106	451	7036	1032	1579	44.90	1527	656	18.7	29
32.99	.0070	1282	990	423	7057	465	1226	45.36	1378	618	16.7	30
27.31	.0186	2059	1539	707	8574	4729	4252	55.49	2364	1550	19.6	31
27.75	.0170	1973	1461	686	8574	4386	3913	55.85	2265	1492		32
27.91	.0155	1885	1389	660	8590	3955	3608	56.10	2169	1432		33
27.76	.0127	1703	1252	588	8574	2819	2961	56.48	1955	1285		34
29.76	.0083	1416	1041	513	8590	843	1962	56.75	1629	1117		35
26.89	.0175	1989	1479	654	8360	4423	3918	54.22	2284	1427	20.2	36
27.36	.0161	1908	1410	633	8360	4040	3611	54.45	2186	1372		37
27.23	.0146	1820	1345	607	8345	3581	3292	54.84	2080	1360		38
27.60	.0141	1778	1309	603	8391	3565	3244	55.46	2055	1314		39
27.58	.0114	1597	1175	541	8376	2399	2636	55.89	1838	1181		40
29.29	.0075	1347	989	468	8391	681	1750	56.08	1557	1016		41
26.21	.0163	1913	1427	595	8146	3974	3539	52.58	2192	1299	20.9	42
26.21	.0154	1856	1384	573	8093	3598	3288	52.50	2103	1237		43
26.08	.0152	1833	1362	571	8146	3661	3321	53.06	2100	1248		44
26.35	.0139	1758	1305	554	8131	3222	3044	53.39	2010	1200		45
25.97	.0112	1580	1172	495	8146	2225	2497	54.09	1814	1083		46
28.00	.0074	1324	979	442	8146	693	1678	55.31	1520	966		47
24.83	.0160	1864	1405	536	7947	3638	3308	50.04	2145	1168	21.5	48
24.78	.0151	1814	1364	523	7961	3404	3170	50.45	2097	1147		49
25.21	.0137	1720	1288	512	7976	3058	2934	51.23	1997	1115		50
25.18	.0111	1562	1167	455	7947	2075	2374	51.60	1797	996		51
26.41	.0072	1286	961	393	7961	636	1590	53.15	1487	855		52
23.72	.0152	1811	1377	479	7731	3155	3015	47.96	2084	1048	22.0	53
23.39	.0150	1790	1364	462	7695	2958	2930	47.66	2042	1015		54
23.36	.0147	1779	1356	459	7695	2923	2874	47.77	2029	1008		55
24.03	.0134	1711	1296	462	7717	2647	2684	48.69	1965	1006		56
23.94	.0106	1518	1145	408	7717	1803	2157	49.46	1739	889		57
24.60	.0072	1286	973	359	7731	586	1518	50.67	1480	786		58
21.79	.0118	1568	1208	360	7302	1905	2194	44.82	1804	783	22.5	59
22.35	.0109	1507	1159	351	7309	1692	2056	45.29	1738	768		60
23.43	.0100	1431	1100	351	7288	1368	1881	45.77	1643	771		61
22.49	.0071	1251	962	311	7302	597	1392	47.06	1440	678		62
17.99	.0195	2078	1545	481	8759	5088	4678	55.67	2485	1624	26.2	63
17.90	.0180	2005	1486	458	8743	4809	4318	55.75	2392	1547		64
18.09	.0167	1925	1420	441	8759	4324	3999	55.68	2302	1487		65
18.34	.0134	1731	1262	401	8767	3212	3271	56.50	2075	1355		66
18.68	.0088	1435	1052	333	8767	992	2145	56.69	1720	1134		67
17.33	.0185	2025	1505	436	8524	4744	4276	53.96	2416	1473	26.7	68
17.83	.0171	1940	1437	436	8524	4485	4042	55.19	2314	1474		69
17.83	.0152	1825	1340	412	8540	3989	3641	55.68	2182	1396		70
18.08	.0125	1656	1211	377	8540	2872	3028	56.25	1980	1281		71
17.78	.0088	1428	1044	313	8548	1258	2134	56.09	1712	1069		72



2308

TABLE I - PERFORMANCE DATA FOR PYTHON

(a) Standard tail

Run	Altitude (ft)	Ram pressure ratio $P_1/P_0$	Cowl-inlet total pressure $P_1$ (lb/sq ft abs.)	Tunnel static pressure $P_0$ (lb/sq ft abs.)	Cowl-inlet total temperature $T_1$ (°R)	Tunnel static temperature $T_0$ (°R)	Engine speed N (rpm)	Torque-meter pressure $P_{TM}$ (lb/sq in. gage)	Shaft horse-power (shp)	Engine fuel flow $W_f$ (lb/hr)	Specific fuel consumption $W_f/shp$ (lb)/(hr) (shp)	Engine air flow (recalculated) $W_{a,1}$ (lb/sec)
73	30,000	1.027	641	624	439	436	7606	109	1173	1050	0.895	17.22
74		1.024	645	630	438	435		103.5	1114	1020	.916	17.46
75		1.025	644	628	444	441		94.5	1016	935	.920	17.20
76		1.027	639	622	440	437	69.5	742	774	1.043	17.40	
77		1.026	634	618	437	434	28	276	540	1.957	17.80	
78		1.025	644	628	437	434	7406	100.3	1052	960	.913	16.52
79		1.027	643	626	437	434		95	995	910	.915	16.46
80		1.026	641	625	436	433		85	889	845	.951	16.92
81		1.027	643	626	438	435	64	664	720	1.084	17.11	
82		1.027	640	623	437	434	31	302	525	1.738	17.39	
83	1.027	643	626	437	434	7205	85.5	870	840	.966	16.16	
84	1.026	642	626	435	432		81	824	805	.977	16.49	
85	1.027	642	625	435	432		75	761	765	1.005	16.53	
86	1.027	640	623	436	433	57	573	665	1.161	16.68		
87	1.026	639	623	436	433	30.5	288	500	1.736	16.72		
88	1.027	640	623	441	438	6805	61	580	670	1.155	14.83	
89	1.026	640	624	436	433		58	551	635	1.152	15.04	
90	1.027	647	630	440	437		51	481	595	1.237	15.19	
91	1.027	641	624	438	435	39.5	366	525	1.434	15.35		
92	1.025	645	629	439	436	8006	29.5	262	472	1.802	15.58	
93	1.025	406	396	441	438		71	799	755	.945	11.10	
94	1.025	406	396	443	440		68	764	720	.942	11.04	
95	1.028	403	392	441	438	60	671	660	.984	11.17		
96	1.026	400	390	439	436	46	507	560	1.105	11.07		
97	1.026	399	389	446	443	23	232	410	1.767	11.17		
98	1.025	407	397	434	431	7806	68	745	700	.940	10.93	
99	1.025	404	394	436	433		64	699	670	.959	10.88	
100	1.020	399	391	437	435		58	632	630	.997	10.98	
101	1.023	404	395	438	435	24	237	400	1.688	11.13		
102	1.028	402	391	438	435	7606	59	626	620	.990	10.48	
103	1.030	406	394	438	434		56	593	590	.995	10.59	
104	1.028	402	391	442	439		49	515	550	1.068	10.58	
105	1.025	408	398	439	436	41	426	490	1.150	10.78		
106	1.026	400	390	439	436	26	253	400	1.581	10.67		
107	1.028	405	394	442	439	7406	48	491	520	1.059	10.13	
108	1.028	404	393	442	439		41	415	470	1.133	10.15	
109	1.030	406	394	444	440		28	268	390	1.455	10.41	

(b) Performance deterioration

1	10,000	1.027	1505	1466	518	514	8006	230	2589	2320	0.896	37.46
2		1.027	1492	1453	518	514		199.5	2246	2100	.935	37.48
3		1.027	1497	1458	520	516		163	1831	1850	1.010	37.87
4		1.026	1498	1460	522	518	119	1328	1560	1.175	37.74	
5		1.027	1498	1458	517	513	223	2510	2320	.924	36.63	
6		1.026	1485	1447	514	510	195	2195	2100	.957	37.11	
7		1.027	1494	1455	525	521	163	1831	1870	1.021	37.22	
8		1.026	1488	1450	520	516	123	1374	1580	1.150	37.67	
9		1.026	1497	1459	510	506	54	595	1195	2.008	38.74	
10		1.025	1503	1466	523	519	8006	221	2498	2290	.920	35.98
11	1.027	1496	1457	517	513	188		2116	2020	.955	36.50	
12	1.026	1490	1452	520	516	122		1363	1600	1.174	36.94	
13	1.026	1496	1458	517	513	33	349	1100	3.152	37.81		
14	1.027	1491	1452	518	514	223.5	2516	2300	.918	36.29		
15	1.028	1489	1449	516	512	180	2025	2000	1.167	36.75		
16	1.026	1482	1444	519	515	122	1363	1590	2.072	37.51		
17	1.026	1487	1449	518	514	50.5	555	1150	.937	35.46		
18	1.026	1485	1448	519	515	211	2391	2240	1.170	35.38		
19	1.026	1488	1450	521	517	180	2039	2010	2.085	36.68		
20	1.026	1494	1456	520	516	121.5	1376	1610	.900	28.02		
21	1.025	1489	1452	519	515	50	554	1155	.939	28.01		
22	20,000	1.028	1002	975	451	447	171	1922	1730	.899	28.24	
23		1.027	997	971	449	446	159.5	1790	1610	.948	28.19	
24		1.028	996	969	450	446	139	1556	1475	1.104	28.43	
25	1.027	995	969	450	447	103	1146	1265	1.887	28.35		
26	1.028	995	968	451	447	43	469	885	.914	18.30		
27	30,000	1.029	643	625	441	437	120.5	1345	1230	.914	18.02	
28		1.027	648	631	442	439	111	1237	1130	.914	18.30	
29		1.027	641	624	441	438	99.5	1107	1045	.944	18.17	
30	1.029	641	623	440	436	74.5	824	870	1.056	18.24		
31	1.027	646	629	443	440	29.5	306	610	1.993	18.35		
32	40,000	1.026	400	390	442	439	69.5	768	745	.970	10.94	
33		1.026	397	387	438	435	67.5	746	725	.972	11.00	
34		1.028	397	386	439	436	61.5	678	665	.981	10.99	
35		1.028	398	387	441	438	48	526	570	1.084	11.03	
36	1.028	407	396	440	437	29	300	450	1.500	11.30		

TURBINE-PROPELLER ENGINE - Continued

pipe - Concluded

Engine air flow (initial) $W_{a,1}$ (lb/sec)	Engine fuel-air ratio f/a	Turbine-inlet total temperature $T_3$ ( $^{\circ}R$ )	Exhaust-nozzle-inlet total temperature $T_5$ ( $^{\circ}R$ )	Jet thrust $F_j$ (lb)	Corrected engine speed $N/\sqrt{\theta_0}$ (rpm)	Corrected shaft horsepower $shp/\theta_0\sqrt{\theta_0}$	Corrected fuel flow $W_f/\theta_0\sqrt{\theta_0}$ (lb/hr)	Corrected air flow $W_{a,1}/\sqrt{\theta_0/\theta_0}$ (lb/sec)	Corrected turbine-inlet temperature $T_3/\theta_0$ ( $^{\circ}R$ )	Corrected jet thrust $F_j/\theta_0$ (lb)	Approximate engine time (hr)	Run
17.16	0.0169	1927	1434	405	8298	4340	3885	53.52	2294	1375	27.1	73
17.34	.0162	1886	1399	400	8306	4086	3741	53.71	2250	1344		74
17.25	.0151	1810	1340	376	8253	3713	3417	53.41	2130	1268		75
17.40	.0124	1631	1203	347	8291	2751	2870	54.31	1937	1182		76
17.95	.0084	1366	1006	299	8321	1034	2023	55.71	1634	1024		77
16.67	.0161	1864	1391	365	8102	3878	3539	50.87	2229	1230	27.6	78
16.58	.0154	1814	1355	353	8102	3680	3365	50.85	2169	1191		79
16.96	.0139	1715	1272	346	8110	3296	3133	52.32	2056	1171		80
16.97	.0117	1567	1167	319	8087	2451	2658	52.96	1869	1077		81
17.61	.0084	1373	1016	288	8102	1122	1950	53.98	1642	976		82
16.03	.0144	1737	1306	324	7882	3217	3106	49.93	2077	1094	28.0	83
16.35	.0136	1696	1269	324	7897	3052	2982	50.85	2037	1095		84
16.31	.0129	1635	1221	316	7897	2824	2839	51.07	1964	1069		85
16.13	.0111	1521	1136	292	7889	2131	2473	51.73	1823	991		86
17.03	.0083	1350	1011	268	7889	1071	1859	51.85	1818	908	28.5	87
14.50	.0125	1581	1207	248	7411	2145	2478	46.25	1873	842		88
14.69	.0117	1538	1173	246	7451	2046	2358	46.58	1843	834		89
14.81	.0109	1492	1138	239	7417	1761	2178	46.81	1772	804		90
15.09	.0095	1400	1068	236	7431	1355	1944	47.67	1670	799		91
16.21	.0084	1332	1019	235	7424	962	1732	48.04	1586	790		92
11.28	.0189	2050	1517	283	8719	4649	4393	54.46	2429	1510	30.8	93
11.16	.0181	2015	1498	272	8695	4433	4177	54.32	2377	1455	31.7	94
11.10	.0164	1908	1410	263	8719	3944	3879	55.37	2261	1420		95
11.11	.0141	1754	1290	239	8735	3001	3315	55.06	2088	1297		96
10.90	.0102	1519	1121	203	8662	1366	2413	56.16	1780	1105		97
10.90	.0178	1976	1470	261	8563	4356	4093	53.11	2379	1390	30.4	98
10.79	.0171	1924	1425	251	8548	4111	3940	53.37	2306	1350		99
10.85	.0159	1850	1365	245	8524	3735	3723	54.42	2207	1325		100
10.79	.0100	1512	1120	198	8524	1366	2340	54.60	1804	1060		101
10.51	.0164	1889	1413	235	8306	3700	3664	51.94	2254	1273	32.0	102
10.81	.0155	1835	1361	232	8321	3484	3467	51.99	2194	1246		103
10.53	.0144	1764	1308	221	8268	3030	3236	52.68	2085	1195		104
10.89	.0126	1670	1243	215	8298	2471	2842	52.54	1988	1144		105
10.35	.0104	1518	1131	187	8298	1498	2368	53.07	1807	1012		106
10.14	.0143	1742	1310	200	8050	2866	3036	50.05	2059	1076	32.8	107
10.39	.0129	1667	1215	196	8050	2429	2750	50.27	1971	1055		108
9.99	.0104	1497	1122	172	8043	1563	2275	51.48	1766	924		109

data, standard tail pipe

37.60	0.0172	2052	1531	893	8046	3754	3364	53.79	2072	1288	2.0	1
37.88	.0156	1936	1439	846	8046	3286	3072	54.30	1955	1232		2
38.01	.0136	1807	1344	788	8030	2664	2692	54.79	1818	1144		3
37.52	.0115	1684	1252	721	8014	1926	2262	54.63	1687	1044		4
36.91	.0176	2068	1552	874	8054	3665	3387	52.83	2092	1268	6.3	5
37.49	.0157	1938	1448	837	8078	3238	3098	53.77	1972	1223		6
37.16	.0140	1845	1374	784	7991	2657	2713	54.22	1838	1159		7
37.54	.0117	1695	1258	726	8030	2010	2312	54.80	1705	1059		8
38.92	.0086	1482	1096	658	8110	874	1755	55.45	1520	955		9
36.23	.0177	2082	1570	847	8006	3590	3304	51.92	2082	1222	16.1	10
36.82	.0154	1936	1453	801	8054	3091	2951	52.68	1959	1163		11
37.05	.0120	1714	1284	714	8030	1991	2338	53.66	1724	1041		12
37.49	.0081	1448	1084	608	8054	510	1606	54.54	1465	882		13
36.71	.0176	2075	1562	862	8046	3683	3367	52.61	2095	1256	18.1	14
37.16	.0151	1918	1437	807	8062	2977	2940	53.28	1944	1179		15
37.14	.0120	1722	1287	717	8038	2005	2339	53.68	1735	1050		16
37.24	.0085	1494	1112	617	8046	814	1687	54.49	1508	901		17
35.43			1563		8038	3508	3286				24.7	18
36.05	.0157	1962	1476	772	8022	2981	2939	51.63	1970	1127		19
36.59	.0123	1738	1305	699	8030	2005	2346	52.70	1748	1015		20
36.79	.0087	1503	1127	601	8038	811	1690	53.23	1515	875		21
28.41	.0172	1973	1457	715	8622	4492	4043	56.46	2291	1551	4.5	22
28.57	.0160	1906	1404	687	8638	4208	3785	56.57	2218	1497		23
28.54	.0145	1794	1314	651	8638	3667	3477	57.16	2088	1421		24
27.93	.0125	1667	1221	591	8622	2695	2975	57.17	1935	1291		25
28.12	.0086	1423	1036	516	8622	1104	2083	57.70	1652	1127		26
18.15	.0190	2042	1510	473	8727	4964	4540	55.98	2425	1803	9.3	27
18.27	.0172	1958	1444	459	8703	4509	4119	56.45	2315	1539		28
18.35	.0160	1883	1382	441	8719	4088	3859	56.58	2251	1496		29
18.27	.0133	1717	1256	403	8735	3053	3223	56.78	2044	1368		30
18.38	.0092	1460	1071	337	8695	1118	2228	56.84	1722	1135		31
10.94	.0189	2044	1515	276	8703	4530	4394	54.61	2416	1497	10.1	32
11.03	.0183	2006	1487	278	8743	4454	4329	55.08	2393	1522		33
10.92	.0168	1925	1419	262	8735	4055	3977	55.22	2291	1455		34
10.65	.0144	1780	1310	245	8719	3132	3394	55.38	2109	1338		35
11.10	.0111	1583	1166	218	8727	1747	2621	55.39	1880	1166		36



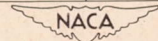
2308

TABLE I - PERFORMANCE DATA FOR PYTHON  
(c) 24-inch-diameter tail pipe;

Run	Altitude (ft)	Ram pressure ratio $P_1/P_0$	Cowl-inlet total pressure $P_1$ (lb/sq ft abs.)	Tunnel static pressure $P_0$ (lb/sq ft abs.)	Cowl-inlet total temperature $T_1$ (°R)	Tunnel static temperature $T_0$ (°R)	Engine speed N (rpm)	Torque-meter pressure $P_{TM}$ (lb/sq in. gage)	Shaft horsepower (shp)	Engine fuel flow $W_f$ (lb/hr)	Specific fuel consumption $W_f/shp$ (lb)/(hr) (shp)	Engine air flow (recalculated $W_{a,1}$ (lb/sec)
1	10,000	1.026	1487	1450	492	488	8006	183.5	2079	2180	1.049	37.40
2		1.025	1492	1455	488	485		159	1801	1990	1.105	38.10
3		1.026	1487	1450	483	479		80.5	909	1460	1.606	39.11
4		1.026	1488	1451	488	485	7806	184	2033	2120	1.043	36.36
5		1.025	1487	1451	490	487		171	1889	2010	1.064	36.38
6		1.026	1485	1447	483	479		146.5	1618	1820	1.125	37.50
7		1.026	1487	1450	487	483		143.5	1585	1820	1.148	37.11
8		1.026	1485	1448	486	482		77	847	1390	1.641	37.82
9		1.025	1486	1450	489	485	7606	160.5	1727	1890	1.094	34.96
10		1.026	1486	1449	486	482		149	1603	1790	1.117	34.25
11		1.026	1486	1449	486	482		128	1377	1655	1.202	35.81
12		1.026	1485	1448	487	483		70	748	1280	1.711	36.20
13	30,000	1.027	643	626	444	441	8006	106	1201	1200	.999	17.78
14		1.025	644	628	444	441		98	1110	1130	1.018	17.78
15		1.026	641	625	441	438		80	903	985	1.091	17.80
16		1.025	648	632	445	442		80	903	985	1.091	18.05
17		1.026	642	626	445	442		47	519	765	1.474	18.00
18		1.025	646	630	445	442		33	351	685	1.952	18.11
19		1.025	645	629	441	438	7806	99	1094	1090	.996	17.31
20		1.025	644	628	445	442		93	1026	1050	1.023	17.35
21		1.027	641	624	438	435		89	982	1000	1.018	17.56
22		1.025	648	632	443	440		77	847	925	1.092	17.78
23		1.026	642	626	442	439		76	835	910	1.090	17.47
24		1.026	643	627	439	436		45	483	710	1.470	17.92
25		1.025	645	629	444	441		37	390	665	1.705	17.77
26		1.025	645	629	443	440	7606	94	1011	1025	1.014	16.57
27		1.025	646	630	442	439		87	935	970	1.037	16.95
28		1.025	644	628	442	439		85	913	955	1.046	16.86
29		1.024	647	632	439	436		75	803	880	1.096	17.20
30		1.027	646	629	444	441		70	748	850	1.136	16.98
31	1.027	646	629	445	442		48	504	690	1.369	17.23	
32	1.025	648	632	441	438		36	369	680	1.843	17.52	
33	40,000	1.028	403	392	438	435	8006	67	753	785	1.042	11.08
34		1.026	401	391	437	434		61	683	720	1.054	11.02
35		1.031	401	389	438	434		50	554	605	1.092	11.04
36		1.028	402	391	436	433		38	412	520	1.262	11.14
37		1.028	404	393	440	437	7606	58	615	650	1.057	10.38
38		1.026	402	392	439	436		53	560	610	1.089	10.31
39		1.028	406	395	436	433		46	482	560	1.162	10.56
40		1.030	408	396	436	432		42	437	530	1.213	10.74

(d) 24-inch-diameter tail pipe;

1	10,000	1.027	1495	1456	493	489	8006	227	2572	2410	0.937	36.90	
2		1.027	1493	1454	499	495		200	2266	2255	.995	36.45	
3		1.026	1490	1452	487	483		200	2266	2190	.968	37.72	
4		1.026	1488	1450	487	483	7806	205	2265	2190	.967	36.04	
5		1.025	1488	1451	486	483		179	1977	1980	1.002	36.57	
6		1.026	1490	1452	489	485		150	1657	1780	1.074	36.77	
7		1.026	1481	1443	484	480		80	881	1350	1.532	37.76	
8		1.026	1489	1451	489	485	7606	178	1916	1940	1.013	34.56	
9		1.025	1490	1453	488	485		161	1733	1820	1.050	34.87	
10		1.026	1483	1446	487	483		137	1475	1650	1.119	35.23	
11		1.026	1487	1449	485	481		80	858	1300	1.515	36.25	
12		30,000	1.027	641	624	441	438	8006	100	1133	1225	1.081	17.79
13	1.025		647	631	444	441		92	1042	1050	1.008	17.91	
14	1.027		644	627	445	442		88	995	1030	1.035	17.85	
15	1.027		646	629	444	441		74	833	890	1.068	18.00	
16	1.025		644	628	444	441		44	484	695	1.436	18.20	
17	1.027		644	627	444	441	7806	103.5	1144	1090	.953	17.24	
18	1.027		640	623	443	440		94	1037	1000	.964	17.38	
19	1.026		641	625	442	439		80	881	900	1.022	17.52	
20	1.026		639	623	443	440		47	506	700	1.383	17.71	
21	30,000		1.026	640	624	442	439	7606	98	1054	1015	.963	16.67
22			1.029	645	627	441	437		92	989	980	.991	16.97
23			1.027	645	628	442	439		77.5	830	865	1.042	17.12
24		1.026	643	627	441	438		45	471	630	1.338	17.37	
25		40,000	1.028	402	391	442	439	8006	68	764	750	.982	10.94
26			1.025	405	395	443	440		58.5	654	665	1.017	11.03
27			1.025	403	393	443	440		53	589	630	1.070	11.06
28			1.028	405	394	442	439		45	496	575	1.159	11.16
29			1.025	408	398	438	435	7606	63	671	660	.984	10.63
30			1.023	408	399	440	437		56	593	600	1.012	10.55
31			1.026	400	390	444	441		44.5	465	490	1.054	10.52
32			1.025	404	394	440	437		44	459	500	1.089	10.61
33	1.026		399	389	439	436		26	253	360	1.423	10.65	



2308

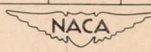
TURBINE-PROPELLER ENGINE - Continued

20-inch-diameter exhaust nozzle

Engine air flow (initial) $W_{a,1}$ (lb/sec)	Engine fuel-air ratio $f/a$	Turbine-inlet total temperature $T_3$ (°R)	Exhaust-nozzle-inlet total temperature $T_5$ (°R)	Jet thrust $F_j$ (lb)	Corrected engine speed $N/\sqrt{\theta_0}$ (rpm)	Corrected shaft horsepower $shp/\theta_0\sqrt{\theta_0}$	Corrected fuel flow $W_f/\theta_0\sqrt{\theta_0}$ (lb/hr)	Corrected air flow $W_{a,1}\sqrt{\theta_0}/\theta_0$ (lb/sec)	Corrected turbine-inlet temperature $T_3/\theta_0$ (°R)	Corrected jet thrust $F_j/\theta_0$ (lb)	Approximate engine time (hr)	Run
38.13	0.0162	1959	1478	1108	8262	3131	3283	52.87	2084	1617	46.5	1
39.39	.0145	1845	1389	1080	8278	2707	2991	53.58	1975	1571		2
40.91	.0104	1570	1173	953	8334	1381	2218	54.81	1701	1390		3
36.61	.0162	1933	1464	1041	8071	3066	3197	51.27	2069	1518	46.8	4
37.00	.0153	1886	1429	1016	8056	2843	3025	51.40	2010	1482		5
39.11	.0135	1761	1329	1006	8126	2463	2770	52.67	1908	1470		6
38.85	.0136	1774	1341	995	8095	2398	2754	52.21	1906	1452		7
39.07	.0102	1541	1157	879	8103	1285	2109	53.23	1659	1284		8
35.97	.0150	1847	1409	932	7857	2603	2848	49.38	1972	1360	47.2	9
36.69	.0145	1789	1360	889	7895	2429	2712	48.17	1926	1297		10
37.31	.0123	1702	1292	892	7895	2086	2507	50.37	1833	1303		11
36.29	.0098	1506	1139	787	7887	1133	1939	51.00	1618	1150		12
17.98	.0187	2055	1545	598	8687	4404	4400	55.39	2419	2022	60.0	13
17.89	.0177	1985	1492	576	8687	4057	4130	55.21	2336	1941		14
17.59	.0154	1857	1383	540	8719	3329	3632	55.35	2200	1829		15
18.30	.0152	1844	1379	546	8679	3277	3575	55.75	2165	1829	55.9	16
18.35	.0118	1632	1220	486	8679	1902	2803	56.13	1916	1644	60.0	17
19.02	.0105	1549	1160	465	8679	1278	2494	56.12	1819	1562	55.9	18
17.35	.0175	1968	1482	547	8501	4007	3993	53.47	2332	1841	60.3	19
17.51	.0168	1932	1449	539	8462	3747	3835	53.92	2269	1817	56.1	20
17.49	.0158	1867	1397	531	8524	3636	3703	54.53	2227	1802	60.4	21
17.90	.0144	1781	1333	511	8477	3080	3363	54.81	2101	1711	56.2	22
17.24	.0145	1792	1338	500	8485	3068	3343	54.32	2118	1689	60.4	23
18.47	.0110	1562	1166	460	8516	1778	2614	55.44	1859	1554	60.3	24
19.04	.0104	1530	1149	447	8470	1424	2427	55.10	1801	1504	56.1	25
16.58	.0172	1940	1469	496	8260	3693	3744	51.33	2288	1670	60.5	26
17.47	.0159	1862	1404	499	8268	3414	3541	52.38	2201	1676	56.4	27
16.45	.0157	1856	1399	486	8268	3343	3497	52.26	2194	1637	60.7	28
17.05	.0142	1757	1319	473	8298	2933	3215	52.78	2091	1584	56.5	29
16.56	.0139	1735	1307	460	8253	2730	3103	52.65	2042	1547	60.7	30
17.47	.0111	1573	1178	430	8245	1838	2516	53.47	1847	1446	60.6	31
17.91	.0108	1501	1133	423	8283	1345	2479	53.86	1779	1416	56.4	32
11.28	.0197	2098	1587	381	8743	4439	4628	54.77	2503	2059	61.3	33
11.16	.0181	2025	1522	365	8759	4044	4263	54.52	2422	1973		34
11.08	.0152	1857	1381	335	8759	3297	3600	54.90	2221	1823		35
10.61	.0130	1723	1276	308	8767	2442	3082	55.06	2065	1666		36
10.38	.0174	1967	1493	316	8291	3609	3815	51.27	2336	1699	62.2	37
10.36	.0164	1918	1453	305	8298	3298	3592	51.01	2283	1644		38
10.35	.0147	1810	1366	296	8329	2827	3285	51.66	2169	1585		39
10.58	.0137	1733	1303	291	8336	2559	3104	52.36	2082	1556		40

22-inch-diameter exhaust nozzle

37.36	0.0181	2080	1570	982	8246	3850	3608	52.05	2208	1427	66.2	1
36.81	.0172	2017	1529	932	8198	3376	3360	51.79	2115	1356	67.4	2
37.85	.0161	1941	1456	947	8302	3424	3309	53.00	2086	1380	68.4	3
36.55	.0169	1969	1488	893	8095	3427	3313	50.71	2116	1303	68.6	4
36.58	.0150	1864	1399	851	8095	2989	2994	51.42	2003	1241		5
38.06	.0134	1758	1321	821	8071	2497	2682	51.81	1881	1196		6
39.37	.0099	1521	1136	736	8118	1344	2059	53.23	1645	1079		7
34.68	.0156	1888	1433	784	7865	2889	2926	48.73	2020	1143	68.9	8
35.39	.0145	1808	1374	764	7865	2610	2741	49.10	1935	1112		9
36.83	.0130	1724	1303	750	7887	2238	2503	49.70	1853	1098		10
37.71	.0100	1513	1139	676	7903	1302	1972	50.94	1632	987		11
18.05	.0191	2057	1557	520	8719	4184	4524	55.40	2437	1765	63.1	12
18.14	.0163	1915	1427	479	8687	3791	3820	55.35	2254	1607		13
17.88	.0160	1887	1406	471	8679	3641	3759	55.58	2216	1590		14
17.98	.0137	1756	1299	439	8687	3040	3249	55.81	2067	1476		15
18.64	.0106	1557	1149	398	8687	1769	2540	56.51	1832	1339		16
17.67	.0176	1975	1485	471	8470	4189	3992	53.63	2324	1591	63.5	17
17.70	.0160	1884	1404	452	8477	3824	3688	54.35	2222	1536		18
17.63	.0143	1779	1321	428	8485	3243	3313	54.57	2103	1449		19
17.86	.0110	1567	1165	381	8477	1866	2562	55.38	1848	1285		20
17.05	.0169	1927	1451	429	8261	3985	3741	52.00	2278	1455	63.8	21
17.25	.0160	1860	1395	429	8284	3639	3605	52.54	2209	1448		22
17.10	.0140	1740	1297	399	8261	3039	3168	53.06	2057	1344		23
17.70	.0101	1506	1122	356	8276	1731	2315	53.83	1785	1202		24
11.13	.0190	2059	1536	310	8703	4495	4412	54.47	2434	1676	70.5	25
11.42	.0167	1939	1442	296	8695	3805	3869	54.41	2287	1586		26
11.25	.0158	1874	1389	288	8695	3444	3684	54.83	2210	1552		27
11.24	.0143	1781	1318	274	8703	2896	3357	55.14	2105	1470		28
10.71	.0172	1921	1453	273	8306	3896	3832	51.76	2292	1452	73.2	29
10.56	.0158	1855	1396	256	8291	3428	3468	51.33	2203	1360		30
10.57	.0129	1740	1274	240	8253	2737	2885	52.61	2048	1302		31
10.69	.0131	1736	1300	246	8291	2687	2927	52.28	2062	1319		32
10.96	.0094	1504	1104	213	8298	1502	2137	53.10	1790	1160		33



2308

TABLE I - PERFORMANCE DATA FOR PYTHON

(e) 24-inch-diameter tail pipe;

Run	Altitude (ft)	Ram pressure ratio $P_1/P_0$	Cowl-inlet total pressure $P_1$ (lb/sq ft abs.)	Tunnel static pressure $P_0$ (lb/sq ft abs.)	Cowl-inlet total temperature $T_1$ ( $^{\circ}$ R)	Tunnel static temperature $t_0$ ( $^{\circ}$ R)	Engine speed N (rpm)	Torque-meter pressure $P_{TM}$ (lb/sq in. gage)	Shaft horsepower (shp)	Engine fuel flow $W_f$ (lb/hr)	Specific fuel consumption $W_f$ (shp) (lb)/(hr)	Engine air flow (recalculated) $W_{a,1}$ (lb/sec)
1	10,000	1.027	1490	1451	492	488	8006	242	2741	2400	0.876	37.41
2		1.027	1487	1448	492	488		224	2538	2255	.888	37.38
3		1.026	1486	1448	493	489		122.5	1387	1580	1.139	38.46
4		1.026	1489	1451	489	485		42	460	1105	2.402	39.58
5		1.026	1488	1450	493	489	7806	223	2463	2200	.893	36.04
6		1.026	1484	1446	485	481		206	2275	2100	.923	36.41
7		1.025	1491	1454	484	481		206	2275	2090	.919	37.17
8		1.025	1489	1452	494	491		183	2021	1910	.945	36.53
9		1.023	1490	1457	494	491		122.5	1353	1520	1.123	37.18
10		1.025	1491	1454	488	485		35	366	1015	2.773	38.55
11		1.025	1489	1452	488	485	7806	196.5	2115	1960	.927	35.21
12		1.025	1490	1453	489	486		181	1948	1860	.955	35.26
13		1.025	1483	1447	486	483		155	1668	1680	1.007	35.98
14		1.025	1492	1455	488	485		105	1130	1390	1.230	36.67
15		1.025	1490	1453	484	481		37	380	985	2.592	37.50
16		1.025	1490	1453	488	485	7205	153	1560	1610	1.032	32.57
17		1.025	1493	1456	486	483		140	1427	1520	1.065	32.94
18		1.025	1487	1451	487	484		126	1285	1430	1.113	33.01
19		1.026	1480	1443	484	480		90	916	1210	1.321	33.77
20		1.025	1485	1449	485	482		33.5	322	880	2.733	34.20
21	30,000	1.025	645	629	439	436	8006	120	1359	1240	.912	17.90
22		1.027	641	624	438	435		114	1291	1170	.906	17.94
23		1.027	641	624	438	435		102	1155	1060	.918	18.10
24		1.025	644	628	437	434		75	845	870	1.030	18.33
25		1.026	641	625	436	433		29	302	590	1.954	18.31
26		1.027	644	627	439	436	7806	115	1270	1150	.906	17.55
27		1.027	643	626	437	434		108.5	1198	1080	.902	17.72
28		1.024	641	626	437	434		100	1105	1030	.932	17.83
29		1.025	646	630	437	434		70	768	785	1.022	18.20
30		1.025	645	629	437	434		28	283	570	2.014	18.22
31		1.026	643	627	436	433	7606	112.5	1211	1090	.900	16.95
32		1.024	642	627	436	433		104	1120	1010	.902	17.11
33		1.026	643	627	435	432		99	1066	980	.919	17.29
34		1.026	641	625	435	432		76.5	820	800	.976	17.58
35		1.026	640	624	435	432		35	357	545	1.527	17.69
36		1.026	643	627	435	432	7205	92	937	950	1.014	15.86
37		1.025	647	631	435	432		88	896	860	.960	16.14
38		1.024	642	627	434	431		82	834	800	.959	16.18
39		1.024	642	627	435	432		59.5	599	650	1.085	16.51
40		1.025	644	628	432	429		29	272	495	1.820	16.93
41	40,000	1.028	402	391	436	433	8006	68	764	750	.982	11.16
42		1.031	401	389	433	429		61	683	640	.937	11.13
43		1.031	406	394	437	433		60	671	660	.984	11.24
44		1.028	402	391	436	433		43	472	550	1.165	11.34
45		1.023	402	393	433	430		23	232	400	1.724	11.31
46		1.028	401	390	436	433	7606	55	582	600	1.031	10.62
47		1.031	402	390	441	437		48	504	535	1.062	10.61
48		1.026	399	389	437	434		33	334	400	1.198	10.77
49		1.023	400	391	438	435		15	141	290	2.057	10.99

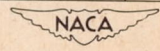
NACA

2308

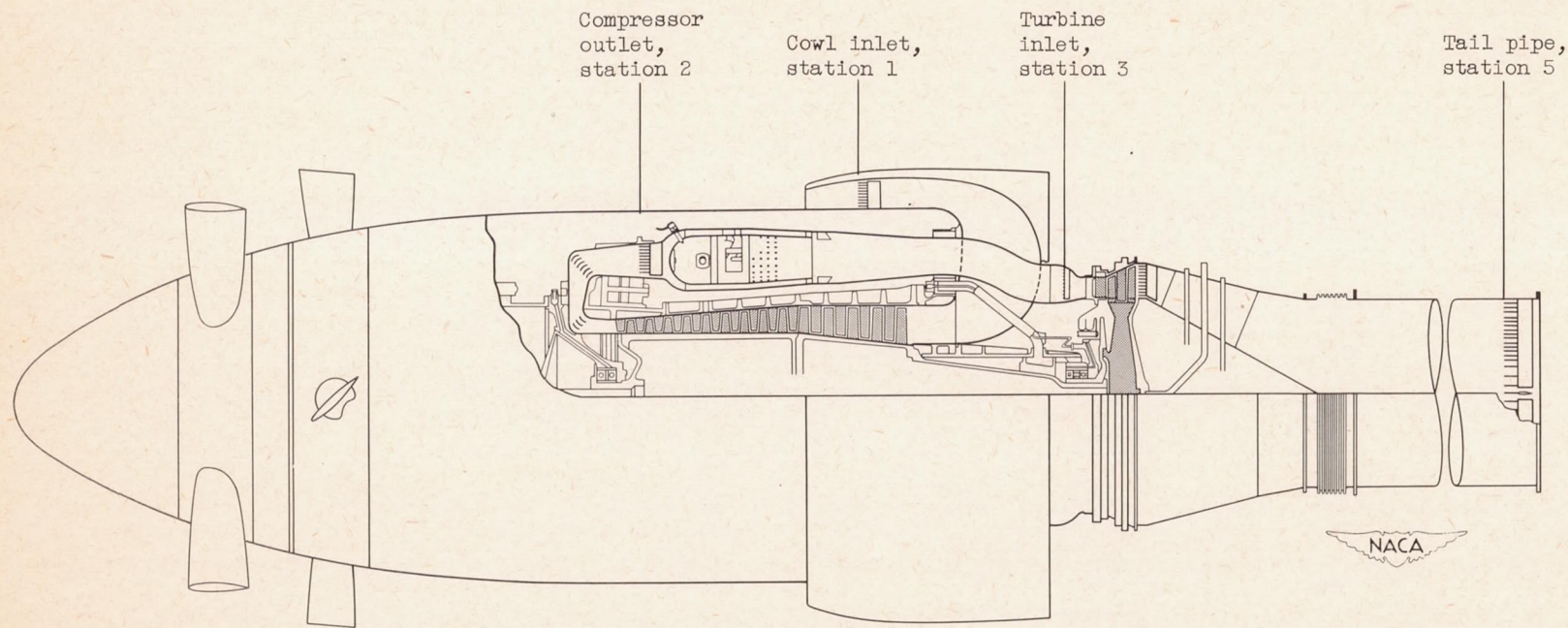
TURBINE-PROPELLER ENGINE - Concluded

24-inch-diameter exhaust nozzle

Engine air flow (initial) $W_{a,1}$ (lb/sec)	Engine fuel-air ratio f/a	Turbine-inlet total temperature $T_3$ (°R)	Exhaust-nozzle-inlet total temperature $T_5$ (°R)	Jet thrust $F_j$ (lb)	Corrected engine speed $N/\sqrt{\theta_0}$ (rpm)	Corrected shaft horsepower $shp/\delta_0\sqrt{\theta_0}$	Corrected fuel flow $W_f/\delta_0\sqrt{\theta_0}$ (lb/hr)	Corrected air flow $W_{a,1}\sqrt{\theta_0}/\delta_0$ (lb/sec)	Corrected turbine-inlet temperature $T_3/\theta_0$ (°R)	Corrected jet thrust $F_j/\delta_0$ (lb)	Approximate engine time (hr)	Run
38.82	0.0178	2058	1536	832	8262	4125	3612	52.85	2189	1213	35.8	1
37.76	.0168	1990	1484	794	8262	3827	3401	52.92	2116	1160		2
40.16	.0114	1651	1221	691	8246	2087	2378	54.55	1752	1009		3
39.54	.0078	1395	1029	579	8278	694	1666	55.81	1493	844		4
36.72	.0170	1984	1494	747	8040	3702	3307	51.05	2106	1090	36.3	5
36.74	.0160	1914	1433	731	8110	3458	3192	51.27	2065	1070		6
37.73	.0156	1890	1413	741	8110	3440	3162	52.05	2039	1077	37.9	7
37.92	.0145	1837	1373	689	8025	3027	2861	51.77	1942	1004	36.4	8
38.78	.0114	1629	1217	626	8025	2020	2269	52.51	1722	909		9
38.24	.0074	1358	1008	529	8071	550	1527	53.96	1453	769		10
35.67	.0155	1875	1417	672	7865	3187	2954	49.61	2006	979	37.0	11
35.60	.0147	1826	1376	646	7857	2930	2797	49.70	1950	941		12
36.61	.0130	1712	1283	628	7887	2529	2547	50.73	1840	919		13
38.36	.0105	1547	1157	586	7865	1698	2089	51.56	1655	853		14
37.36	.0073	1328	993	501	7903	575	1490	52.55	1433	730	37.8	15
33.42	.0137	1736	1333	541	7450	2349	2425	45.86	1858	787	37.6	16
34.24	.0128	1673	1278	534	7472	2150	2291	46.15	1798	776		17
34.50	.0120	1621	1237	515	7457	1939	2158	46.50	1738	750		18
35.14	.0100	1480	1126	485	7493	1397	1845	47.60	1600	711		19
33.67	.0071	1299	989	413	7479	488	1333	48.10	1399	603		20
18.06	.0192	2064	1535	426	8735	4988	4551	55.19	2457	1431	39.8	21
18.09	.0181	1979	1459	413	8743	4781	4333	55.71	2361	1399		22
18.56	.0163	1880	1376	399	8743	4277	3925	56.21	2243	1352		23
18.30	.0132	1695	1233	356	8759	3115	3207	56.45	2027	1200		24
18.72	.0090	1430	1045	299	8767	1120	2188	56.62	1714	1011		25
17.55	.0182	1988	1473	395	8516	4676	4234	54.29	2366	1333	40.3	26
17.95	.0169	1914	1412	389	8540	4430	3994	54.75	2289	1313		27
18.36	.0160	1840	1350	379	8540	4086	3809	55.09	2200	1281		28
18.20	.0120	1630	1185	335	8540	2822	2885	55.88	1949	1125		29
18.81	.0087	1385	1012	289	8540	1041	2098	56.03	1656	972		30
17.05	.0179	1953	1456	365	8329	4476	4029	52.24	2341	1233	40.7	31
17.72	.0164	1880	1392	360	8329	4140	3733	52.74	2253	1216		32
17.83	.0157	1827	1350	359	8336	3943	3625	53.24	2195	1210		33
17.62	.0126	1652	1213	328	8336	3043	2969	54.31	1985	1111		34
18.24	.0086	1396	1024	277	8336	1327	2026	54.73	1677	958		35
16.18	.0166	1783	1338	300	7897	3466	3514	48.84	2142	1013	41.3	36
16.26	.0148	1748	1313	299	7897	3293	3161	49.38	2100	1001		37
16.34	.0137	1687	1258	287	7904	3087	2962	49.78	2032	969		38
16.30	.0109	1523	1131	261	7897	2216	2404	50.84	1830	882		39
17.98	.0081	1320	975	245	7926	1008	1834	51.85	1597	825		40
11.31	.0187	2033	1519	261	8767	4527	4445	55.16	2437	1414	42.4	41
11.18	.0160	1900	1397	239	8807	4087	3830	55.04	2299	1297		42
11.46	.0163	1880	1379	240	8767	3946	3881	55.13	2253	1291		43
11.40	.0135	1734	1277	225	8767	2797	3259	56.05	2078	1218		44
11.49	.0098	1513	1110	189	8799	1373	2367	55.41	1826	1018		45
10.91	.0157	1839	1373	217	8329	3458	3565	52.62	2204	1176	42.7	46
10.78	.0140	1747	1299	205	8291	2981	3164	52.82	2075	1111		47
10.60	.0103	1534	1124	173	8321	1988	2380	53.55	1834	942		48
11.68	.0073	1329	969	161	8306	833	1714	54.47	1586	870		49



CONFIDENTIAL



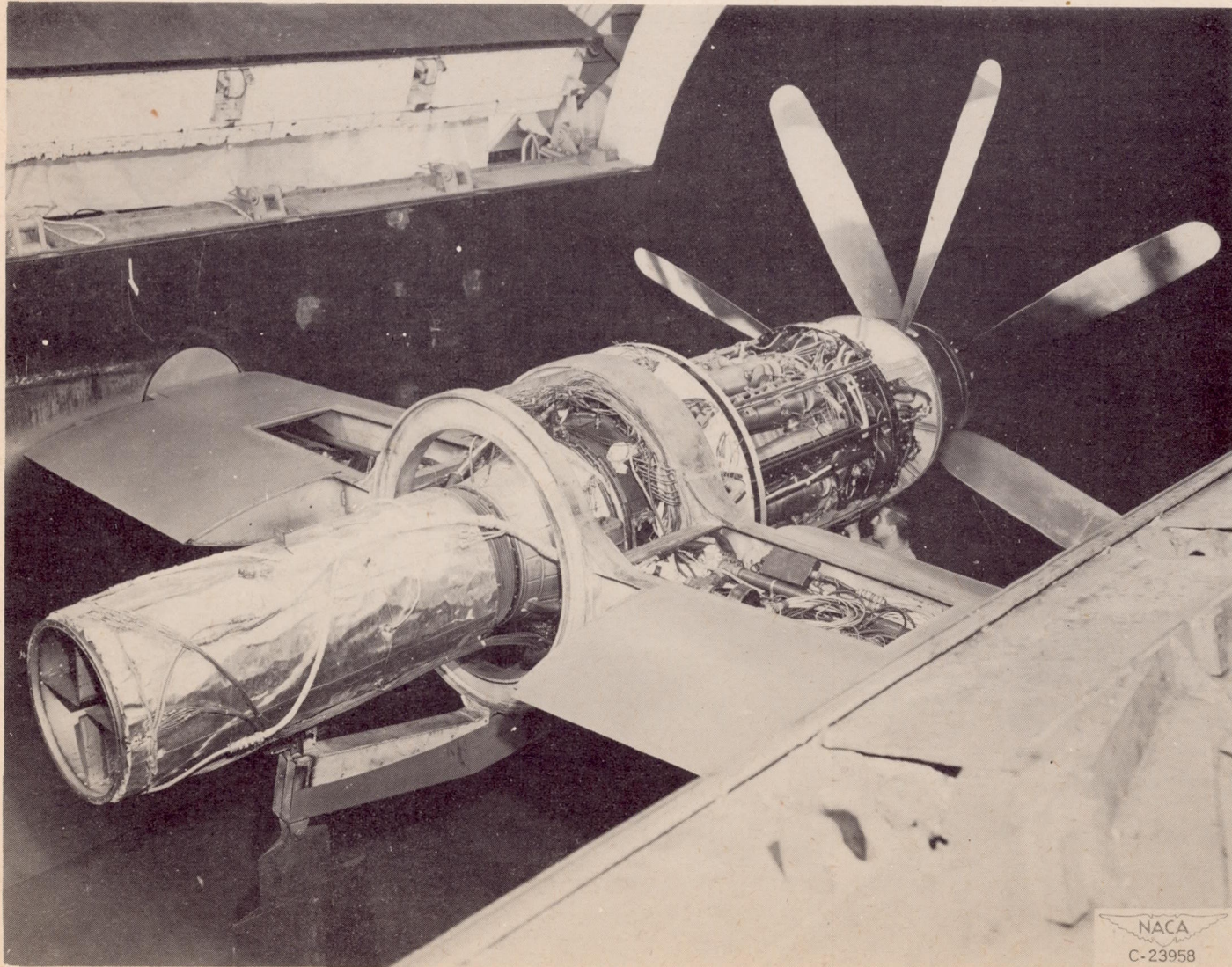
CONFIDENTIAL

Figure 1. - Cross section of Python turbine-propeller engine.

NACA RM E51114

NACA RM E51114

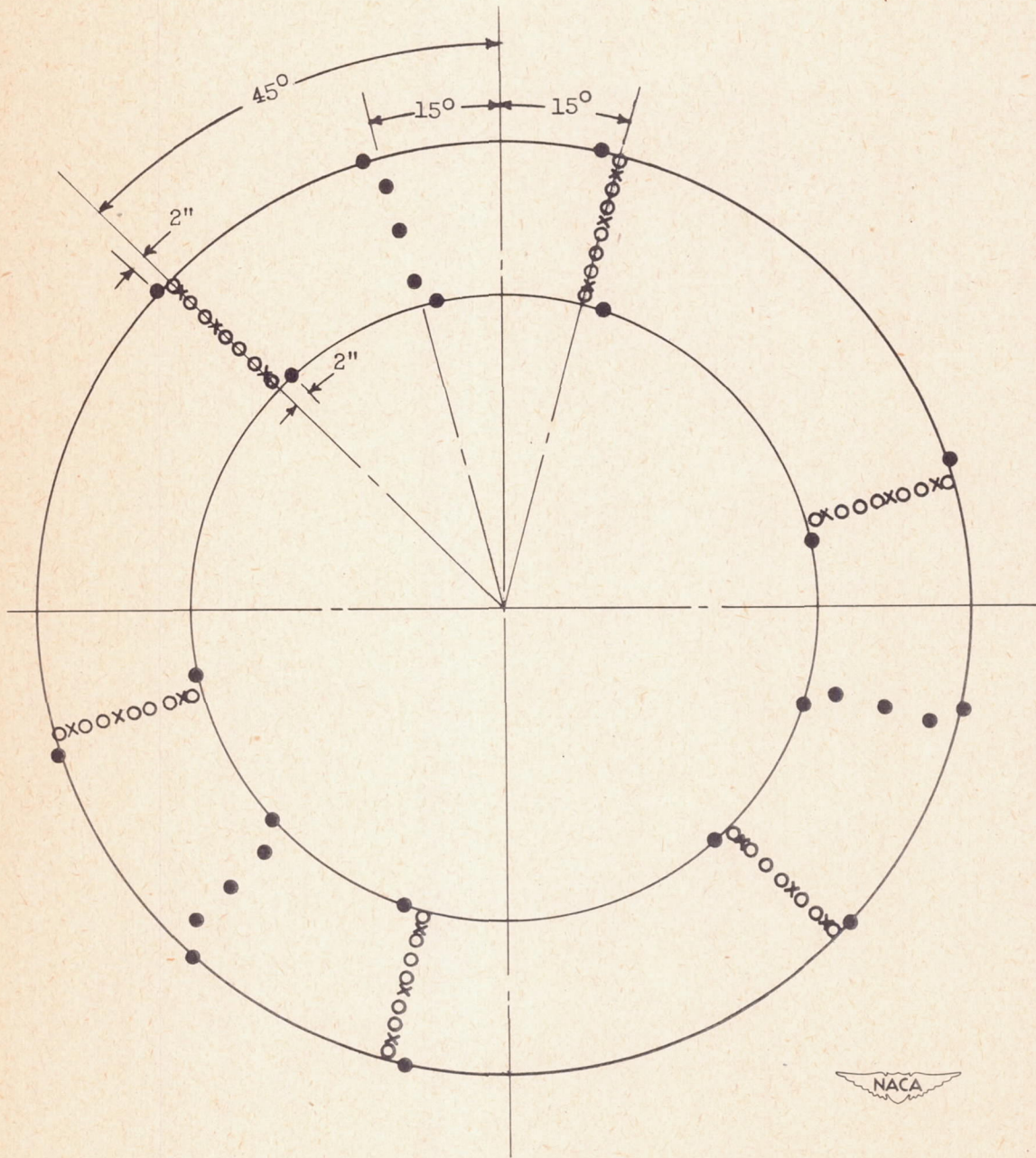
CONFIDENTIAL



CONFIDENTIAL

Figure 2. - Installation of Python turbine-propeller engine in altitude wind tunnel (cowling removed).

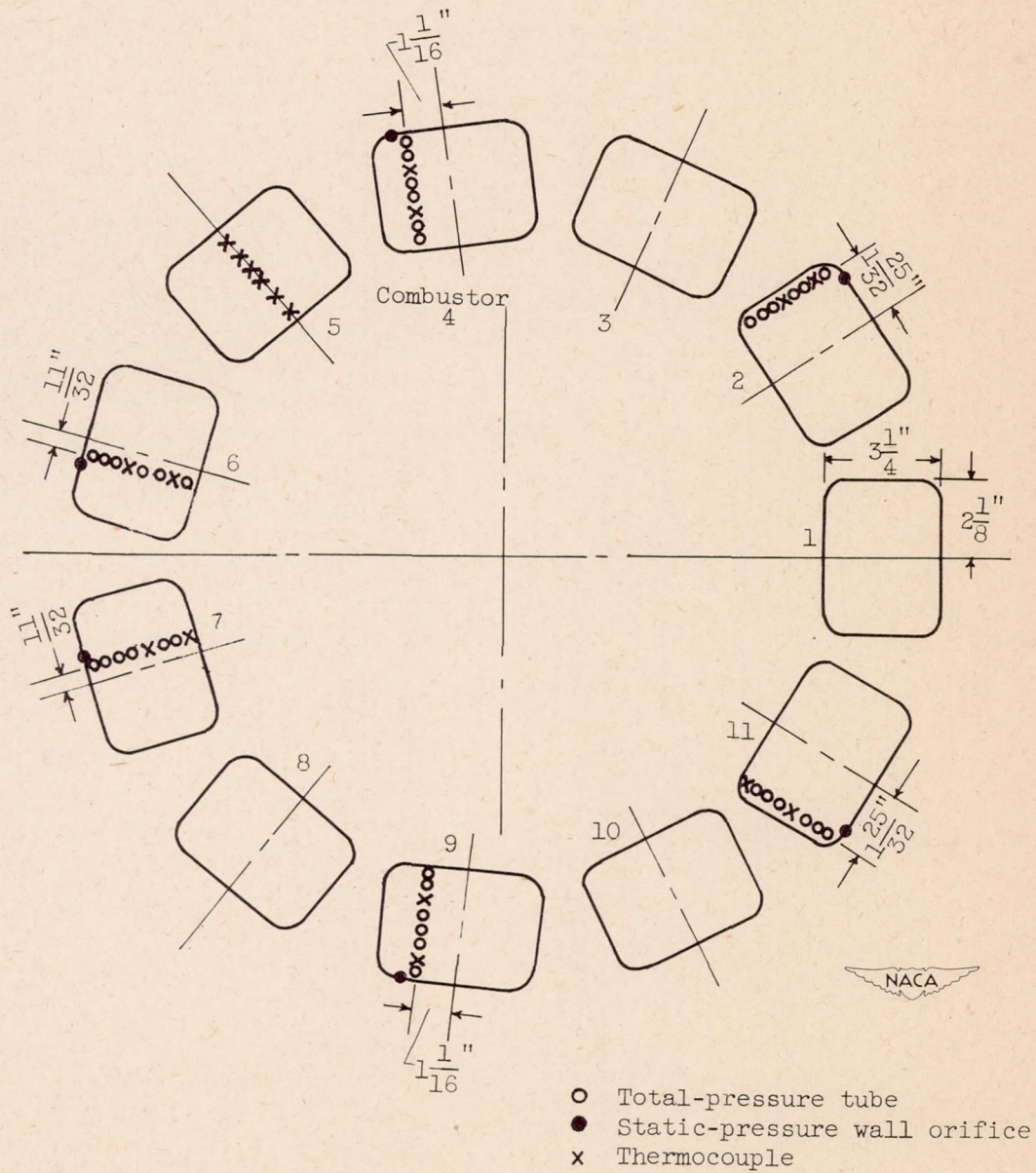
2308



- Total-pressure tube
- Static-pressure tube or wall orifice
- x Thermocouple

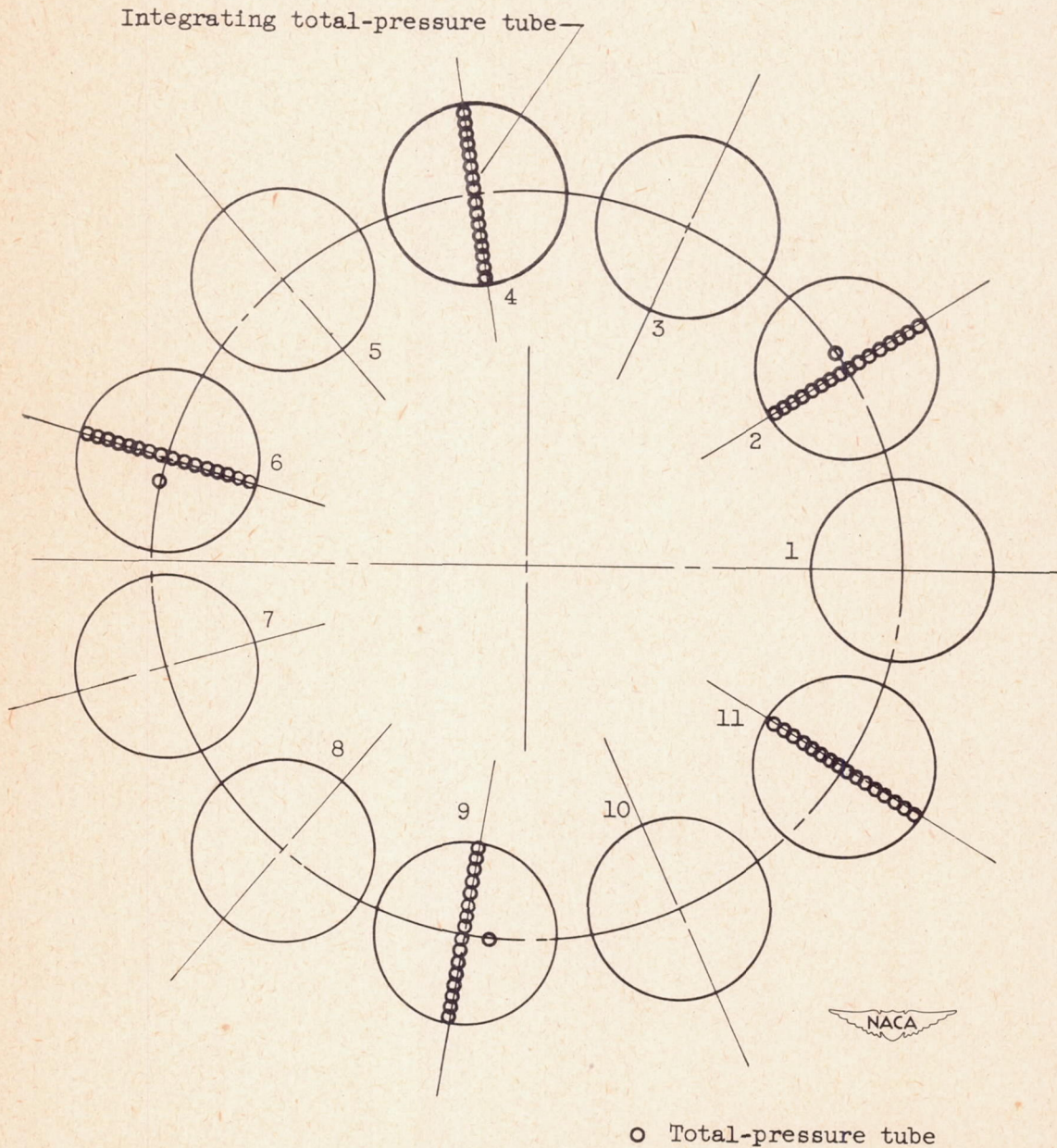
(a) Cowl inlet, station 1, 8 inches downstream of tip of cowling.

Figure 3. - Schematic diagram of instrumentation viewed from upstream.



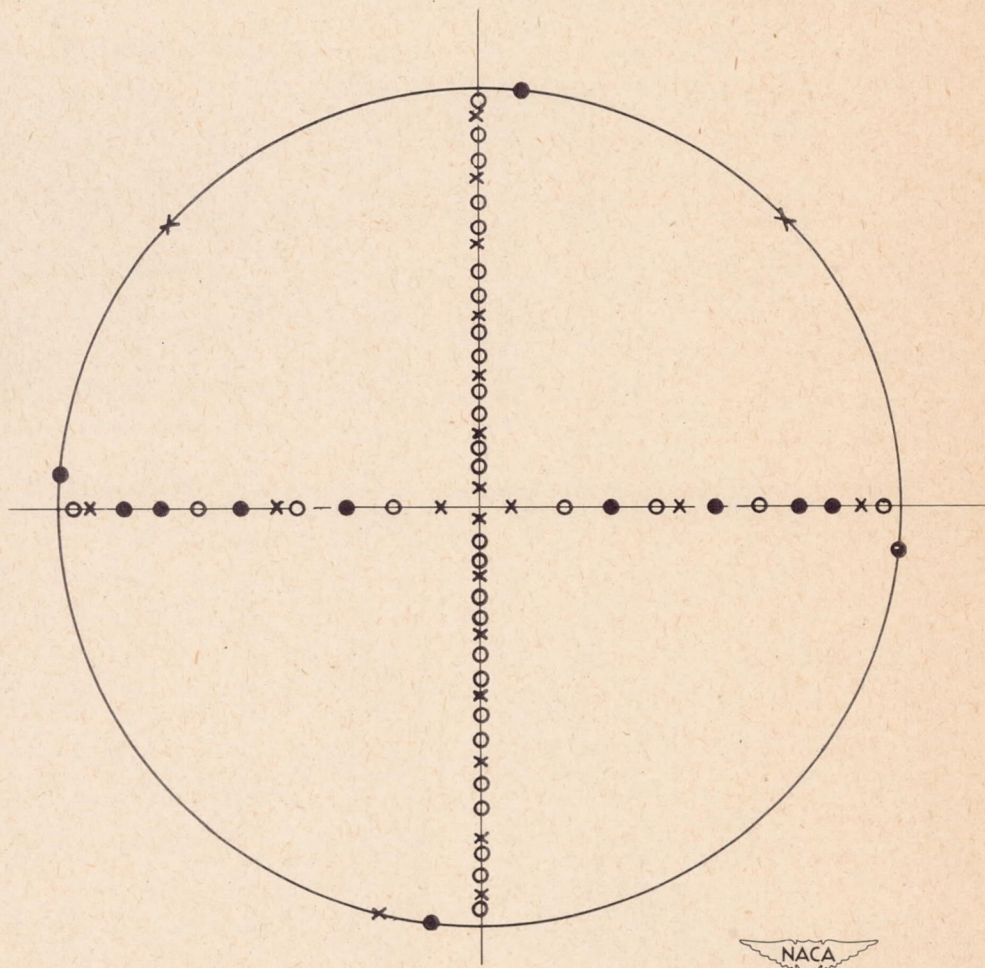
(b) Compressor outlet, station 2,  $3\frac{1}{4}$  inches upstream of burner-inlet flange.

Figure 3. - Continued. Schematic diagram of instrumentation viewed from upstream.



(c) Turbine inlet, station 3, 3 inches upstream of turbine flange.

Figure 3. - Continued. Schematic diagram of instrumentation viewed from upstream.

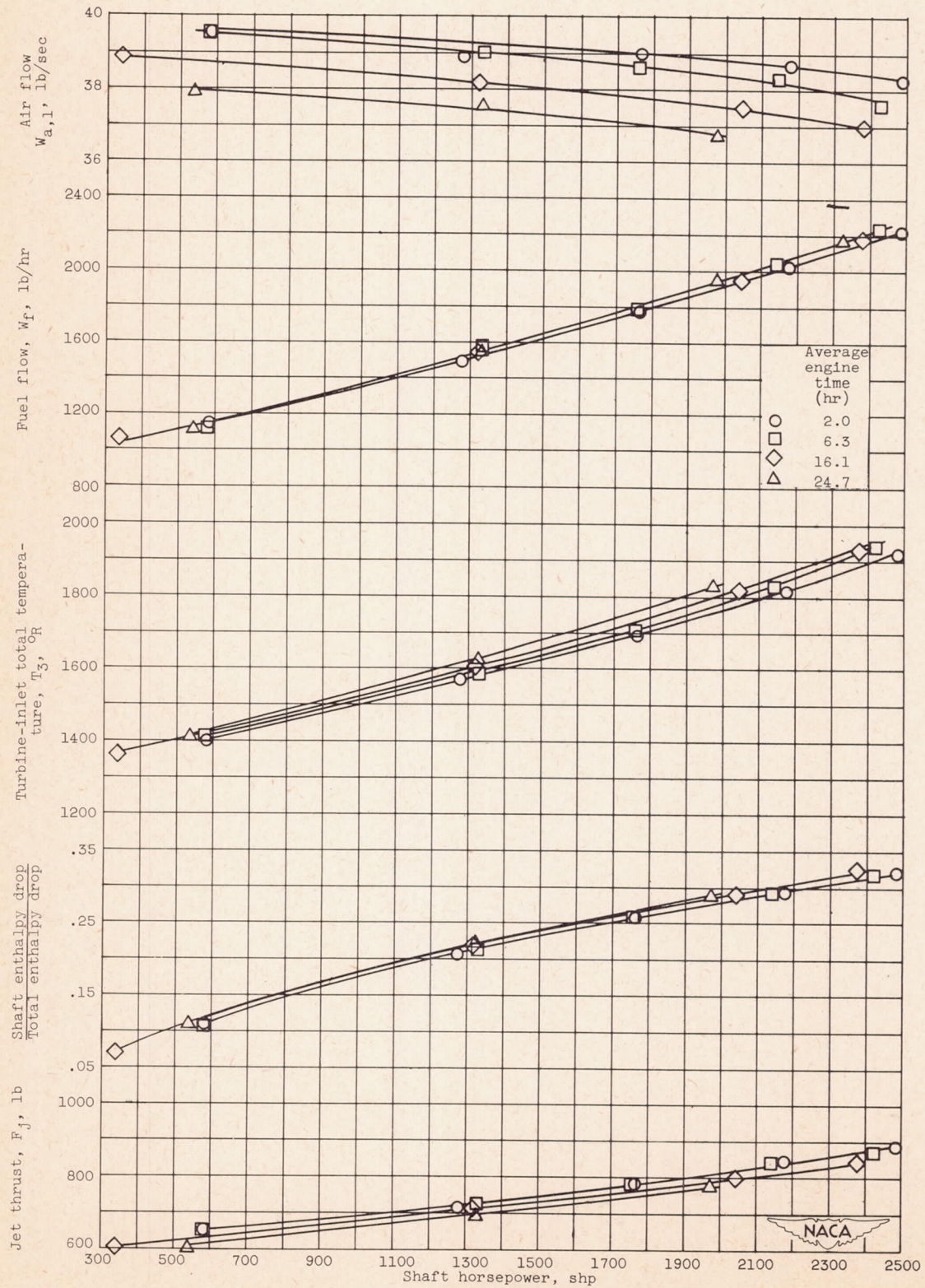


- Total-pressure tube
- Static-pressure tube or wall orifice
- x Thermocouple

(d) Tail pipe, station 5,  $5\frac{1}{4}$  inches upstream of exit of constant diameter tail pipe.

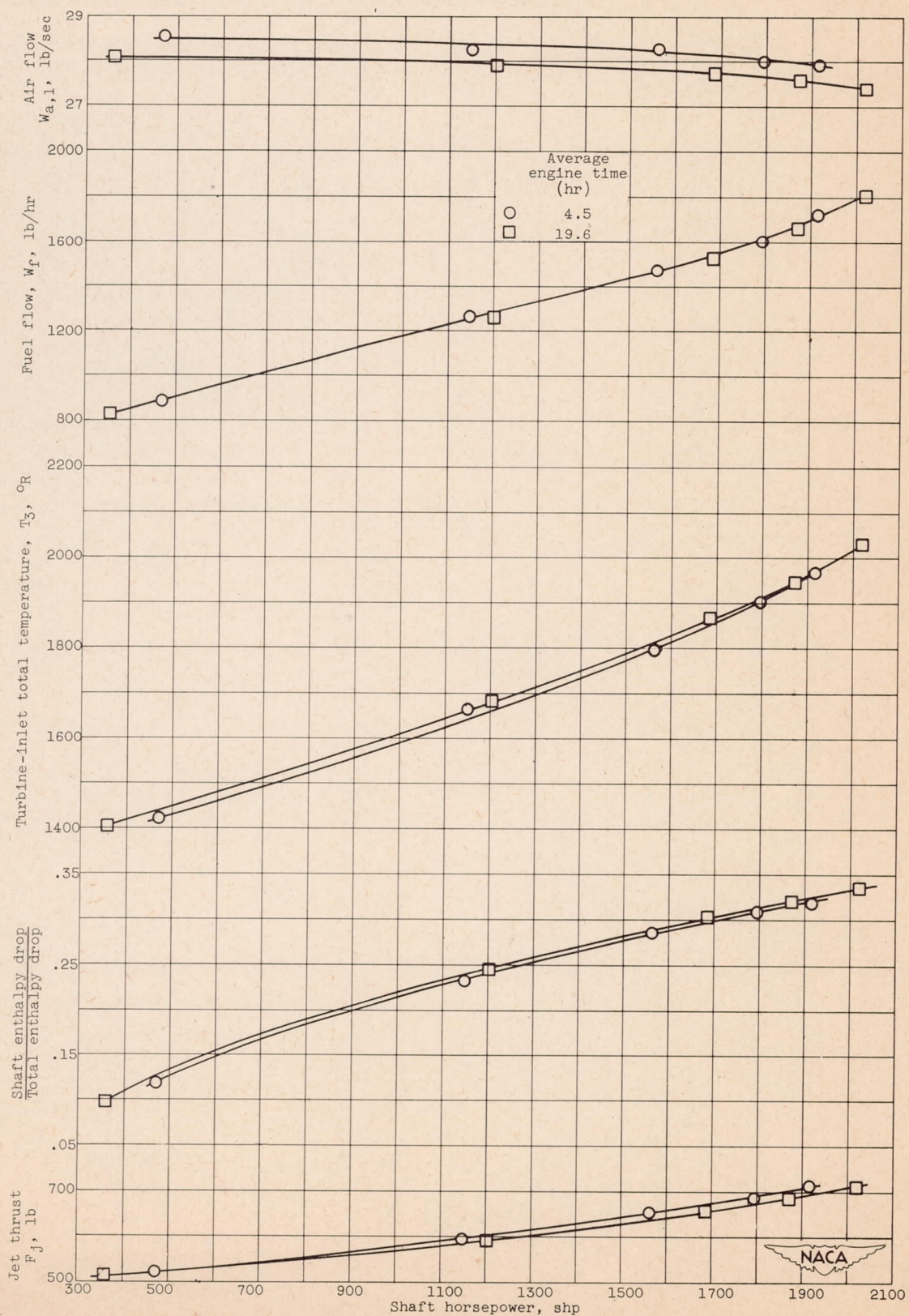
Figure 3. - Concluded. Schematic diagram of instrumentation viewed from upstream.

2308



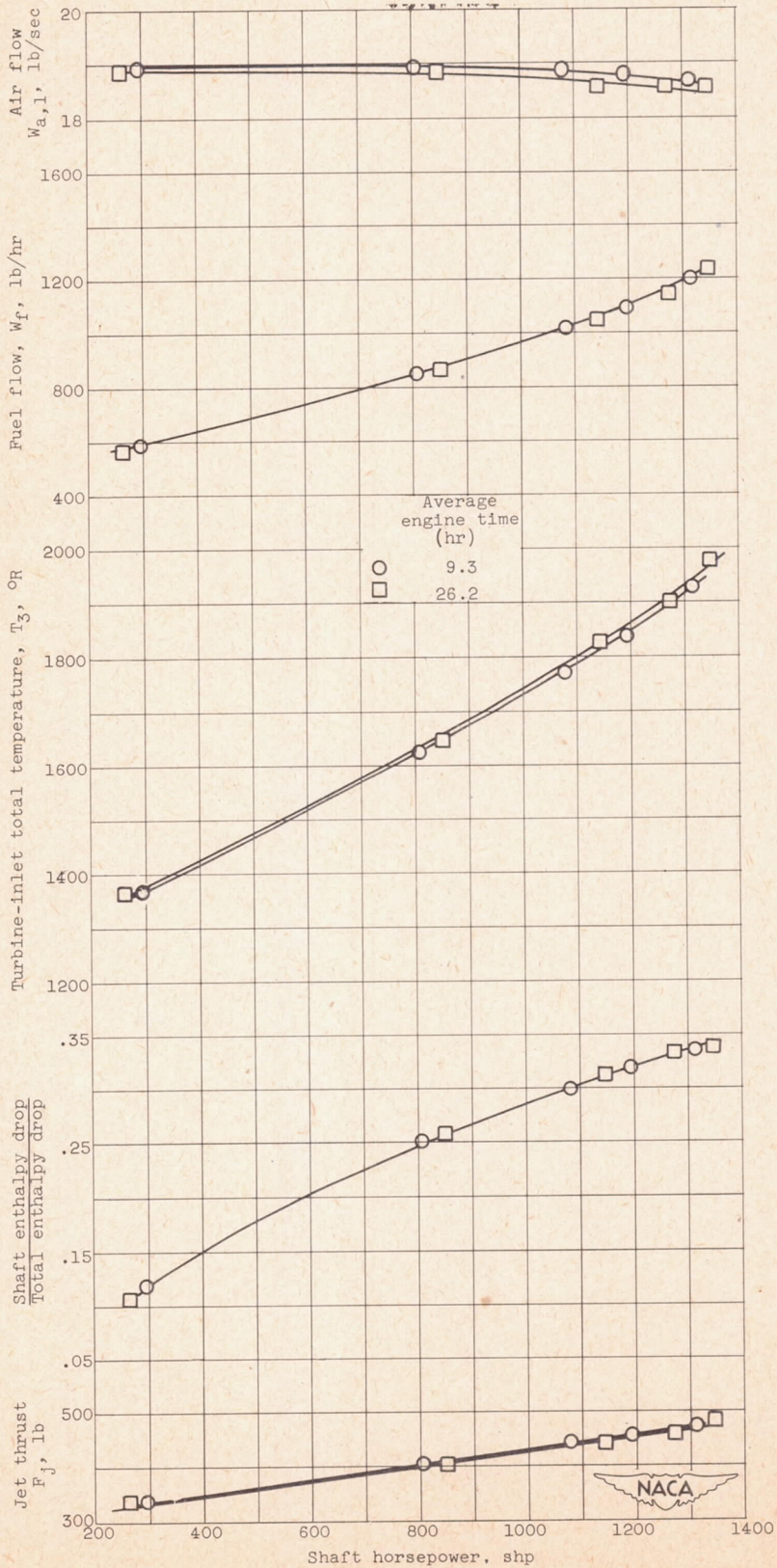
(a) Altitude, 10,000 feet; engine speed, 7760 rpm.

Figure 4. - Variation of engine performance with operating time. Cowl-inlet ram pressure ratio, 1.03.



(b) Altitude, 20,000 feet; engine speed, 7990 rpm.

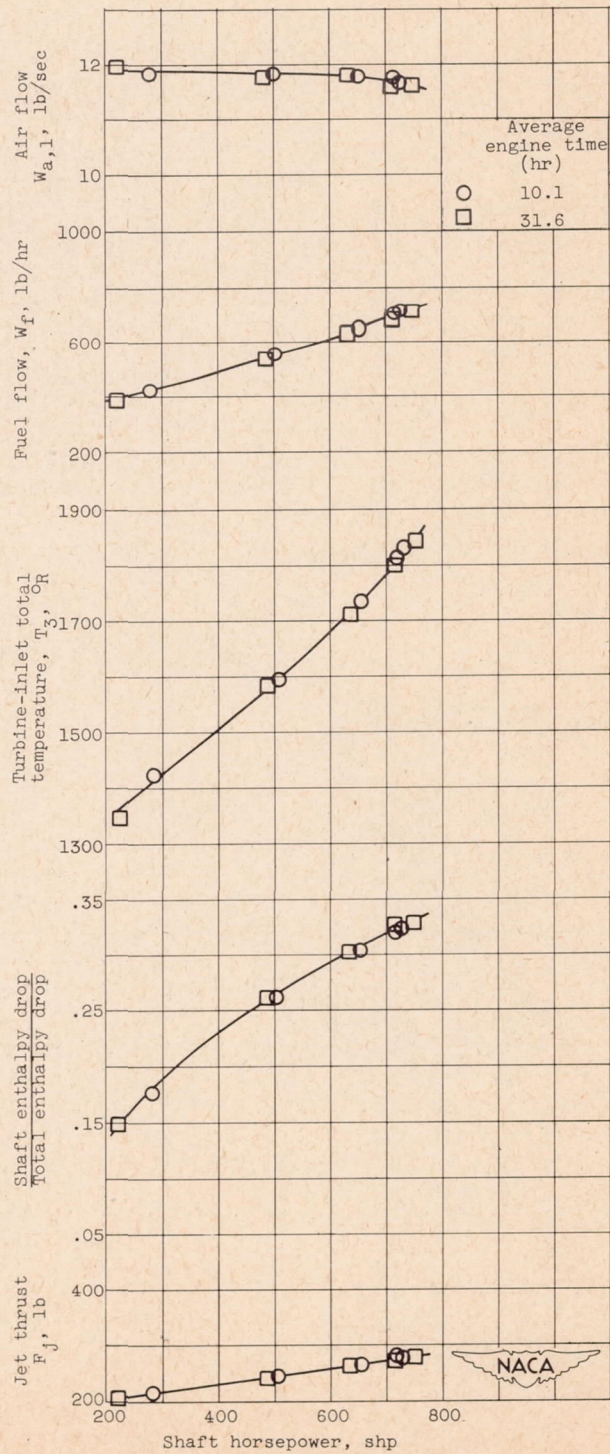
Figure 4. - Continued. Variation of engine performance with operating time. Cowl-inlet ram pressure ratio, 1.03.



(c) Altitude, 30,000 feet; engine speed, 7780 rpm.

Figure 4. - Continued. Variation of engine performance with operating time, Cowl-inlet ram pressure ratio, 1.03.

2308



(d) Altitude, 40,000 feet; engine speed, 7590 rpm.

Figure 4. - Concluded. Variation of engine performance with operating time. Cowl-inlet ram pressure ratio, 1.03.

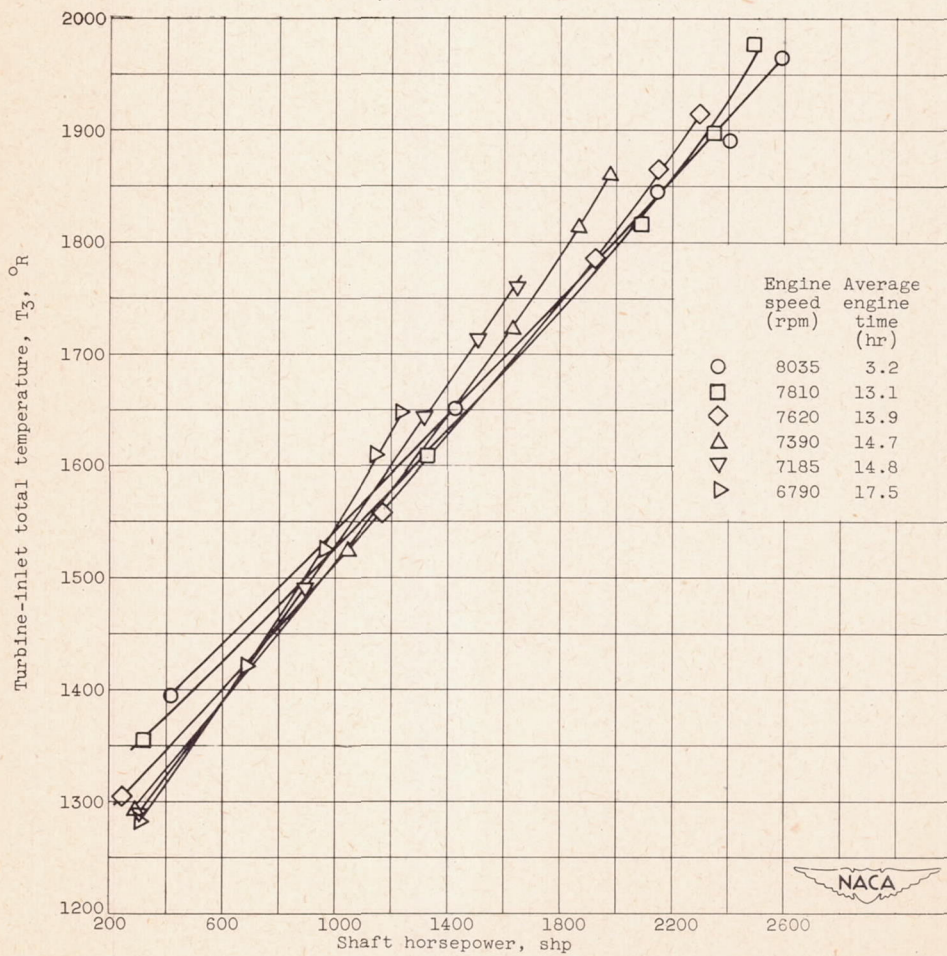
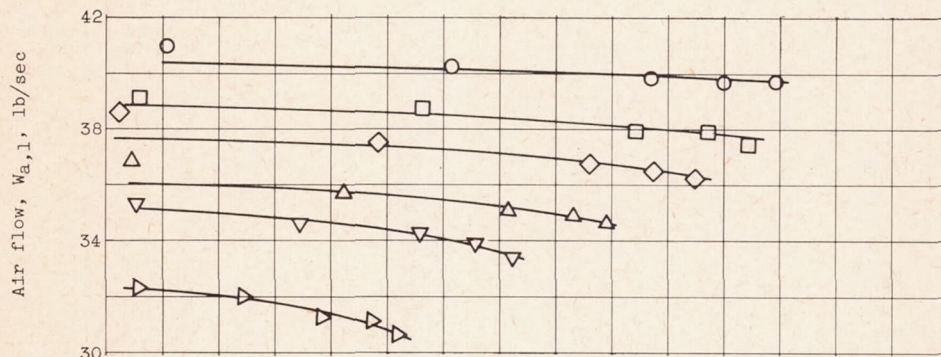
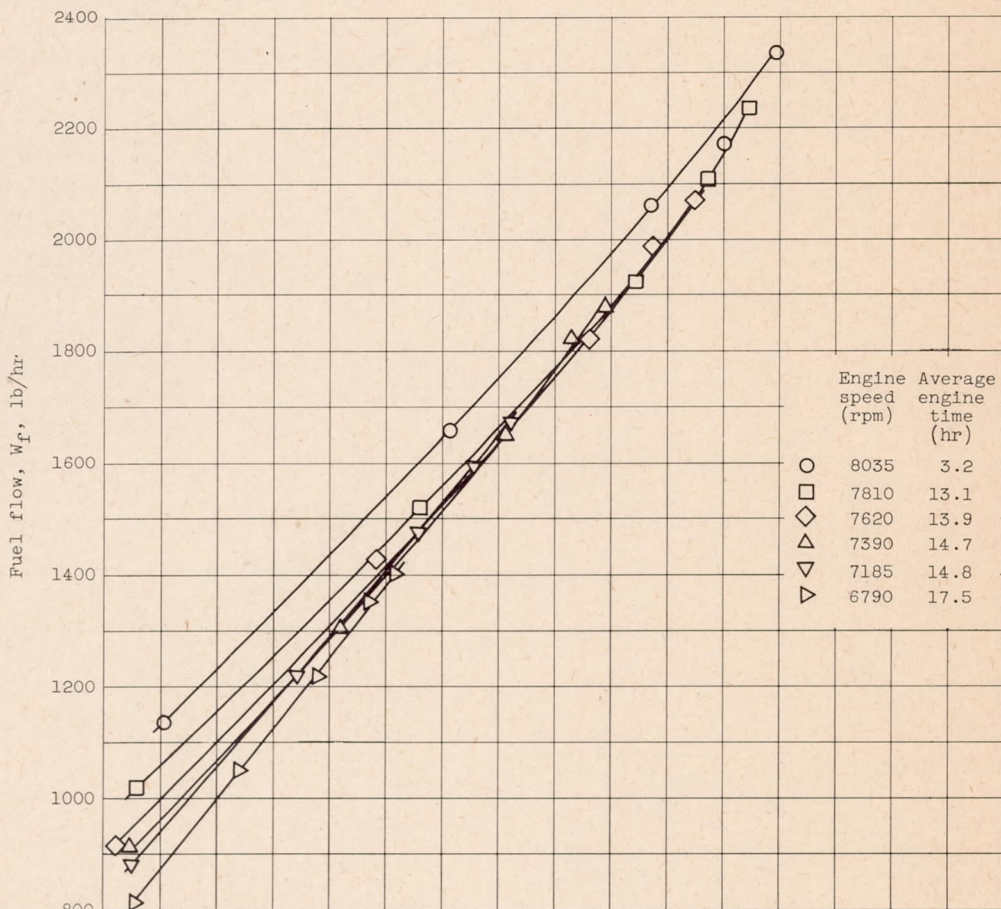


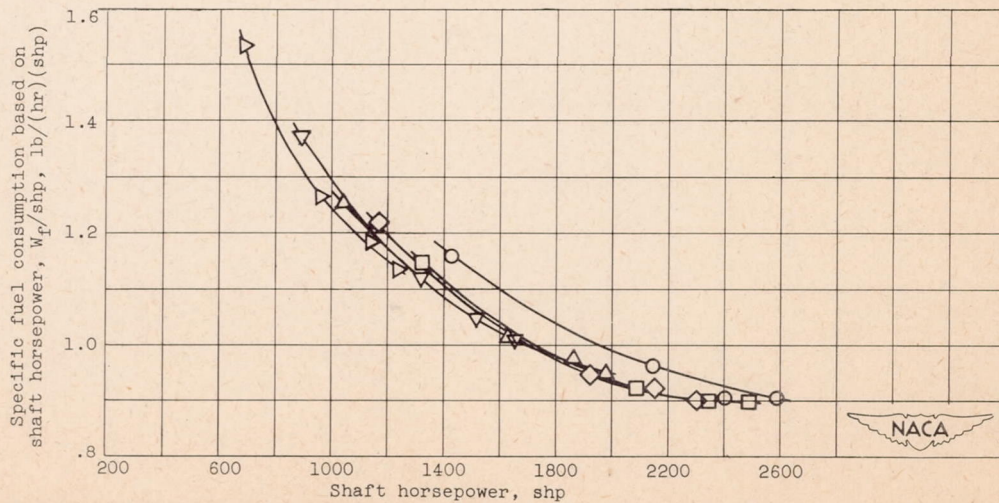
Figure 5. - Effect of shaft horsepower on engine-performance parameters at various engine speeds. Altitude, 10,000 feet; cowl-inlet ram pressure ratio, 1.03.

2308

2308

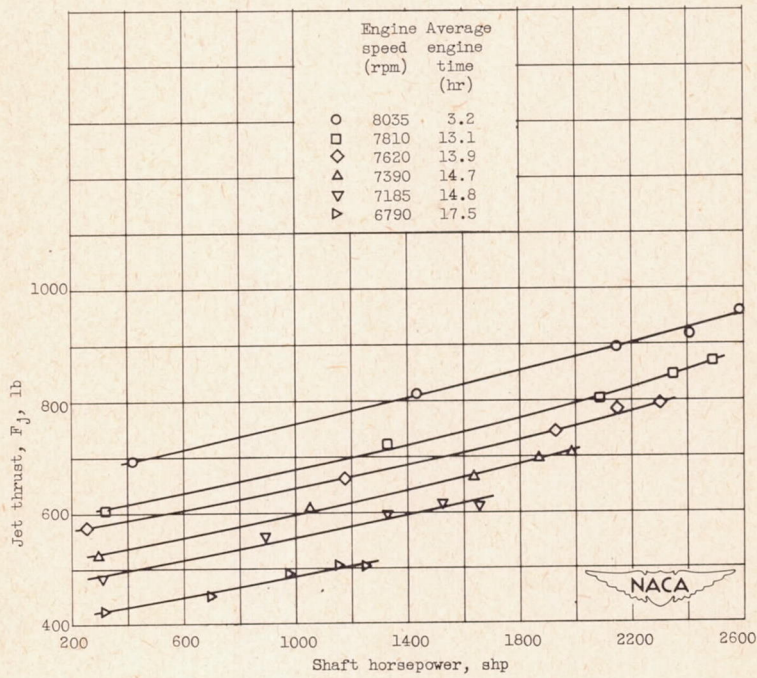


(c) Fuel flow.



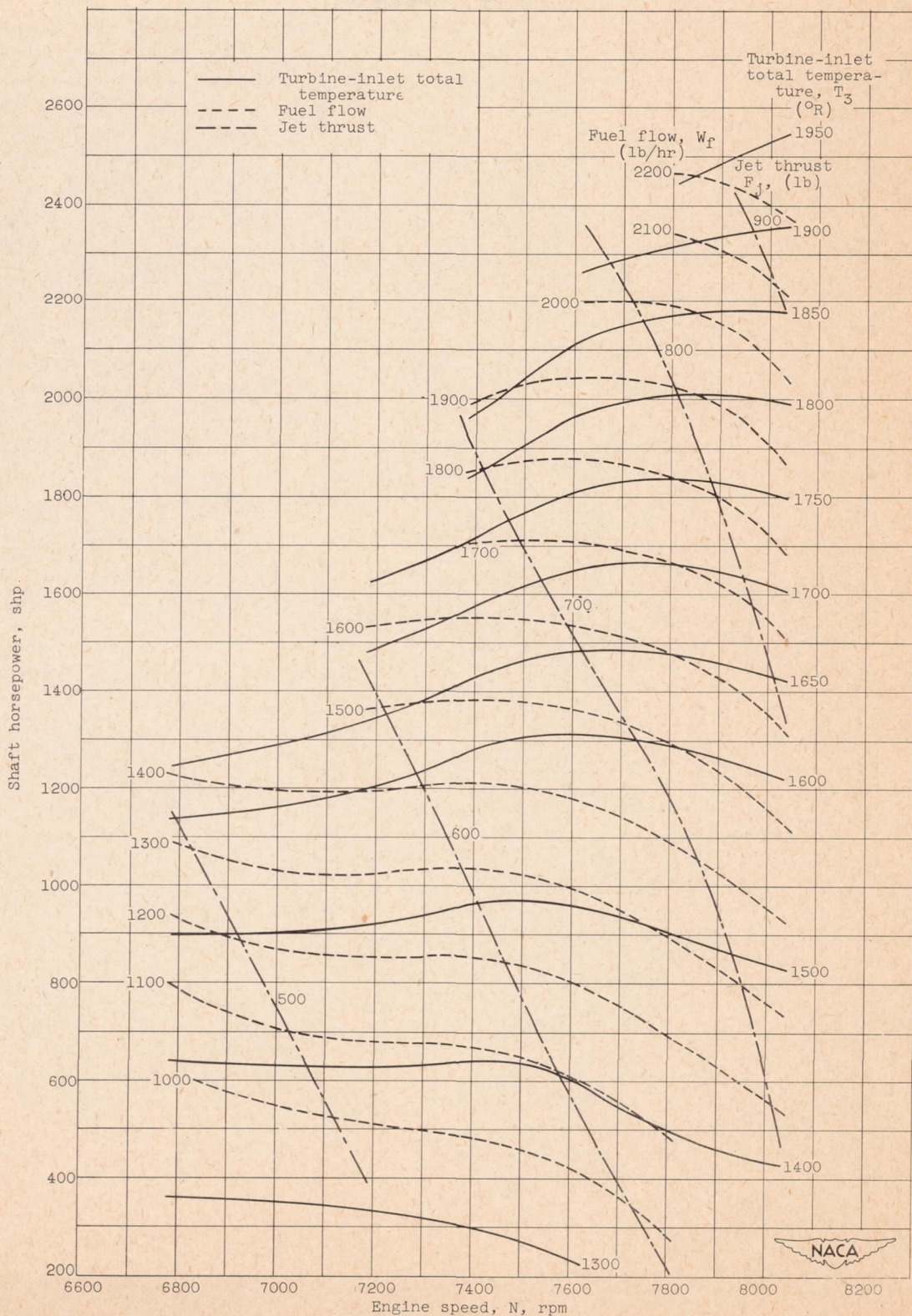
(d) Specific fuel consumption based on shaft horsepower.

Figure 5. - Continued. Effect of shaft horsepower on engine-performance parameters at various engine speeds. Altitude, 10,000 feet; cowl-inlet ram pressure ratio, 1.03.



(e) Jet thrust.

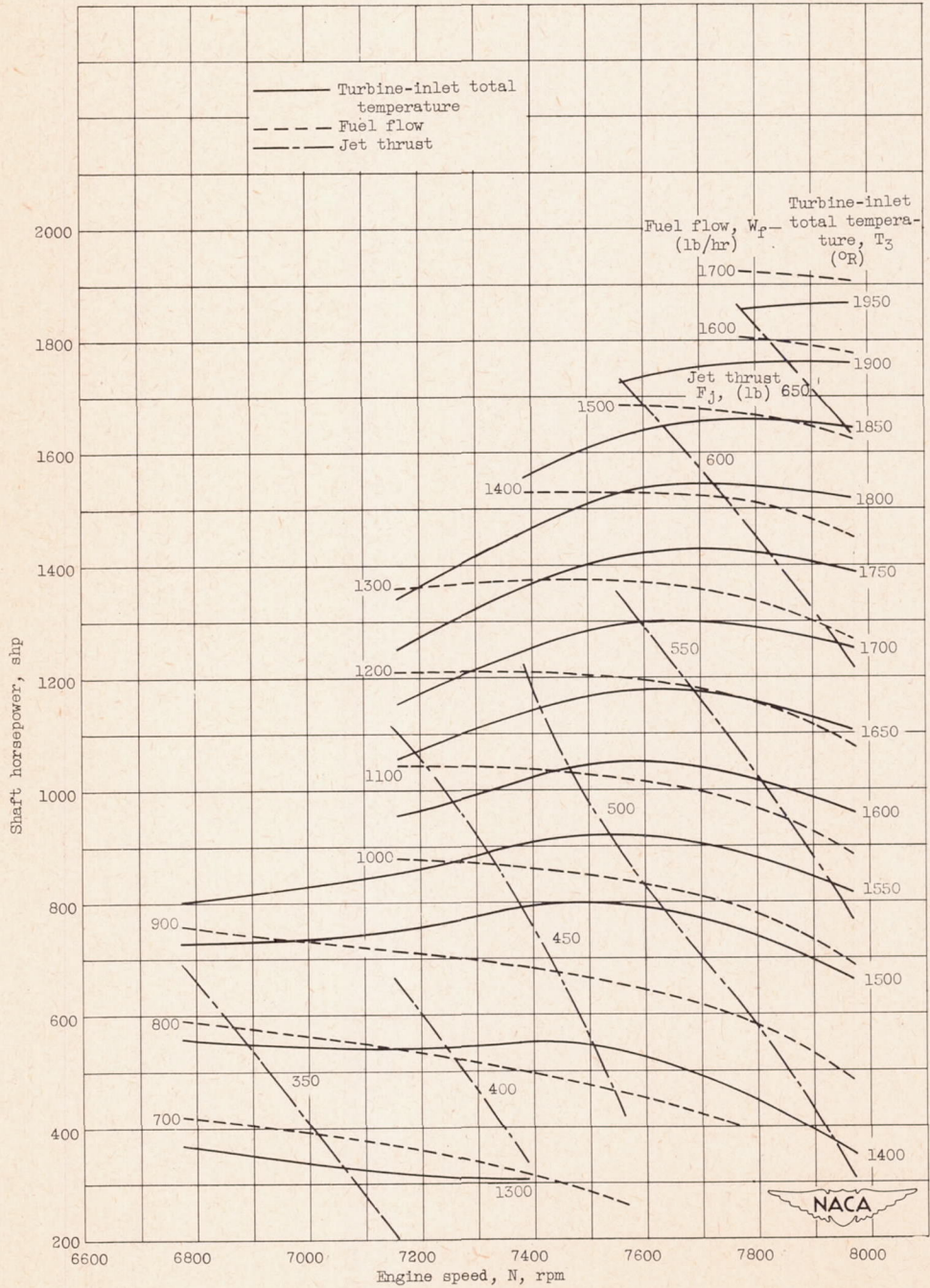
Figure 5. - Concluded. Effect of shaft horsepower on engine-performance parameters at various engine speeds. Altitude, 10,000 feet; cowl-inlet ram pressure ratio, 1.03.



(a) Altitude, 10,000 feet.

Figure 6. - Engine performance map. Cowl-inlet ram pressure ratio, 1.03.

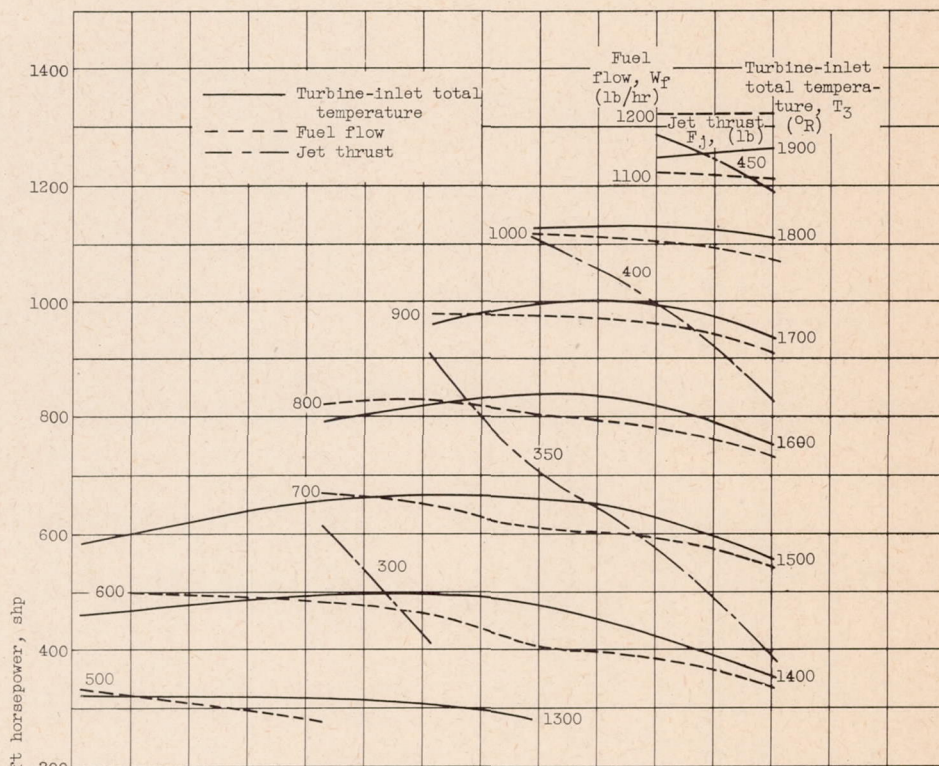
2308



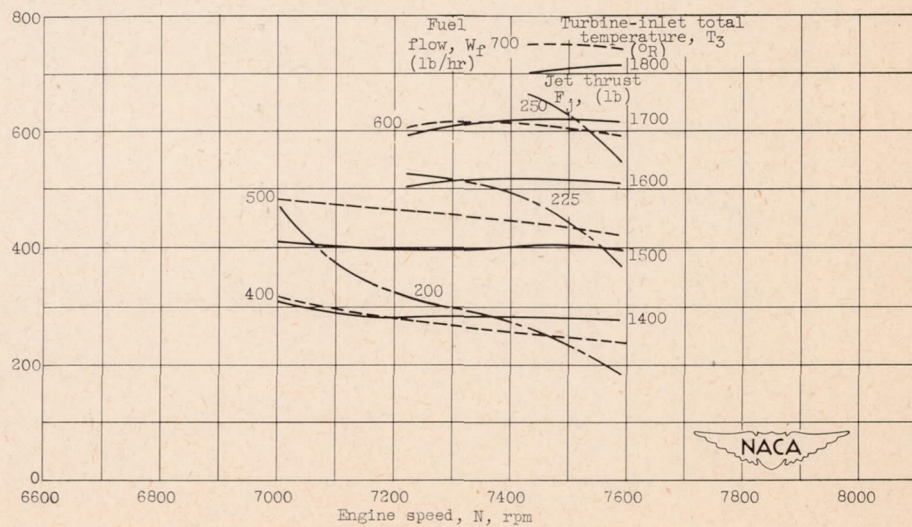
(b) Altitude, 20,000 feet.

Figure 6. - Continued. Engine performance map. Cowl-inlet ram pressure ratio, 1.03.

2308

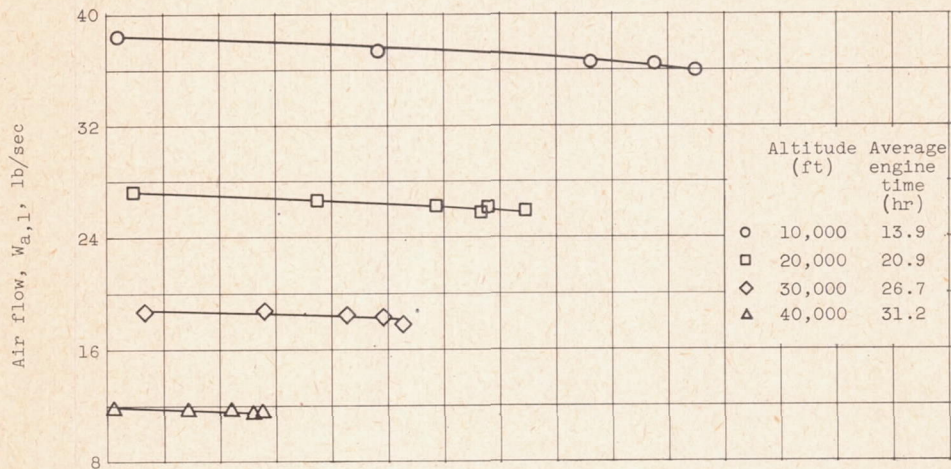


(c) Altitude, 30,000 feet.

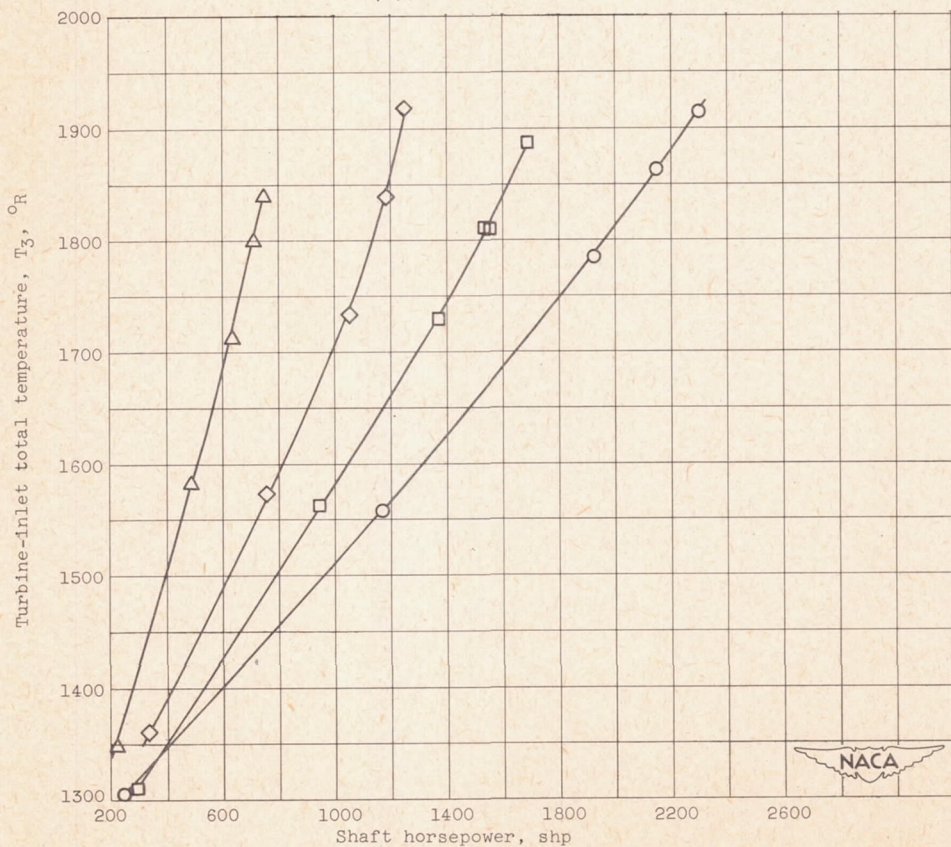


(d) Altitude, 40,000 feet.

Figure 6. - Concluded. Engine performance map. Cowl-inlet ram pressure ratio, 1.03.



(a) Air flow.

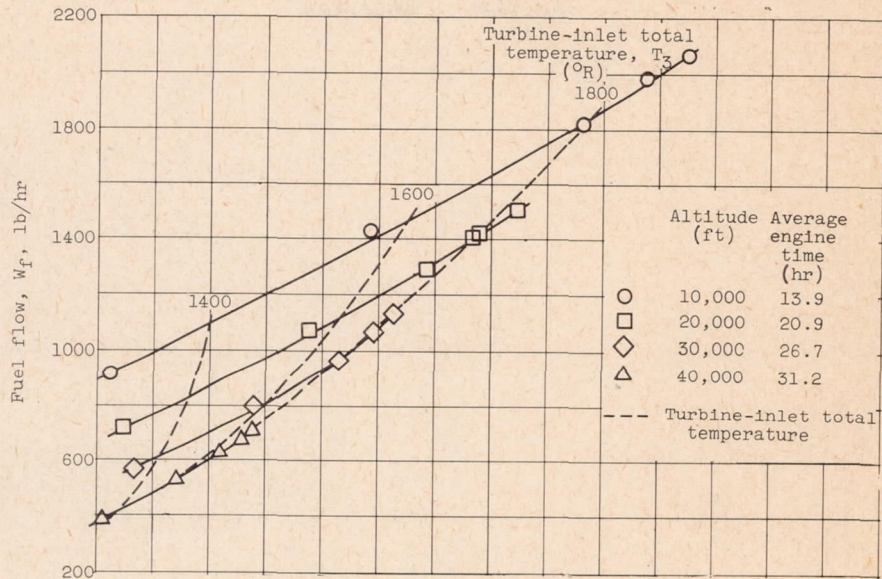


(b) Turbine-inlet total temperature.

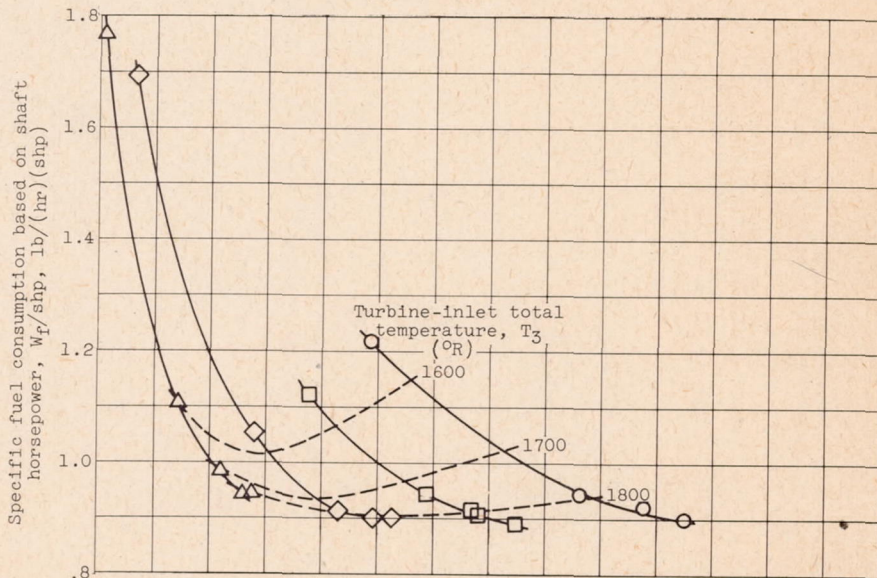
Figure 7. - Effect of shaft horsepower on engine-performance parameters at various altitudes. Engine speed, 7600 rpm; cowl-inlet ram pressure ratio, 1.03.

2308

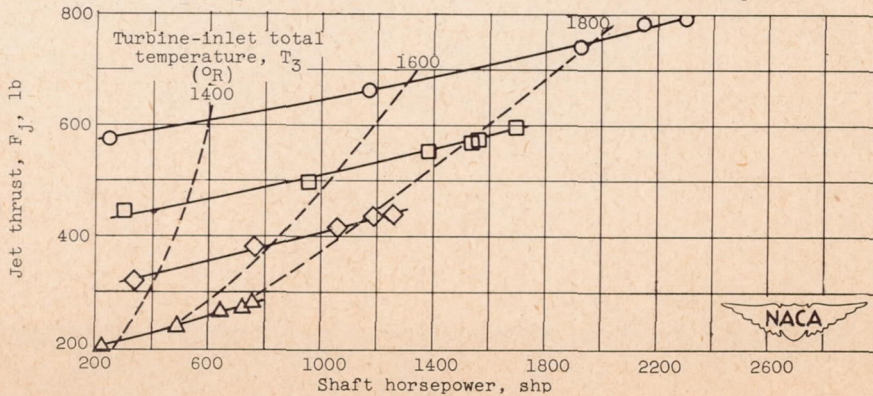
2308



(c) Fuel flow.

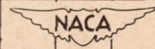


(d) Specific fuel consumption based on shaft horsepower



(e) Jet thrust.

Figure 7. - Concluded. Effect of shaft horsepower on engine-performance parameters at various altitudes. Engine speed, 7600 rpm; cowl-inlet ram pressure ratio, 1.03.



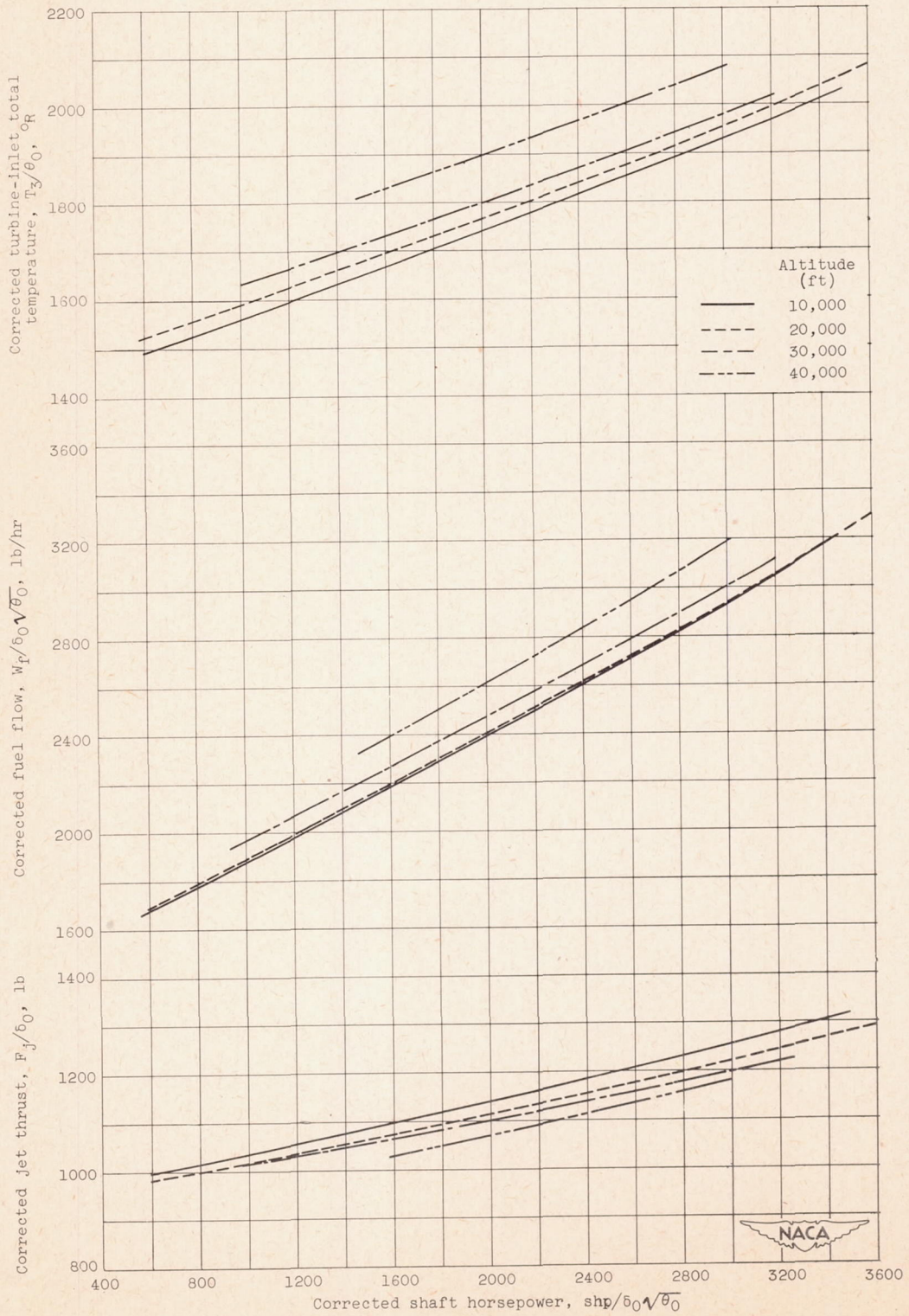


Figure 8. - Generalized engine-performance parameters. Corrected engine speed, 8300 rpm; cowl-inlet ram pressure ratio, 1.03.

2308

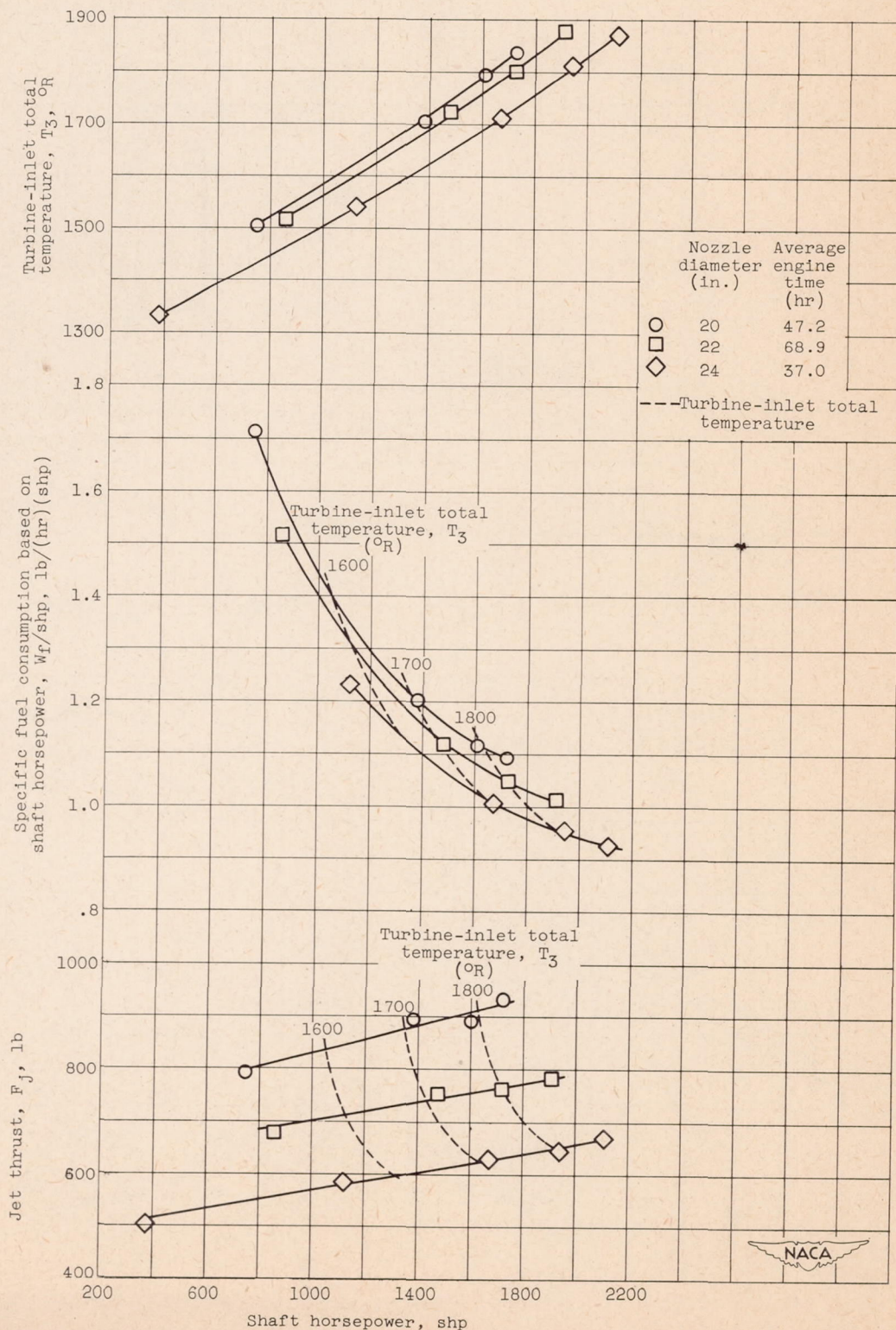


Figure 9. - Effect of shaft horsepower on engine-performance parameters at various exhaust-nozzle areas. Engine speed, 7600 rpm; altitude, 10,000 feet; cowl-inlet ram pressure ratio, 1.03.

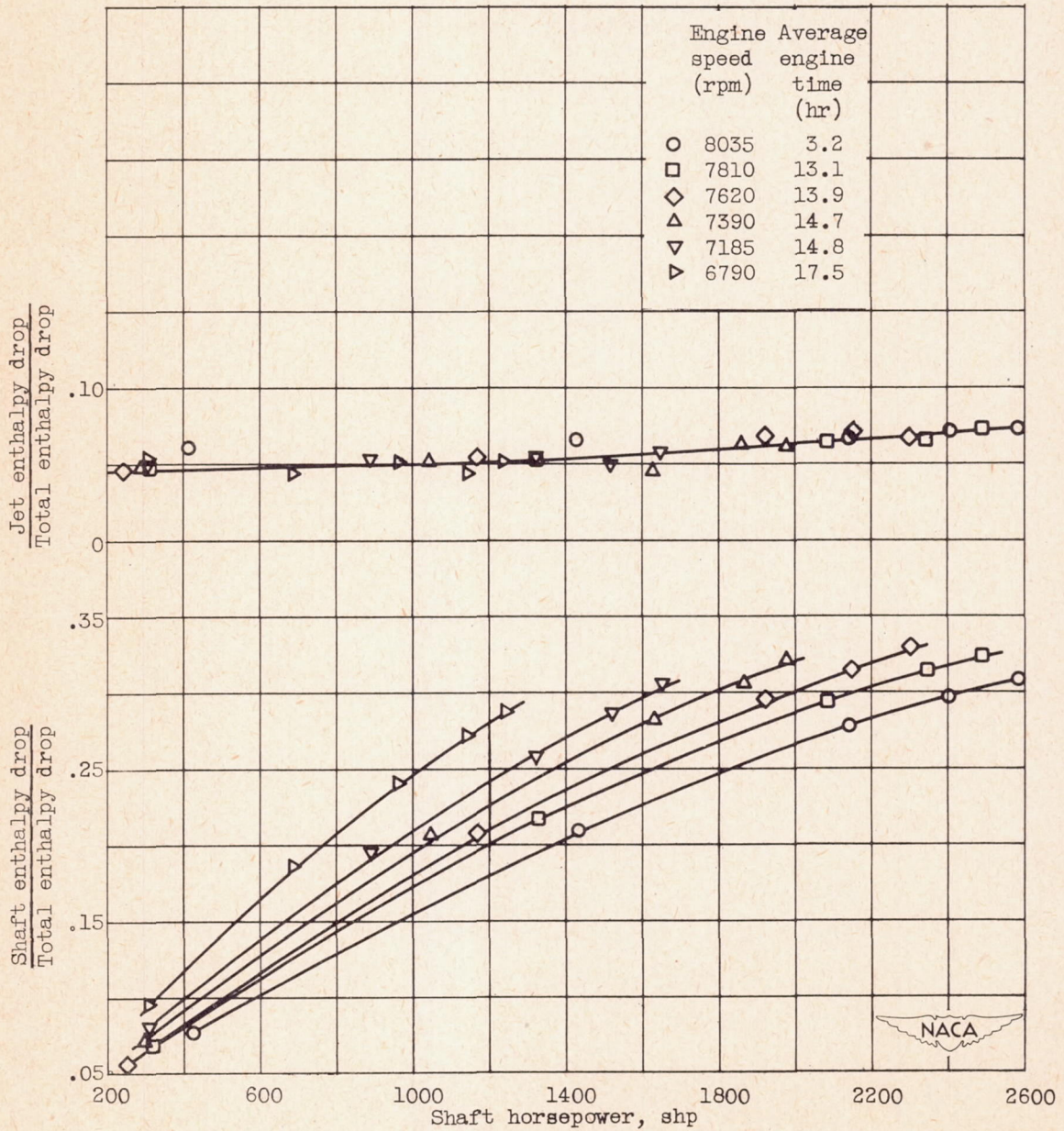


Figure 10. - Effect of engine speed on ratios of jet and shaft enthalpy drops to total enthalpy drop. Altitude, 10,000 feet; cowl-inlet ram pressure ratio, 1.03; standard tail pipe.

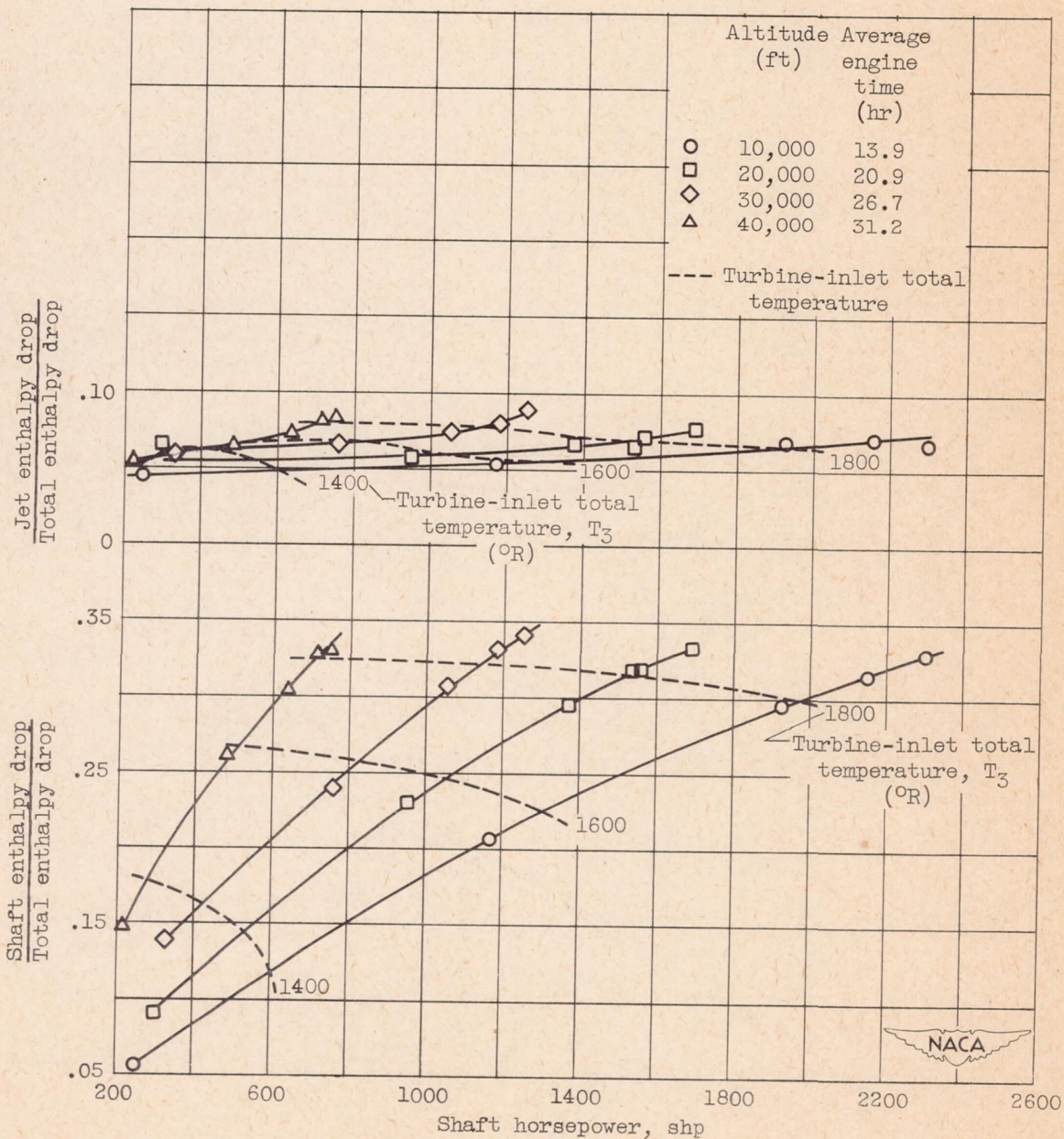


Figure 11. - Effect of altitude on ratios of jet and shaft enthalpy drops to total enthalpy drop. Engine speed, 7600 rpm; cowl-inlet ram pressure ratio, 1.03; standard tail pipe.

2308

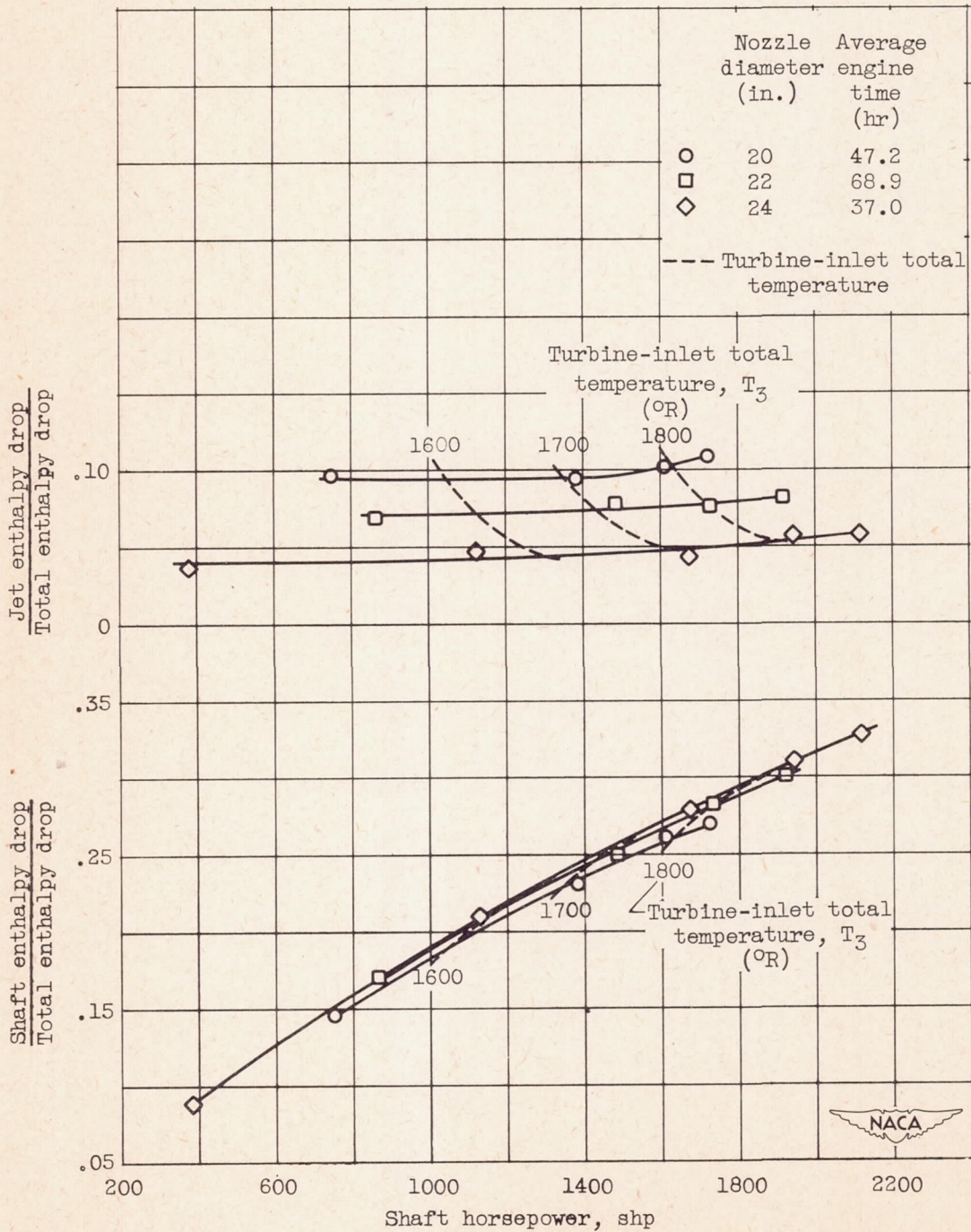
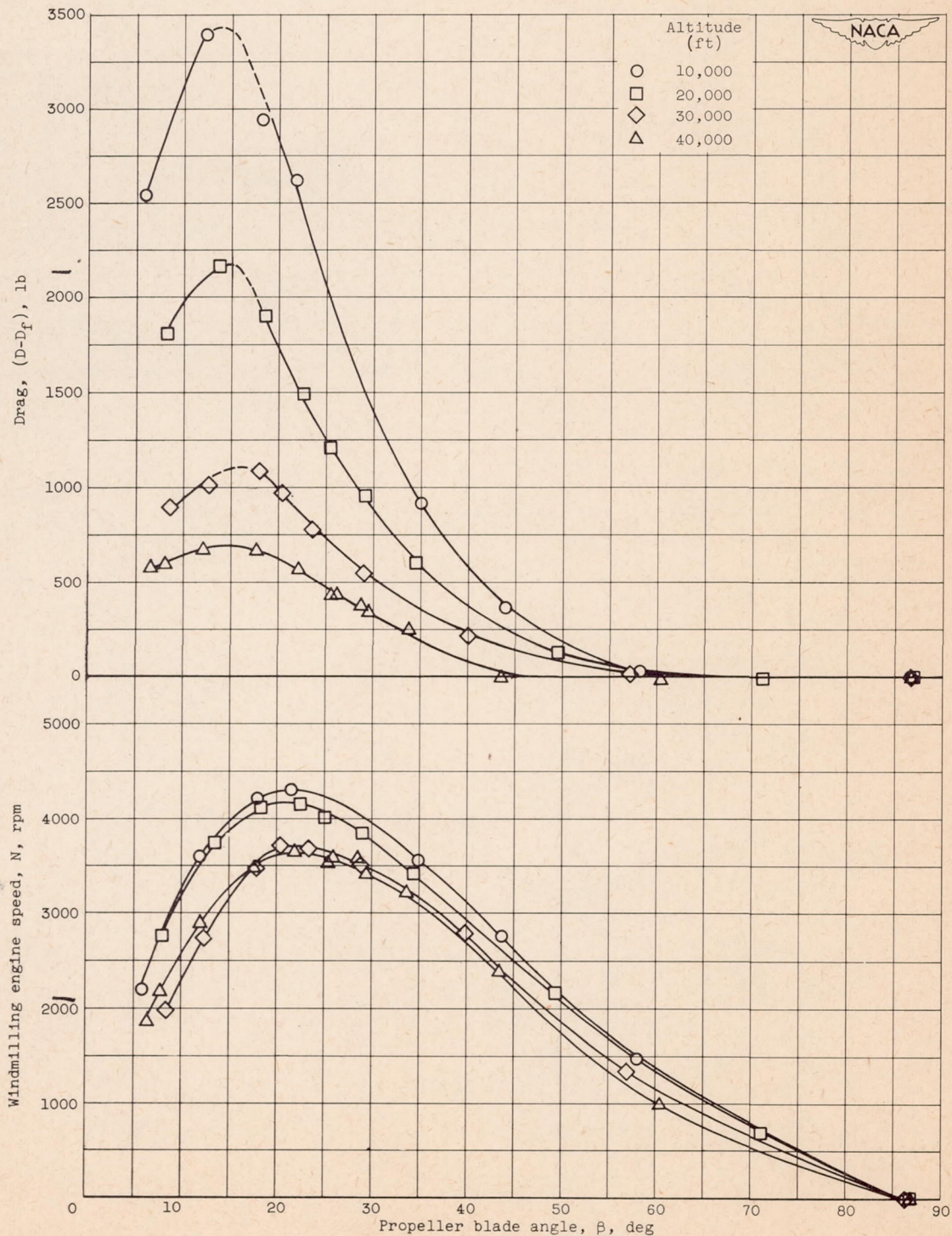


Figure 12. - Effect of exhaust nozzle area on ratios of jet and shaft enthalpy drops to total enthalpy drop. Engine speed, 7600 rpm; altitude, 10,000 feet; cowl-inlet ram pressure ratio, 1.03.

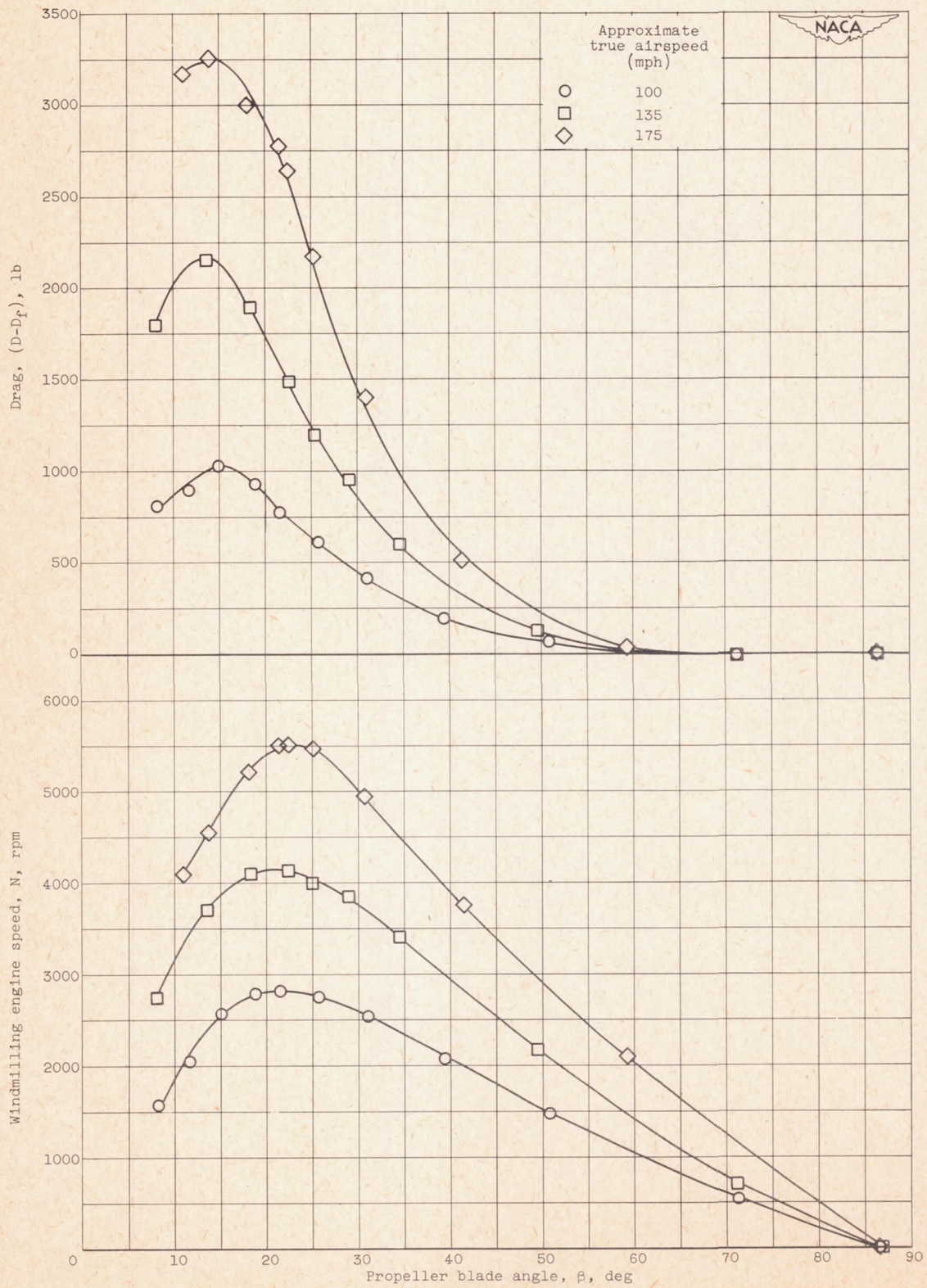
2308

2308



(a) Various altitudes; true airspeed, 135 miles per hour.

Figure 13. - Variation of windmilling drag and windmilling engine speed with propeller blade angle.



(b) Various true airspeeds; altitude, 20,000 feet.

Figure 13. - Concluded. Variation of windmilling drag and windmilling engine speed with propeller blade angle.

2308

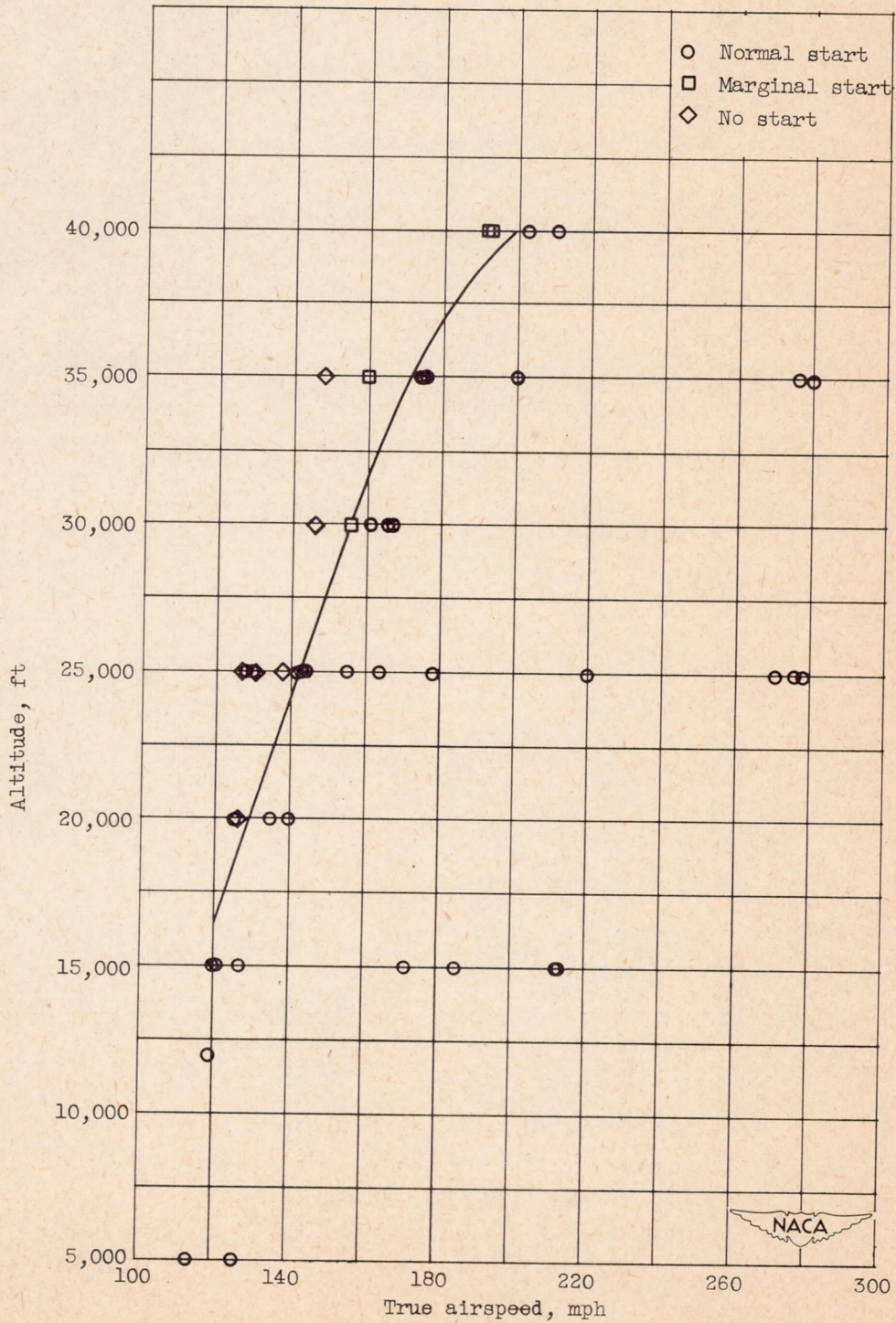
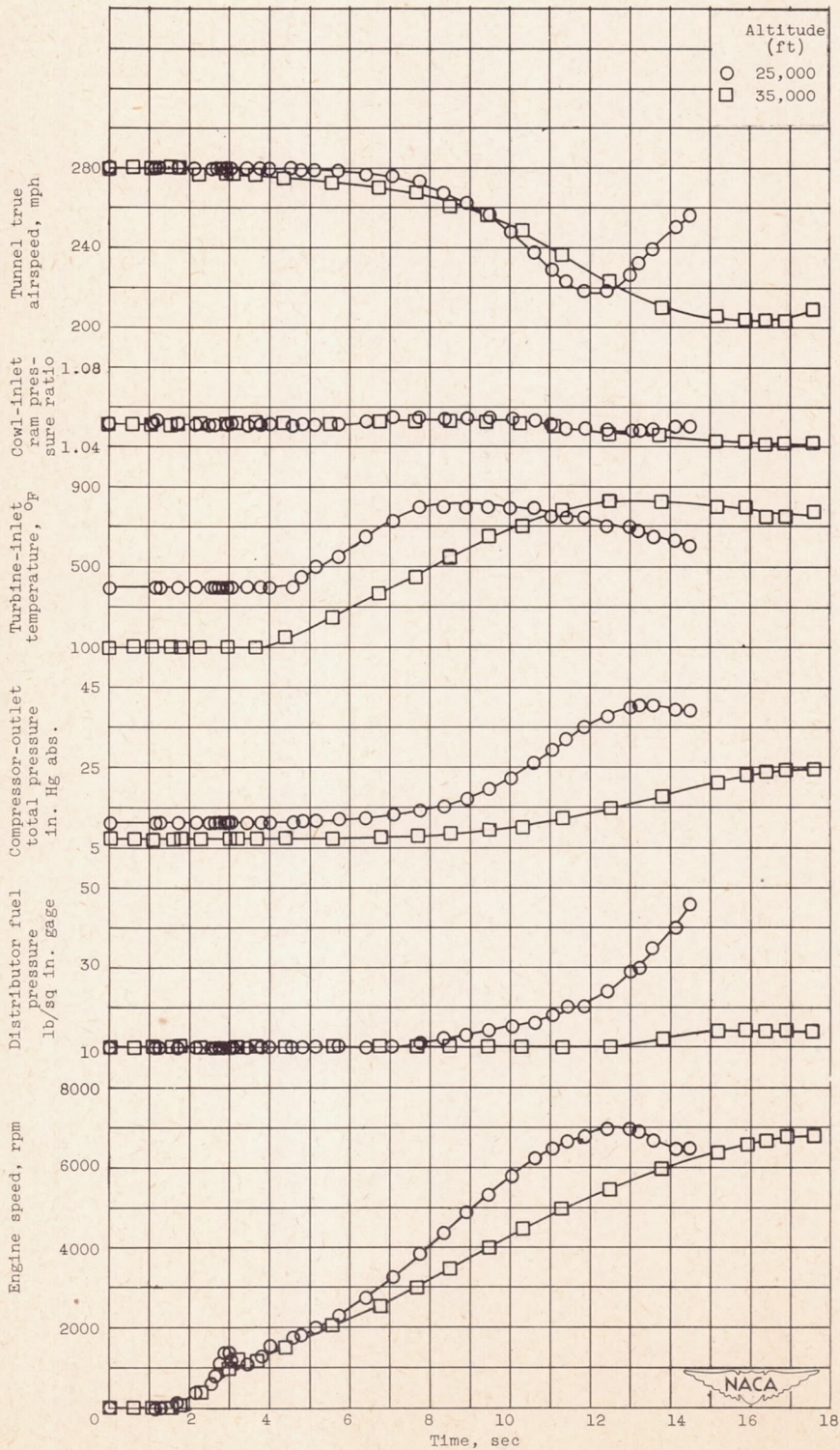
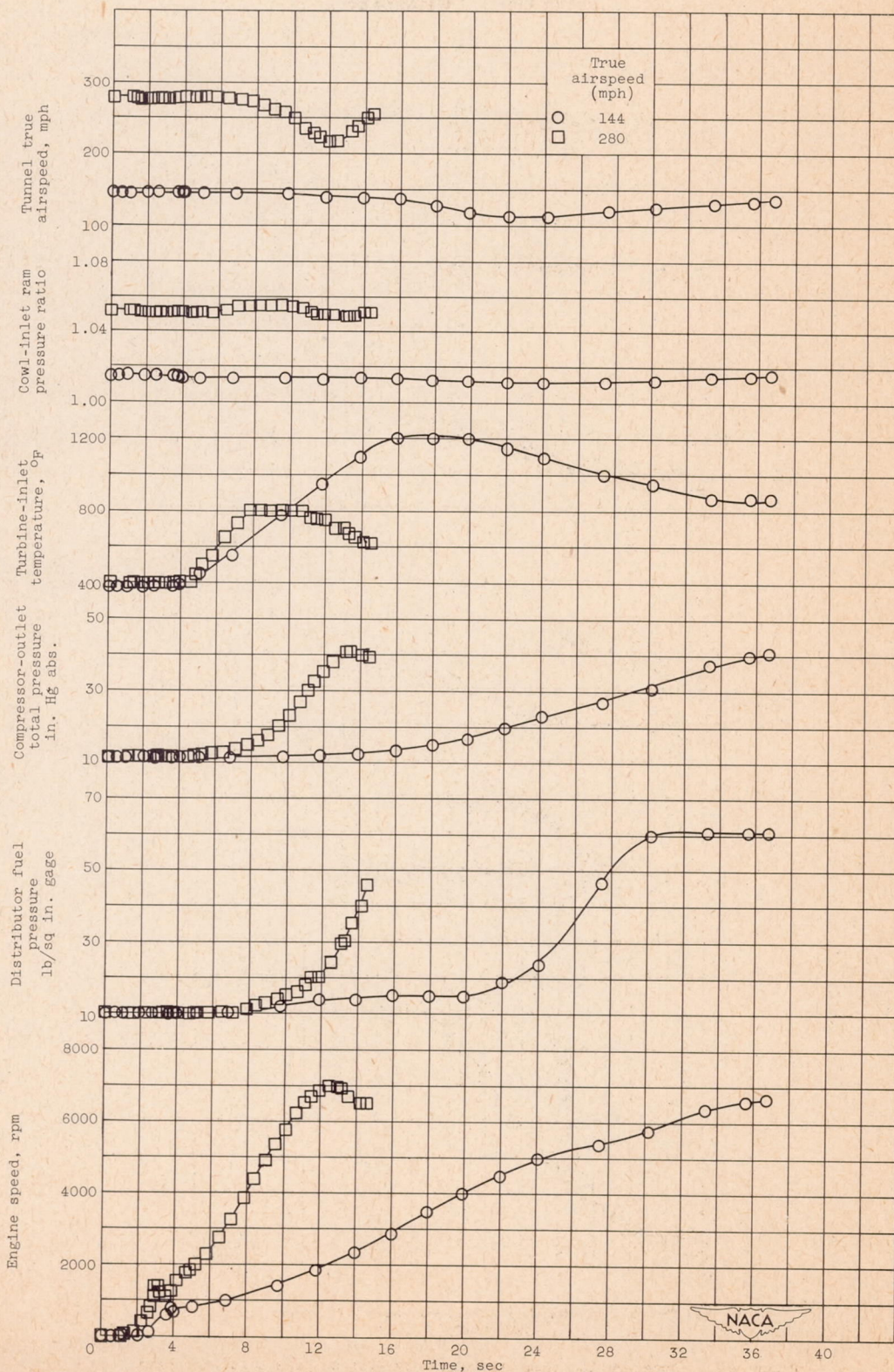


Figure 14. - Effect of altitude on minimum true airspeed required for successful windmilling starts. Normal engine control system.



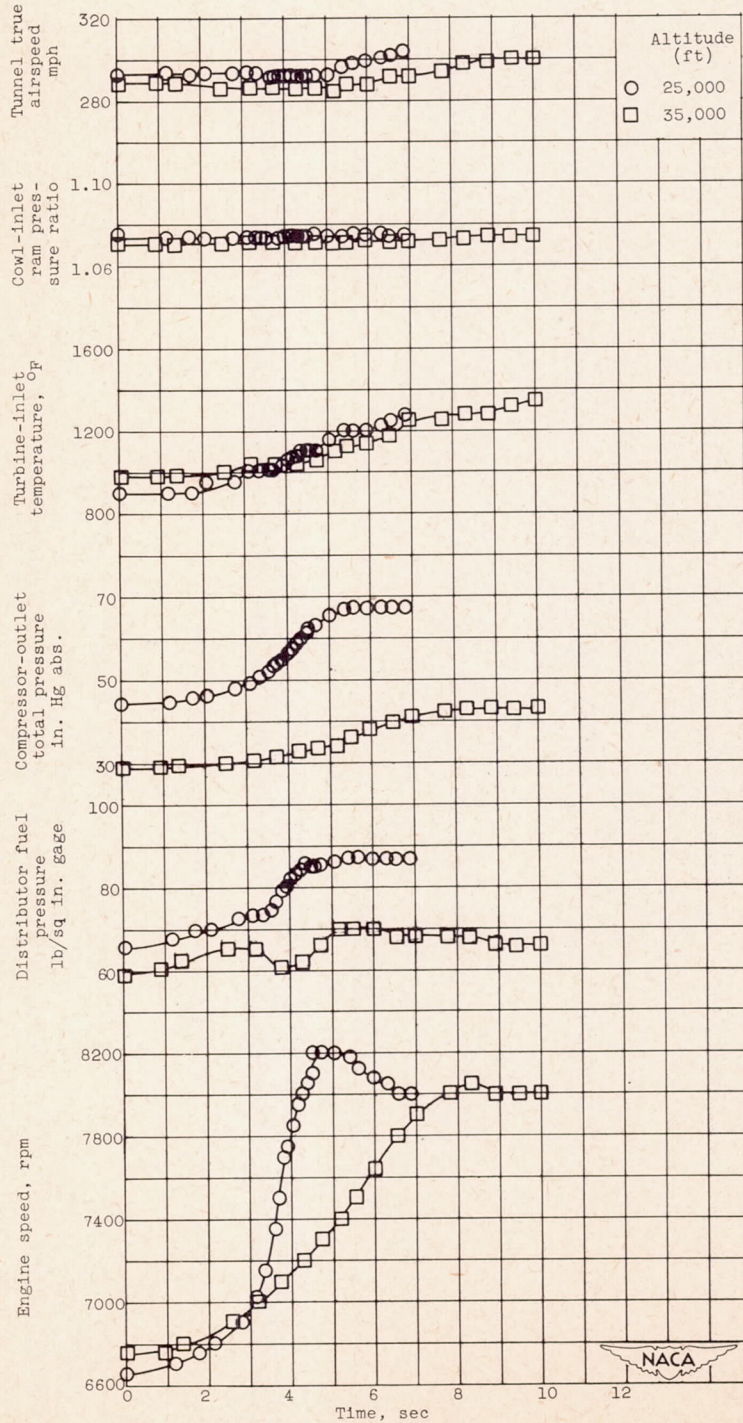
(a) Two altitudes; true airspeed, 280 miles per hour.

Figure 15. - Windmilling starts including acceleration to approximately minimum flight idling engine speed. Normal engine control system.



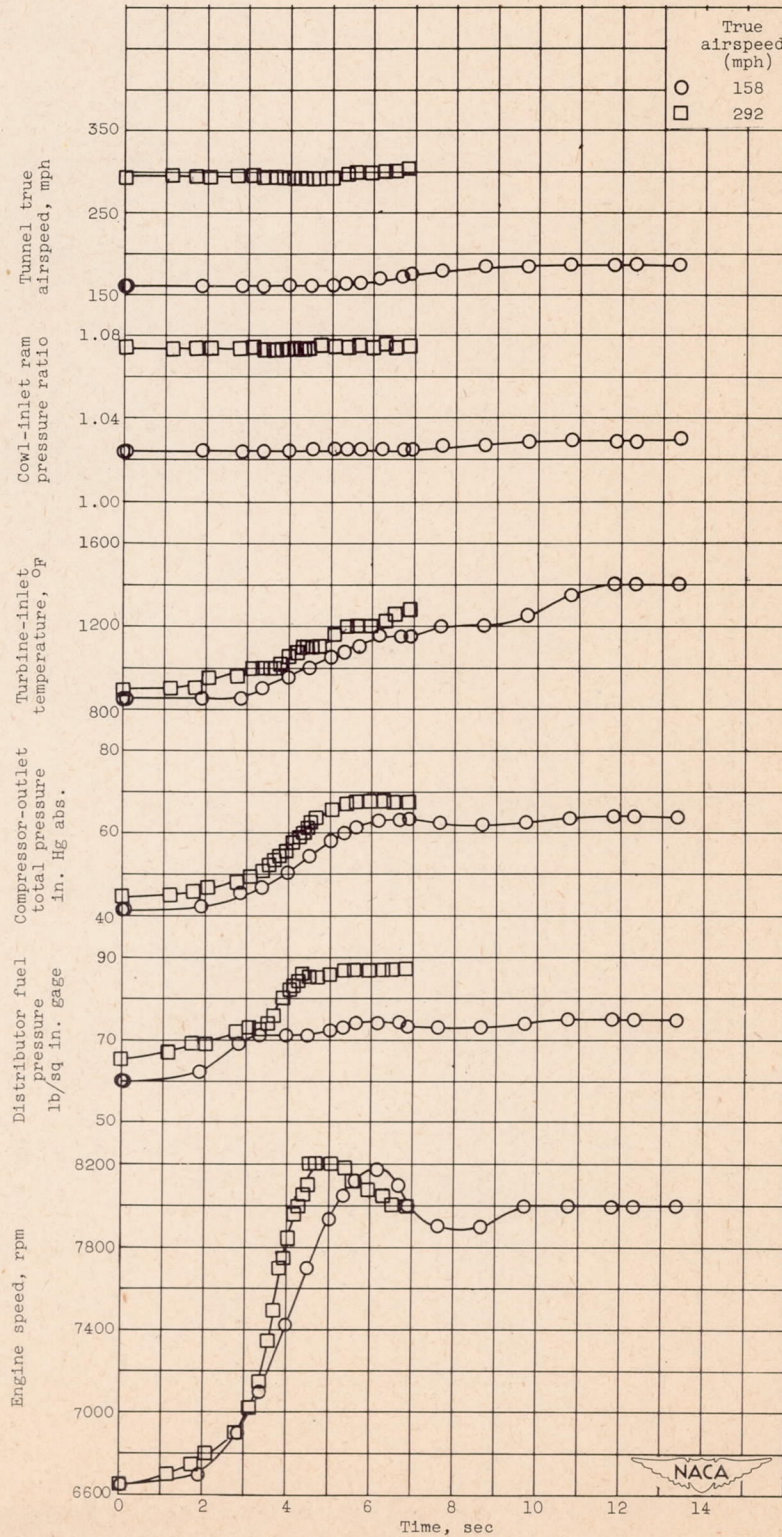
(b) Two true airspeeds; altitude, 25,000 feet.

Figure 15. - Concluded. Windmilling starts including acceleration to approximately minimum flight idling engine speed. Normal engine control system.



(a) Two altitudes; true airspeed, about 290 miles per hour.

Figure 16. - Acceleration from approximately minimum flight idling engine speed to maximum engine speed. Normal engine control system.



(b) Two true airspeeds; altitude, 25,000 feet.

Figure 16. - Concluded. Acceleration from approximately minimum flight idling engine speed to maximum engine speed. Normal engine control system.

2308

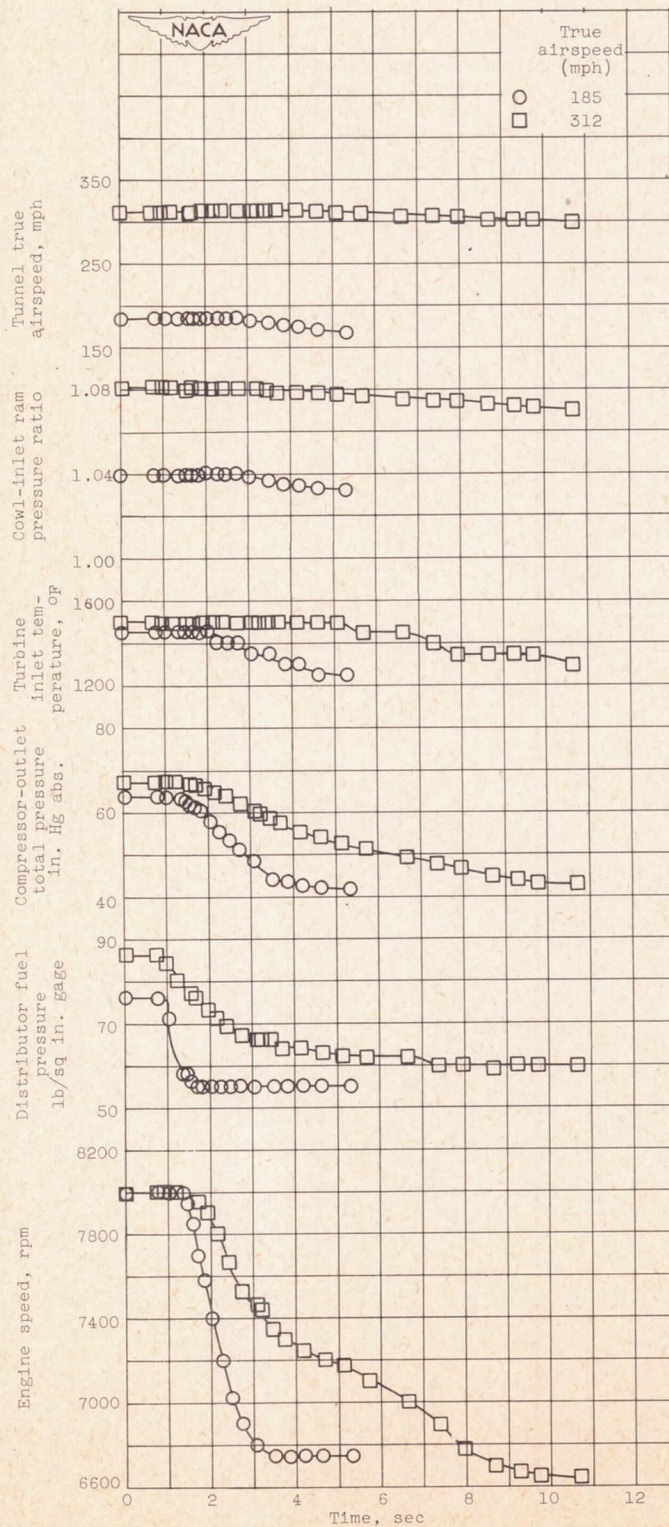


Figure 17. - Decelerations from maximum engine speed to approximately minimum flight idling speed for two true airspeeds at an altitude of 25,000 feet. Normal engine control system.

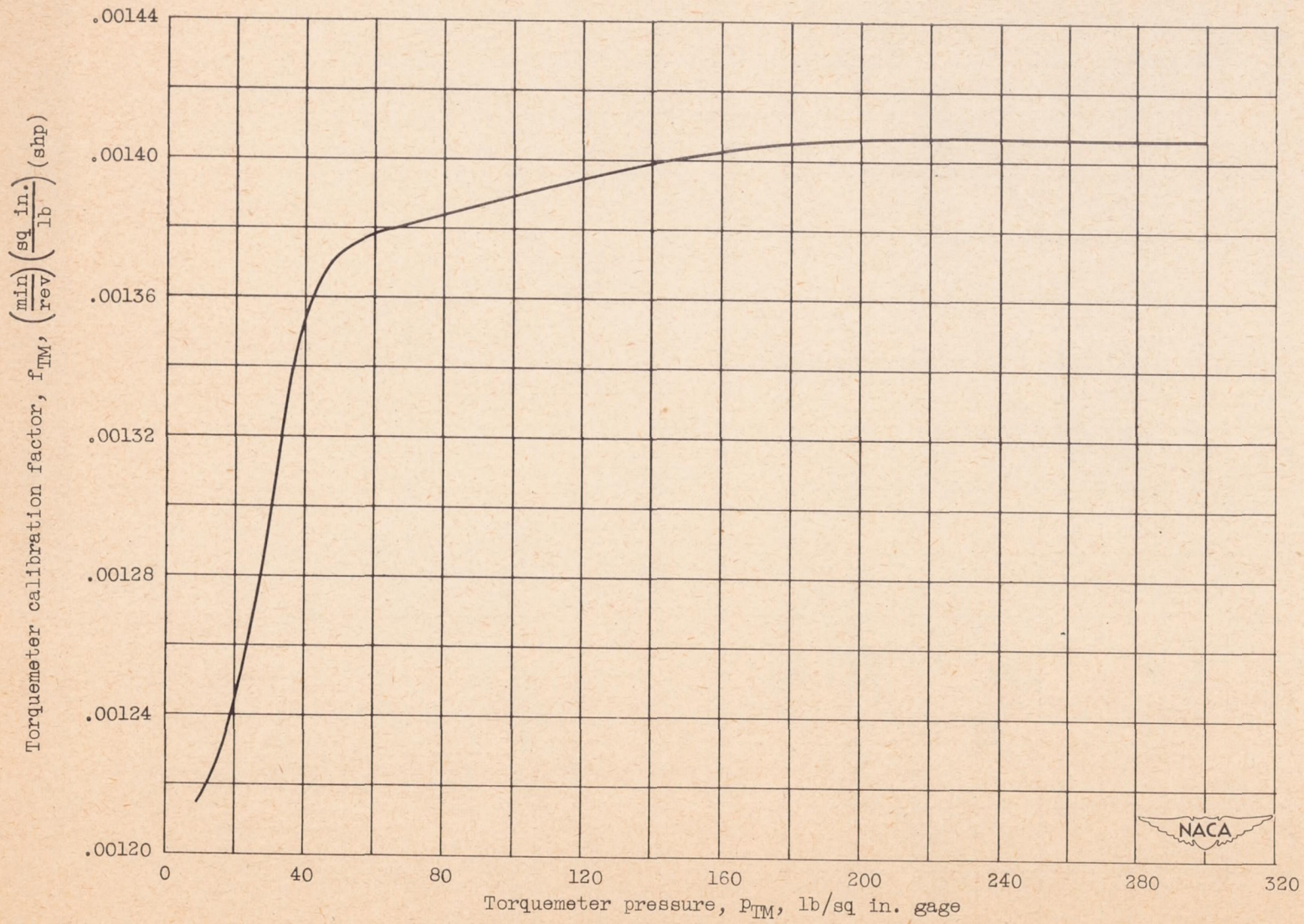


Figure 18. - Torquemeter calibration.

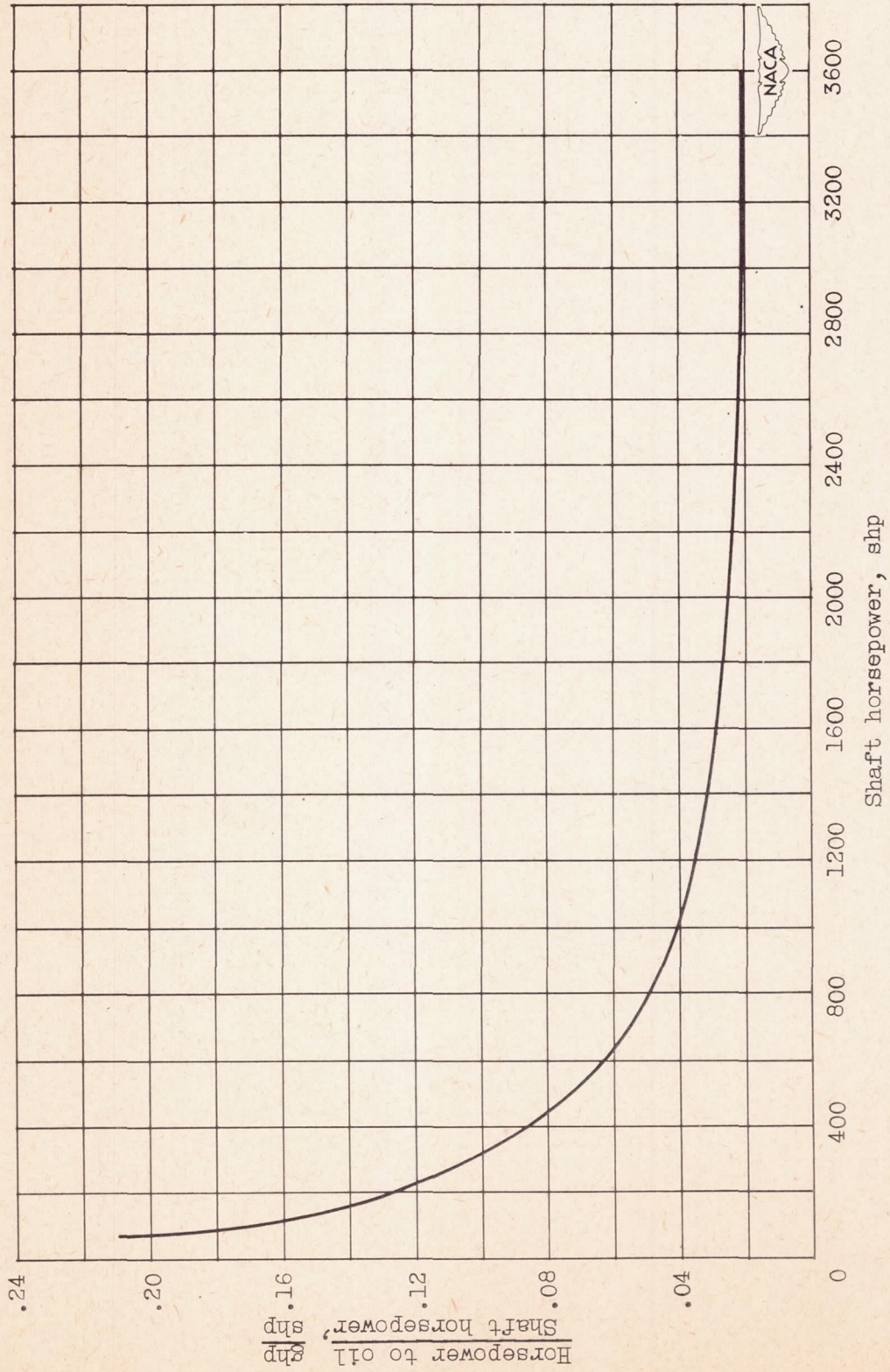


Figure 19. - Gear-horsepower calibration.

2308